Regulation of Human Cripto-1 Expression

Thesis submitted by

POJUL LOYING

For the award of the degree

of

Doctor of Philosophy

DEPARTMENT OF BIOTECHNOLOGY

INDIAN INSTITUTE OF TECHNOLOGY GUWAHATI

GUWAHATI-781039, ASSAM, INDIA

May 2014

Dedicated to my family and friends

Department of Biotechnology

Indian Institute of Technology Guwahati

Date: 23.05.2014

Statement

I do hereby declare that the matter embodied in this thesis entitled "**Regulation of Human Cripto-1 Expression**" is the outcome of research work carried out by me in the Department of Biotechnology, Indian Institute of Technology Guwahati, India, under the supervision of Dr. Biplab Bose.

In keeping with the general practice of reporting scientific observations, due acknowledgement has been made whenever work described here has been based on the findings of other investigators.

May, 2014

Pojul Loying

(Roll No. 08610610)

Department of Biotechnology

Indian Institute of Technology Guwahati

Date: 23.05.2014

Certificate

This is to certify that the thesis entitled "**Regulation of Human Cripto-1 Expression**", is being submitted by **Mr. Pojul Loying (Roll No. 08610610)** for the award of degree of Doctor of Philosophy is an authentic record of the results obtain from the research work carried out under my supervision in the Department of Biotechnology, Indian Institute of Technology Guwahati, India.

The results embodied in this thesis have not been submitted to any other University or Institute for the award of any degree.

May, 2014

Dr. Biplab Bose

(Research Supervisor)

Acknowledgement

The enlightening experience of doing science under the guidance of Dr. Biplab Bose can hardly be described in words. His dedication and commitment to research is truly inspiring. The countless discussions and interactions I had with him expanded my horizons to hitherto unknown frontiers of science and knowledge. I am indebt to this wonderful person for all that he had given me and above all for motivating me towards the scientific research. I am thankful to my doctoral committee members, Prof. Siddhartha S. Ghosh, Prof. Lingaraj Sahoo, Dr.Bhubaneswar Mandal and Dr. Aiyagari Ramesh for their valuable suggestions during my PhD.

I am gratified to Prof. S. S. Ghosh, Prof. L. Sahoo, Prof. Pranab Goswami, Dr. Biplab Bose and Dr. A. Ramesh for providing "state-of-art" laboratory facilities at the 'Centre for Excellence' (DBT Programme support Laboratory) here at Department of Biotechnology, IIT Guwahati. I am grateful to present and past HOCs, Centre for Nanotechnology for providing me the access to valuable instruments without which this study would have not been feasible. I must not forget to thank the past and present HODs of the Department of Biotechnology for creating excellent facilities and a great atmosphere at the department. I feel privileged to work with intelligent, interesting and co-operative present and past members of the Department of Biotechnology.

I am extremely grateful to Dr. Sudip Sen for providing me wonderful laboratory facility to carry out some important part of my PhD work at the Department of Biochemistry, AIIMS, New Delhi. Special thanks to him and his lab members Dr. Sandeep Agrawal, Dr. Janvie Manhas and Aditi Bhattacharya for fostering laboratory environment. I extend my sincere thanks to Dr. Asok Mukhopadhyay, National Institute of Immunology (NII), New Delhi for allowing me to use cell sorter facility in his laboratory at NII.

I thank to Department of Biotechnology (DBT), Govt. of India, for the financial support during my PhD. Special thank to Boehringer Ingelheim Fonds, Germany for providing me entire expenses for the participation in EMBO workshop on "Single Cell Gene Expression Analysis" at EMBL, Heidelberg, Germany (2012). I thank to DBT, Govt. of India for international travel support to attend Cold Spring Harbor Asia conference on "Cell Signaling in Metabolism, inflammation and cancer" at Suzhou, China (2013).

I am heavily indebted to my former lab member Dr Asim Bikas Das, for his unconditional help, support and encouragement during my PhD. I am grateful to my lab members Ashok, Ritika, Mahesh, Poulami, Kaushik for their help and co-operation in the laboratory during my PhD. I am also thankful to all the past and present members of 'Centre for Excellence' especially Manab, Chockalingam, Subhomoy, Mitun, Santoosh, Nidhi, Amaresh, Ankana, Sudeep, Sandipan, Thyago, Somasekhar, Babina, Priyambada,

Archita, Sharmila, Asif, Neha, Mahitosh… for their co-operation during my work in lab. My sincere thank to Departmental of Biotechnology and IIT Guwahati staff.

Several people deserve special acknowledgements. It is worth mentioning the name of Dr. Manabendra Sarma, Department of Chemistry, IIT Guwahati for his kind support and motivation during my entire PhD life. Special acknowledgement to my seniors cum friends; Dr. Subhash Medhi, Dr. Manash Pratim Sarma, Dr. Rajib Kishore Hajam, Dr. Vinod Yata, Dr. Urmila Saxena, Dr. Dipjyoti kalita, Bhaskar Talukdar, Pranab Kumar Das, Phukan Basumatary, Manash Protim Dutta, Rupam Pathak, Aleenndra Brahma, Hrishikesh Duwarah, Madhuri Das, Nithi Phukan… for their exceptional support and encouragement during my PhD. Most especially, the sharing of news and views with my friends Bhaskar (Sr.), Bhupen, Kalpa, Mrinal, Jyoti, Himangshu, Prithiviraj, Bhaskar (Jr.), Prakash, Sumon… in and around IITG campus used to give me outmost relaxation from my tedious work.

Last but not the least, I express my deepest gratitude to my parents, Mr. Gojendra Nath Loying and Mrs. Renu Loying for their love, support and encouragement throughout my life. I am indebt Bornali for her respect towards my profession and for her support & encouragement in each and every moment of my PhD.

May 2014 ***Pojul Loying***

Contents

Abbreviations

ANOVA	Analysis of variance
ActR	Activin receptor
bp	Base pair
cDNA	Complementary deoxyribonucleic acid
CR-1	Cripto-1
CR1ΔC	C-terminal truncated Cripto-1
CR1-GST	GST-tagged Cripto-1
DMEM	Dulbecco's Modified Eagle Medium
DNA`	Deoxyribonucleic acid
dNTP	Deoxyribonucleotide triphosphate
EGF	Epidermal growth factor
EGFR	Epidermal growth factor receptor
Erk	Extracellular signal-regulated receptor
FBS	Fetal bovine serum
GADPH	Glyceraldehyde 3-phosphate dehydrogenase
GSH	Glutathione
GST	Glutahione S-transferase
hr	Hour
HRP	Horseradish peroxidase
kDa	Kilodalton
MAPK	Mitogen-activated protein kinases
mg	Milligram
min	Minutes
ml	Milliliter

mM	Millimolar
MTT	3-(4,5-Dimethylthiazol-2-yl)-2,5-diphenyltetrazolum bromide
mRNA	Messenger ribonucleic acid
ng	Nanogram
nm	Nanometer
nM	Nanomolar
PBS	Phosphate buffer saline
PCR	Polymerase chain reaction
PI3K	Phosphatidylinositol 3-kinase
PMSF	Polymethanesulfonylfluoride
PVDF	Polyvinylidene fluoride
qPCR	Quantitative real-time PCR
rCR-1	Recombinant cripto-1
RIPA	Radioimmunoprecipitation assay
RNA	Ribonucleic acid
rpm	Revoluions per minute
RT-PCR	Reverse transcriptase polymerase chain reaction
s	Seconds
TDGF	Teratocarcinoma derived growth factor
TGF-β	Transforming growth factor beta
TβR	Transforming growth factor receptor
µg	Microgram
µl	Microliter
µM	Micromolar

Abstract

Human Cripto-1 (CR-1) is an oncofetal protein. It is a modulator of embryogenesis and oncogenesis. It is involved in multiple signaling pathways, which are essential for cellular transformation, metastasis and angiogenesis. It is expressed in embryonic cells but is absent in adult tissues. However, CR-1 is overexpressed in several types of cancers. Though extensive work has been done to understand the role of CR-1 in oncogenesis and embryonic development, there is limited information on the control of expression of CR-1. In the present work, we have focused on transcriptional control and cellular heterogeneity in expression of CR-1.

Based on the existing literature, we hypothesized that CR-1 may control its own expression through an autoregulatory pathway involving Nodal/ALk4/SMAD2/3. We have used human glioblastoma cell line, U-87 MG as a model cellular system for our studies. Expression of CR-1 is low in this cell line. We show that treatment with exogenous recombinant CR-1 induces expression of endogenous CR-1 both at mRNA level and at protein level in U-87 MG cells. Experiments were performed to investigate the dose-dependent and time-dependent behavior of such induction. We have confirmed that such an increase in CR-1 is not due to any change of mRNA stability and does not involve expression of Cripto-3, a pseudogene. Using inhibitor-based assays, we show that CR-1 mediated induction of CR-1 indeed involves Alk4/SMAD2 pathway.

During embryonic development, CR-1 is involved in pattern formation. Embryonic pattern formation requires heterogeneous gene expression, with some cells expressing a pattern forming gene at very high level and some having very low expression of the same. Transcriptional networks involving positive feedback often give rise to such cellular heterogeneity. We looked into the single cell expression of CR-1 using flow cytometry. We observed that induction of CR-1 expression by recombinant CR-1 leads to a heterogeneous population, with only a minority subpopulation expressing CR-1. Size of the minority population and level of CR-1 expression in these cells, increases with increase in inducing signal. For further exploration of this heterogeneity, we have analyzed the noise in expression of CR-1 in this heterogeneous population.

Heterogeneity in gene expression in tumor cells is believed to limit chemotherapy and associated with emergence of drug resistance. We have investigated the expression of multi drug resistance protein 1 (MDR1). We observed that MDR1 is expressed only in a minority population of cells.

Treatment with CR-1 increases number of cells expressing MDR1 and most of these cells also have high CR-1 expression. Our observation indicates correlated induction of CR-1 and MDR1.

PI3K and MAPK are two cardinal pathways involved in cell proliferation and survival. Several growth factors activate these pathways. Even CR-1 can contextually activate these pathways. Therefore, we looked into how these pathways may control expression of CR-1. Using combinatorial experiments involving different pathway inhibitors, we show that these two pathways negatively regulate CR-1 expression.

1 Introduction

Human Cripto-1 (CR-1) is an oncofetal protein of EGF-CFC family. It is expressed during embryonic development and is absent or expressed in very low quantity in normal adult tissues. However, it is overexpressed in wide variety of human tumors including colorectal, breast, gastric, pancreatic, ovarian, endometrium, nasopharynx and lung. CR-1 is a typical example of an embryonic protein that is re-expressed in human tumors, promoting cellular proliferation, migration, and tumor angiogenesis. During embryonic development, CR-1 controls formation of germ layers, patterning of anterior posterior axis, specification of mesoderm and endoderm during gastrulation. CR-1 is also involved in mammary gland development and cardiomyogenesis. CR-1 functions through multiple signaling pathways, including Nodal/Alk4/SMAD2/3 and Glypican-1/c-Src/MAPK/Akt. CR-1 overexpression in cancer cells leads to aberrant activation of these pathways, triggering enhanced cell proliferation, migration, EMT and angiogenesis.

Though the role of CR-1 in oncogenesis has been widely investigated, limited information is available on the control of CR-1 expression. Being a crucial molecule in embryonic development, it is expected that that expression of CR-1 must have very stringent regulation through multiple control elements. Expression of molecules involved in embryonic development is regulated, spatially and temporarily, through multiple layers of transcriptional control. Any aberration in these control elements would lead to unwanted expression pattern. Overexpression of CR-1 in tumors can be a manifestation of such aberrations.

It is now well known that gene expression is stochastic in nature. Such stochasticity leads to population heterogeneity in gene expression. Heterogeneous gene expression, in clonally identical cells, is crucial in embryonic development. Such heterogeneity adds another layer of complexity in genesis and progression of cancer. Architecture of transcriptional control circuit affects population heterogeneity in expression of a gene. For example, negative feedback reduces noise in gene expression, thereby reducing population heterogeneity. On the other hand, positive feedback amplifies noise and often gives rise to two separate populations. Therefore, information on population heterogeneity in expression of a particular gene can give clues about the transcriptional network of that gene and *vice versa*.

Existing literature shows that CR-1 promoter has SMAD Binding Elements (SBEs). It is known that TGF-β induces the expression of CR-1 through SMAD2/3 pathway. It is also established that CR-1 can activate SMAD2/3 pathway by forming complex with Nodal and Alk4. Based on these information, we hypothesized that CR-1 may autoregulate its expression. To investigate our hypothesis, we have used human glioblastoma cell line, U-87 MG for our experiments. Using a systematic study, we show that CR-1 induces its own expression in U-87 MG cells thereby creating a possible positive feedback circuit. Such induction has been observed at both mRNA and protein level. We have shown that such an increase in CR-1 is not due to any change of mRNA stability. Using pathway inhibitor, we have confirmed that such induction is mediated through Alk4/SMAD2/3 pathway. Both dose and time dependent experiments have been performed to delineate the positive feedback. The dose dependent induction in CR-1 expression has a sigmoidal behavior with a Hill coefficient greater than one, indicating a possible cooperativity.

Existence of a positive feedback loop that controls induction of CR-1 expression and sigmoidal behavior of such induction indicated that induction of CR-1 may lead to heterogeneous expression of CR-1. Through single cell analysis, using flow cytometry, we observed that CR-1 mediated induction of CR-1 does not happen uniformly. Only a minority sub-population showed measurable level of induction in expression of CR-1. With increase in the inducing signal, two subpopulations of cells emerge, one with high expression of CR-1 and the other with low level of CR-1. With increase in the external signal, the size of subpopulation, with higher expression of CR-1, also increases. We called this subpopulation as CR-1 positive. Appearance of such heterogeneity, with bimodal distribution, is a well known feature of positive feedback circuits. However, we have not observed clear bimodality, with two distinct peaks, in CR-1 expression. We looked into the noise in CR-1 expression and used the change in noise with level of induction, as a marker for hidden bimodality.

We have also looked into the biological significance of CR-1 positive subpopulation that emerges through autoinduction. As CR-1 is a marker of pluripotency, it is believed to be involved in cancer stem cells. We have separated out CR-1 positive and CR-1 negative subpopulations and measured expression of various genes involved in pluripotency and drug resistance. We observed that treatment with exogenous CR-1 co-induced expression MDR1 in the same minor subpopulation that showed higher expression of CR-1. MDR1 is known to be involved in

development of drug resistance in cancer cells. Our observation is important as it indicates that CR-1 and MDR1 are co-regulated.

Further, we have also shown that mitogenic pathways, involving PI3K and Erk1/2, negatively regulate CR-1 expression. These two pathways are aberrantly activated in most cancers, either through overexpression of ligands or receptors or through oncogenic mutations. Several chemotherapeutic agents, used regularly in clinic, block these pathways. Our observation indicates that such inhibition may increase the expression of CR-1, a potential mitogen for cancer cells. Therefore, involvement of mitogenic pathways in CR-1 expression may turn out to be important in development of drug resistance.

The present thesis is organized into separate sections. After this introductory chapter, existing literature on Cripto-1 has been reviewed in Chapter 2, Review of literature. Though all the aspects of CR-1 biology have been discussed in this section, special emphasize is given on transcriptional control of CR-1 expression and on heterogeneity in gene expression. Chapter 3 describes Materials and Methods used in the present work. The methodologies for various experiments have been given in detail. Additional information on common reagents, buffers, solutions, antibodies etc. items used in different experiments are given in appendix. The results of our experiments and thorough discussion of those have been provided in Chapter 4, Results and Discussion. The conclusions drawn from our present work, along with their implications are discussed in brief in Chapter 5, Conclusion.

2 Review of Literature

Human Cripto-1 (CR-1) is a member of the EGF-CFC family of vertebrate signaling molecules [1]. This family also includes Cryptic in mice [2], FRL-1 in *xenopus* [3], and one eyed pinhead in Zebrafish [4]. CR-1 is also known as human teratocarcinoma derived growth factor-1 (TDGF-1) as it was initially derived from undifferentiated human teratocarcinoma cells, NTERA2 [5].

CR-1 is a 188 amino acid long protein and its molecular weight varies from 19 – 36 kDa, depending upon the extent of glycosylation [6]. Like other members of EGF-CFC family of proteins, CR-1 has N-terminal signal peptide, an epidermal growth factor (EGF)-like motif, a conserved cysteine-rich domain (CFC region), and a short hydrophobic C-terminus that is essential for membrane anchorage by a glycosylphosphatydilinositol moiety [7]. However, CR-1 sheds from the membrane, to generate soluble CR-1, by the activity of GPI-phospholipase D and growth factors like EGF stimulate such shedding [8]. Soluble CR-1 has been identified *in vitro* culture system, human milk and in serum of breast and colon cancer patients [9, 10]. Both soluble and membrane-bound CR-1 are functional [11].

Like other members of EGF-CFC, CR-1 is expressed during embryonic development and is absent or expressed in very low quantity in normal adult tissue. However, it is overexpressed in wide variety of human tumors including colorectal, breast, gastric, pancreatic, ovarian, endometrium, nasopharynx and lung [12].

2.1: Structural aspects of Cripto-1:

The domain architecture of human CR-1 is shown in Figure 2.1. Like other members of EGF-CFC family proteins, CR-1 has four distinct regions: signal peptide domain, EGF-like motif, a conserved cysteine rich domain (CFC region), and a region for membrane anchoring through GPI. However, the EGF domain present in CR-1 is a variant EGF-like motif of other members in EGF super-family. It is 40 amino acids long. It has six cysteine residues that can form three intramolecular disulfide bonds. The canonical EGF-motif has three distinct loops (A, B and C). However, EGF-like motif in CR-1 lacks the A-loop, possesses a truncated B-loop and has a

complete C-loop [6]. Bianco *et al.* [13] have shown that due to modified EGF like domain, CR-1 cannot bind to epidermal growth factor receptor (EGFR).

CR-1 gets is fucosylated in the EGF-like domain. However, such fucosylation is not essential for CR-1 signaling [14]. Similarly, C-terminal GPI anchoring domain and membrane anchorage through GPI is not essential for CR-1 signaling [15, 16]. Soluble and functional CR-1 has been identified in human milk [9] and in serum of breast and colon cancer [10]. Various forms of recombinant soluble CR-1 has been used in experiments and found to be functional [17-19]. Even, the EGF-like domain of CR-1, fused either to human Fc or to GST, was found to be functional [20, 21]. Furthermore, refolded peptides corresponding to EGF-like domain of CR-1 also induces CR-1 signaling [22, 23]. Das *et al.* [24] had earlier shown that C-terminal truncated CR-1, fused to GST and expressed using a bacterial expression system, is functional.

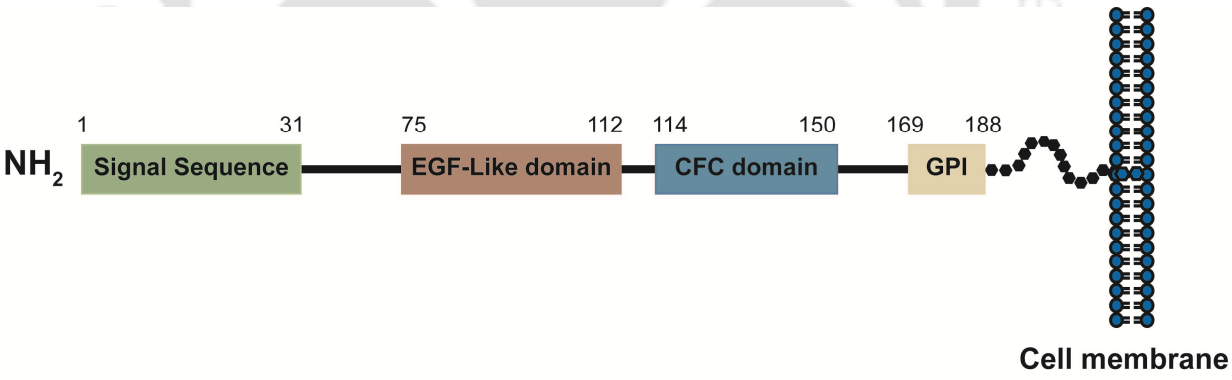

Figure 2.1: Domain architecture of Human Cripto-1. Cripto-1 (1-188 amino acids) has signal peptide, epidermal growth factor-like motif (EGF-Like domain), a conserved cysteine rich domain (CFC domain), and a short hydrophobic C-terminus that is essential for membrane anchorage by a glycosylphosphatydilinositol anchor domain.

2.2: Functions of Cripto-1:

Human Cripto-1 is a signaling molecule involved in various processes from embryonic development to progression of cancer. In playing its versatile role, CR-1 acts either as co-ligand/co-receptor or as an independent ligand to trigger different signaling pathways. Some of these pathways are well characterized and role of CR-1 in those pathways have been clearly elucidated.

Cripto-1 during embryonic development:

Members of EGF-CFC family are involved in early vertebrate development [25]. CR-1 is expressed in various human embryonic stem cell lines [26, 27], as well in human induced pluripotent stem cells [28] and believed to be involved in maintenance of pluripotency [29]. However, the precise role of human CR-1 in human embryonic development is not elucidated. Loss-of-function mutations in human Criptic protein (CFC1), another member of EGF-CFC family, are associated with left-right lateral defects [30]. Mouse homologue of Cripto-1 has been extensively investigated in embryonic development [12].

During embryonic development, mouse cripto-1 (Cr-1) is expressed in a spatially restricted fashion [31]. Xu *et al.* [32] reported three major roles for Cr-1 during mouse embryonic development. Cr-1 is needed to produce the correct number and specification of embryonic precursor cells, gives a spatial signal that is required for morphogenesis of cell layers and forms a morphogenic gradient across the embryonic field, with a high concentration in the mesodermal cells of the primitive streak. Cr-1 is essential for the conversion of a proximal-distal asymmetry into an orthogonal anterior-posterior axis in mouse embryo [33]. Disruption of both the Cr-1 alleles by homologous recombination leads to embryonic lethality due to impaired gastrulation and anterior-posterior (A-P) axis perturbation and the rotation of the anterior–posterior axis fails to occur, resulting in mislocalization of the head- and trunk-organizing centers [33]. It has also been seen that disruption of both Cr-1 alleles by homologous recombination in mES cells leads to a specific block in the *in vitro* differentiation of cardiac myocytes [34]. Cr-$1^{-/-}$ mouse embryonic stem cells, shows extensive neural differentiation, suggesting neuroectodermal differentiations in absence of Cr-1 [35].

One-eyed pinhead, *oep*, the Cripto-1 homologue in zebra fish, is essential for cellular movement during embryonic development [36]. During embryonic development, one eyed pinhead *oep*, is essential for Nodal signaling and regulates germ layer formation and the positioning of the

anterior posterior development. It is also essential for the cell motility throughout the blastoderm during early embryonic development. *Oep* mutant cells are more cohesive and migrate slower than wild-type cells. [36, 37].

Cripto-1 during oncogenesis:

CR-1 is involved in several cellular processes linked to neoplasia, such as stimulation of cell proliferation, migration, branching morphogenesis and transformation [38]. Overexpression of CR-1 in breast cancer cell line, MCF-7, enhance resistance to anoikis and increases invasiveness of these cells [39] and enhances tumor neovascularization in a xenograft model [12]. In addition, overexpression of CR-1 enhances colony formation and anchorage independent growth in normal mammary epithelial cells, NOG-8 [40]. Transfection of CR-1 into mouse mammary epithelial cells, NIH3 induces morphological changes and colony formation [41]. Overexpression of CR-1 in normal rat fibroblasts induces growth in soft agar [23]. *In vivo* overexpression of human CR-1, in mammary glands of transgenic mouse, causes development of hyperplasia and papillary adenocarcinoma [42]. The expression of CR-1 is significantly inhibited by anti-CR-1 second generation antisense oligonucleotides and can inhibits growth of cancer cells in both *in vitro* and *in vivo* [43].

CR-1 is also involved in tumor angiogenesis. It enhances cell migration and invasion of human umbilical endothelial cells, HUVEC and induces formation of vascular-like structures on Matrigel experiments [44]. Moreover, overexpression of CR-1 stimulates various epithelial cell responses that are associated with microvessel formation *in vivo* [44]. Treatment with monoclonal antibody against CR-1 can inhibit such CR-1 induced neovessel formation [44].

CR-1 also play role in inducing epithelial to mesenchymal transition (EMT) of mammary epithelial cells [12]. EMT marker expression study has shown that E-cadherin, which is responsible for intactness of junction complex in epithelial cells, was significantly downregulated in mammary gland hyperplasia, tumors of CR-1 transgenic mice and CR-1 transfected HC-11 cells [45]. Furthermore, zinc finger repressor transcription factor Snail was detected in elevated levels in mammary tumor lesions of CR-1 transgenic mice [45]. Increase in the expression of another EMT marker, vimentin, a major cytoskeletal component of mesenchyme cells, was observed following overexpression of CR-1 human cervical carcinoma cells, Caski. Increased vimentin expression exhibited increased migration and invasion in Caski cells [46, 47].

Involvement of Cripto-1 in different signaling pathways:

CR-1 is a co-receptor for Nodal, a ligand of transforming growth factor (TGF-β) family [48]. Nodal is a morphogen involved in embryonic development [49]. It forms a concentration gradient, thereby provides positional information to cells through dose-dependent activation of signaling pathways [50]. Like other ligands of the TGF-β family, Nodal signals through transmembrane serine/threonine kinase receptor [51]. It signals through type I activin receptor ActRIB (Alk4) and type II receptors, ActRIIA and ActRIIB, leading to phosphorylation and nuclear accumulation of SMAD2 and/or SMAD3 together with SMAD4 [52]. The activated SMAD complex binds to SMAD binding element in the promoter of target genes, interacts with other transcription factors, like transcription factors of FAST subfamily, and induces gene expression [16].

However, Nodal alone cannot activate this pathway. It requires CR-1 for the same. Mutational studies have shown that CR-1 binds to Nodal through its EGF domain and binds to Alk4 (ActRIB) through its CFC domain [14, 53]. That is why CR-1 is considered as a co-receptor of Nodal [54]. Physical association of Nodal, Alk4 and CR-1 is essential for activation of the SMAD2/3 pathway [17]. Alk4 positive mouse mammary epithelial cells showed no phosphorylation of SMAD2 upon treatment with external CR-1 [17]. However, phosphorylation SMAD2 was observed when Nodal was overexpressed in these cells and treated with exogenous CR-1 [17].

It is now well established that both membrane bound CR-1 and soluble CR-1 activate Nodal/Alk4/SMAD2/3 pathway. In association with Nodal and Alk4, membrane bound CR-1 can induce SMAD2 phosphorylation [55] Bianco *et al.* [17] have shown that c-terminal truncated soluble CR-1 (CR1ΔC) that was expressed in CHO cells, functionally forms complex with Alk4 and nodal and induce phosphorylation of SMAD2 in mouse mammary epithelial cells, EpH4. Commercially available soluble recombinant CR-1 (R&D system) expressed in bacterial system also induces phosphorylation of SMAD2 in several human melanoma cells [19]. Further, this commercial recombinant CR-1 shows induction of SMAD2 in mouse extra-embryonic endoderm stem cells, XEN, however, such effects was inhibited by an Alk4 inhibitor , SB431542 [56]. Considering these, CR-1 can be considered as a co-ligand rather than co-receptor of Nodal [16]. This pathway of CR-1 is briefly described in Figure 2.2.

Nodal/Alk4/SMAD2/3 pathway has important role in embryonic development and in cancer. Parisi *et al.* [57] have shown that CR-1 dependant Nodal signaling pathway induces SMAD2 phosphorylation and determines cardiac fate in early embryonic development. Failure in the induction of this pathway, results in the direct conversion of embryonic stem cells into neuronal fate, rather cardiac fate [57]. This signaling pathway is also involved in the establishment of Left/Right embryonic axis [52]. Blocking of CFC domain of CR-1 by using anti-human Cripto-1 mAbs shows functional blockade of Nodal/Alk4/SMAD2/3 pathway and inhibits tumor growth in human breast cancer cells and in human testicular and colon xenograft tumor models [58]. Complex formation of CR-1 and ActRIIB is interrupted by alantolactone and inhibits SMAD3 phosphorylation, thereby results in the inhibition of cell proliferation [59].

CR-1 can also activate PI3K/Akt as well as MAPK pathways. PI3K/Akt pathway is known to regulate cell cycle progression, apoptosis and oncogenic transformation [60]. MAPK pathway maintains normal cell proliferation, survival and differentiation and aberrant regulation of MAPK pathway leads to cancer and other human diseases [61]. These two pathways are activated when CR-1 binds to the heparin sulfate proteoglycan Glypican-1. In turn, it activates the tyrosine kinase c-Src, leading to the activation of downstream Akt and MAPK [17, 18, 62]. In Akt signaling pathway, CR-1 enhances the tyrosine phosphorylation of the p85 regulatory subunit of PI3K and induces the phosphorylation of Akt and GSK [12, 63]. In several *in vitro* experiments, it has been shown that full length CR-1 expressed in mammalian system activates MAPK pathway leading to enhanced phosphorylation of Erk1/2 [44, 64].

CR-1 mediated cell proliferation and survival is regulated by Akt and MAPK signaling pathways. Deregulated activation of these two pathways by CR-1 leads to enhanced cell proliferation. Exogenous CR-1 activates these two pathways and induces proliferation, migration, invasion and angiogenesis in HUVECs cells [44]. CR-1 inhibits phosphorylation through enhanced phosphorylation of Akt and GSK-3β in human cervical carcinoma cells, SiHa and Caski [63]. Mammary tumors from Cr-1 transgenic mice and HC-11 cells overexpressing Cr-1, shows increase in active C-Src and Akt [45].

Kelber *et al.* [65] have recently shown that CR-1 forms complex with the HSP70 family member glucose-regulated protein-78 (GRP78) and participated in various CR-1 mediated signaling in human tumor, mammary epithelial and embryonic stem cells. Using various experiments, they have demonstrated that targeted disruption of the cell surface CR-1/GRP78 complex blocks CR-1

activation of PI3K/MAPK pathways, thereby prevents CR-1 from increasing cellular proliferation [65]. Glypican-1/C-Src/MAPK/Akt signaling pathways of CR-1 are briefly described in Figure 2.3.

Further, *in vitro* experiments shows that CR-1 binds to TGF-β and reduces cross-linking of TGF-β to its receptor TβRI. Eventually, it leads to reduced phosphorylation of downstream SMAD2/3 and induces growth in TGF-β signal dependent cells [53]. Glucose regulated protein 78 (GRP78) associates with CR-1 and enhances cell growth and inhibits cytostatic effects of TGF-β. Cripto and GRP78 had a cooperative ability to block the cytostatic effects of TGF-β under anchorage-independent conditions. This complex leads to increased malignancy and confers a competitive proliferative advantage to tumor cells via inhibition of TGF-β signaling at the receptor level [66].

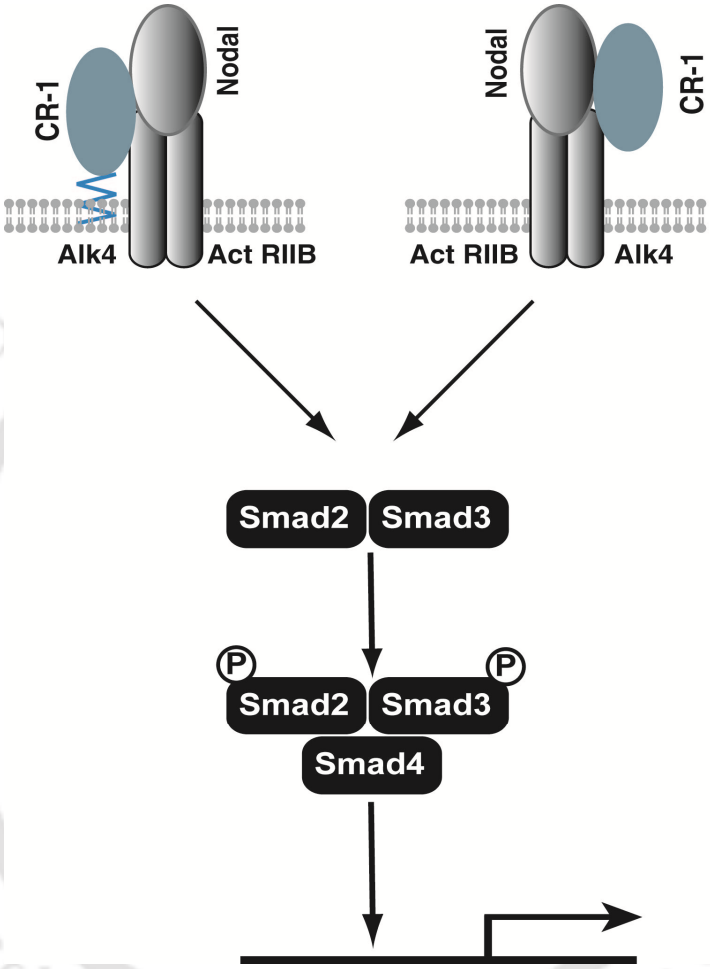

Figure 2.2: Cripto-1 activates SMAD2/3 signaling pathway. Cripto-1 acts as a co-receptor/co-ligand in this signaling pathway. Both membrane bound and soluble Cripto-1 binds to Nodal through EGF domain and recruits Nodal to type I activin receptor ActIB (Alk4). Binding of Nodal to this receptor activates SMAD2/3 pathway. The SMAD complex binds to SMAD binding elements (SBE) in the promoters of target genes and modulates expression of those genes.

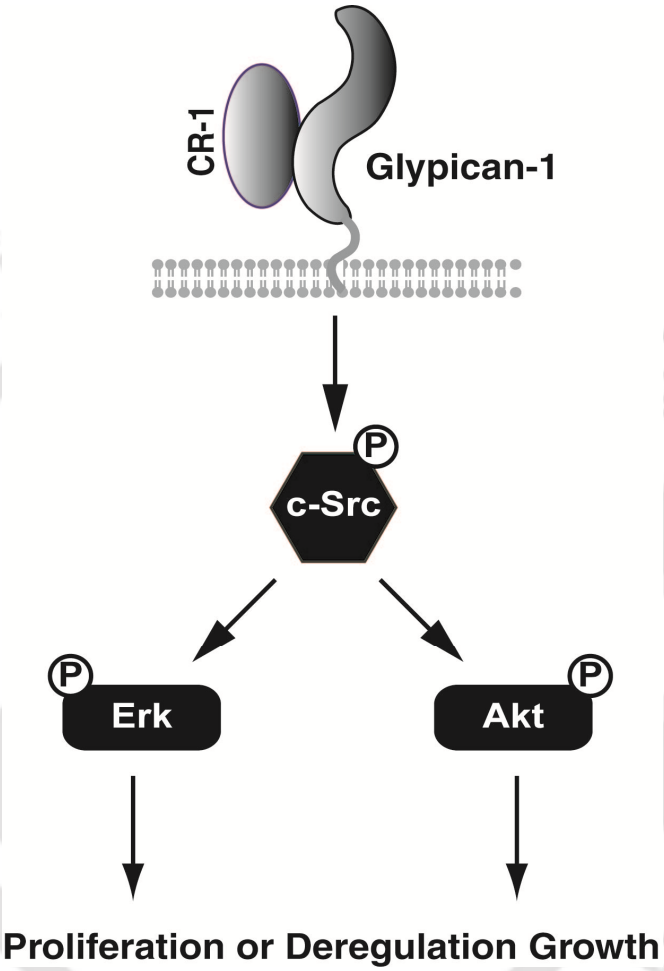

Figure 2.3: Cripto-1 activates MAPK and Akt signaling pathway. Cripto-1 binds with glypican-1, and activates c-Src which subsequently activates Erk1/2 and Akt. Activation of these pathways finally leads to cell proliferation through modulation of molecules involved in cell cycle progression.

2.3: Expression of Cripto-1:

Full-length human CR-1 transcript was initially identified by Ciccodicola *et al.* [1] from a cDNA library derived from undifferentiated human teratocarcinoma cells, NTERA2. The transcript is approximately 2.2 kb long and codes for a 188 amino acid protein. This was further mapped to human chromosomal location 3p21.3. Genomic sequence of CR-1 available in NCBI database NCBI (reference Sequence: NG_017049.1) shows all total seven exons. There are three transcript variants of CR-1 originating from alternate splicing. Transcript variant-1 does not have exon-1 and starts from exon-2. Transcript variant-2 of CR-1 starts from exon-1 but exon-2 is missing in this transcript. Baldassarre *et al.* [21] have described a short form of CR-1 in human colon carcinoma cell line, Geo. This transcript variant of CR1 start form exon-4 and the putative start codon is not ATG but a CTG.

Five pseudo genes related to human CR-1 have been reported [5]. These are CR-2, CR-3, CR-4, CR-5 and CR-6 (also known as TDGF-2, TDGF-3, TDGF-4, TDGF-5 and TDGF-6 respectively). Dono *et al.* [67] have characterized CR-3. CR-3 does not have introns and has seven base differences with CR-1. These differences result in changes in six amino acids. It has been reported that CR-3 transcripts are expressed in breast, lung and colon carcinoma cells [68].

CR-1 is expressed in human embryonic stem (huES) cells and it considered as a marker for stemness [26]. During embryonic development in mouse, Cr-1 is expressed in mouse blastocyst, primitive streak, and later it is restricted to the developing heart [31]. Mouse Cr-1 is expressed in the stromal cells, luminal epithelial cells, and myoepithelial cells of the branching ducts of mouse mammary glands [69]. Expression of Cr-1 in mouse mammary glands increases during pregnancy and lactation [69].

Human CR-1 is generally absent or present in very low level in some normal adult tissue [70]. In normal adult tissues, CR-1 expression has been detected only in mammary gland [9]. Bianco *et al.* [9] have also detected CR-1 in human milk. CR-1 is overexpressed in a majority of human cancers like colorectal carcinomas [71], breast carcinomas [72], testicular germ cell tumors [21], lung cancer [73], ovarian carcinomas [74] and pancreatic cancer [75]. Full-length human cripto-1 is expressed in several human cell lines such as embryonal and colon carcinoma cells [76]. Human cripto-1 is found to be secreted to cytoplasm in uveal melanomas [77]. Human naso-pharyngeal carcinoma, NPC series (C666-1, CNE-1, CNE-2, HNE-1, SUNE-1, and HONE-1) is

also reported to express human cripto-1 and overexpression is connected with the tumorigenesis and progression of NPC [78].

Overexpression of CR-1 has significant correlation with decreased survival rate in breast cancer patients. Overexpression of CR-1 was more often found in high grade tumors and poor prognosis tumors compared to low grade and good prognosis breast cancers [79]. Gastric cancer patients with higher expression of CR-1 also shows worst patient survival rate and has negative correlation with the expression of E-Cadherin indicating metastatic state [80]. Tysnes *et al.* [81] have observed varied level of expression of CR-1 in glioblastoma biopsy samples and have shown that higher expression of CR-1 has association with reduced postoperative survival in young patients. Pilgaard *et al.* [82] have also made similar observation and had shown that high level of CR-1 in blood of glioblastoma patients had significant correlation with shorter survival.

2.4: Control of Cripto-1 expression:

CR-1 is an embryonic gene that is overexpressed in several cancers. Expression of molecules involved in embryonic development is spatially and temporally regulated through multiple layers of transcriptional control. Aberrations in such controls, in adults, are often associated with development and progression of cancer. Expression of CR-1 is also controlled through multiple pathways. NANOG and OCT4 are two core transcription factors of Human ES cells [83] and are overexpressed in cancer stem cells [84]. Watanabe *et al.* [85] have identified binding site for NANOG and OCT4 in the proximal region of Transcription Start Site (TSS) of CR-1 promoter and have shown that these transcription factors directly regulates the expression of CR-1 in embryonic carcinoma (EC) cells, NTERA2/D1. Watanabe *et al.* [85] have also separated out CR-1 high subpopulations of NTERA2/D1 cells and observed the higher expression of NANOG and OCT4 in CR-1 high cells, indicating suitable relation between these molecules.

CR-1 promoter has conserved sequence of Hypoxia Responsive Elements (HREs). Hypoxia-inducible factor-1α (HIF-1α), binds to the HREs of CR-1 promoter and up regulates CR-1 expression in mouse mES and human NCCIT cells [86]. Canonical Wnt pathway regulates the expression of CR-1. It has been shown that CR-1 has three tandem TCF/LEF binding sites. Wnt pathway activates TCF/LEF and TCF/LEF upregulates the expression of short form of CR-1 [87]. A nuclear receptor, liver receptor homolog 1 (LRH-1) known to be expressed in undifferentiated ES cells, maintains expression of CR-1 in embryonic carcinoma cells, NTERA2/D1 [88]. On the other hand, during retinoic acid induced differentiation, another nuclear receptor called germ cell

nuclear factor (GCNF) binds to the DR0 motifs (repeat sequence of AGGTCA) of CR-1 promoter and represses the expression of CR-1 in human teratocarcinoma cell line, NTERA2 [88, 89].

TGF-β signaling controls plethora of cellular responses. TGF-β1 is a member of TGF-β superfamily and binds to two different serine/threonine kinase receptors, TβRI and TβRII. Upon binding to its receptors, TGF-β induces intracellular phosphorylation of SMAD2/3. Phosphorylated SMAD2/3 form complexes with SMAD4 and translocates to the nucleus, where they regulates the expression of target genes [48, 90]. Mancino *et al.* [76] have identified three SMAD Binding Elements (SBEs) in the CR-1 promoter. Treatments with TGF-β activates SMAD2/3 pathway in NTERA-2 and LS174-T cells. Activated SMAD complex binds to SBEs of CR-1 promoter and up-regulates CR-1 expression in these cells. Mancino *et al.* [76] have further shown that Bone Morphogenic Protein (BMP-4), another member of TGF-β superfamily, has the opposite effect. Treatment with BMP-4, induce phosphorylation of SMAD1/5/7 and down regulate the CR-1 expression in these cells. The schematic representation of various controls of CR-1 expression is shown in Figure 2.4.

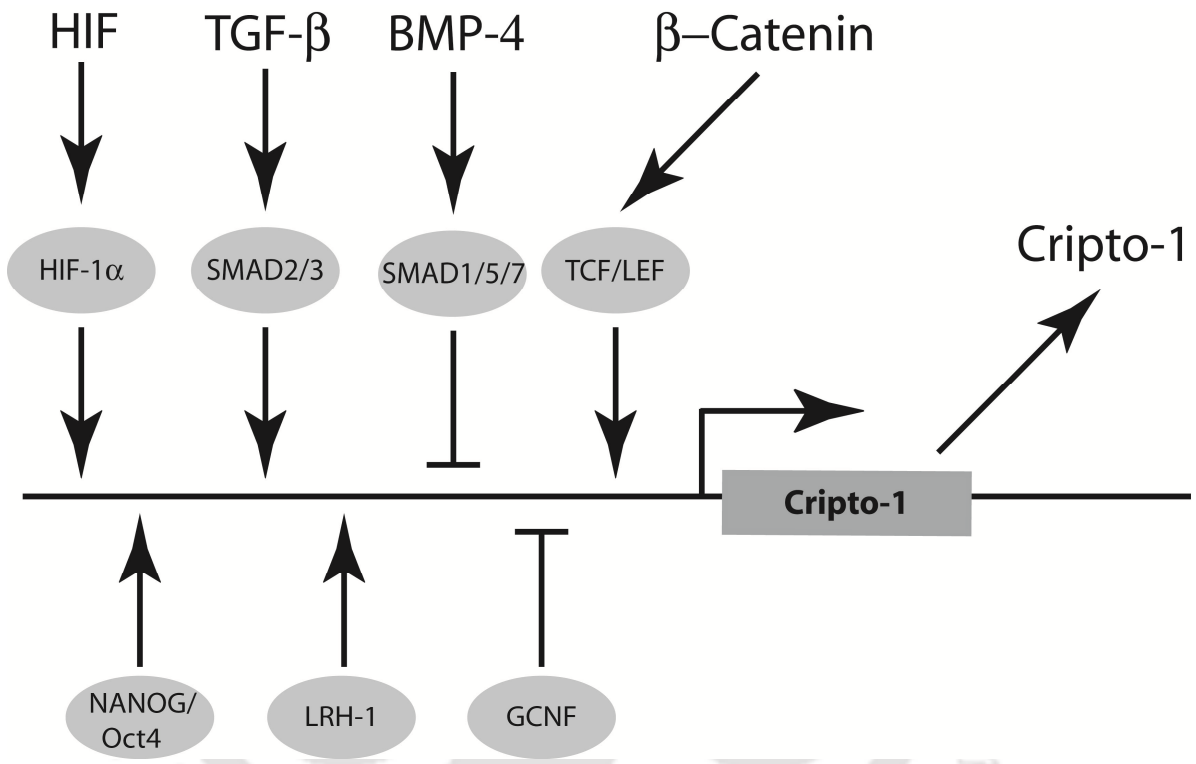

Figure 2.4: Control of expression of Cripto-1. Different molecular pathways and transcription factors that are known to control CR-1 expression are shown here.

2.5: Heterogeneity in gene expression:

Techniques like, RT-PCR, Western Blot, are conventionally used to detect changes in gene expression. These techniques use RNA or protein, isolated from an ensemble of cells to estimate level of gene expression. However, cellular processes are noisy (or have fluctuations). In absence of any noise, in a population of isogenic cells of same type, all cells should have same number of a particular protein (Figure 2.5a). However, in reality such cells never have same amount of the same protein. Rather such ensemble of cells exhibit considerable cell-to-cell variation in the levels of any specific protein [91-93] and amount of a protein per cell in a population often follows certain distributions, like gamma, and log-normal distributions [94-96] (Figure 2.5b). Such variability arises for multiple reasons, including unequal distribution of protein during cell division, and stochastic nature of gene expression [97]. Cell-to-cell variability in protein level plays crucial role in various biological processes like embryonic development, development of drug resistance, and progression of cancer [97, 98].

Elowitz *et al.* [91] proposed that the variability in protein level, in an ensemble of cells, originates from two sources: extrinsic and intrinsic noise. The first one originates from the heterogeneity in cell size, stage of cell cycle, and abundance of protein expression machinery. On the other hand, intrinsic noise originates from the stochastic nature of the biochemical processes involved in transcription and translation [97]. Expression of a protein in a single cell involves molecules in low number. For example, transcription of a gene involves interactions of few copies of transcription factors with one or two promoter regions. At such low abundance of molecules, chemical reactions do not follow deterministic Law of Mass Action. Rather in this regime, biochemical processes are stochastic [99]. Such stochasticity is involved in all processes linked with protein turnover.

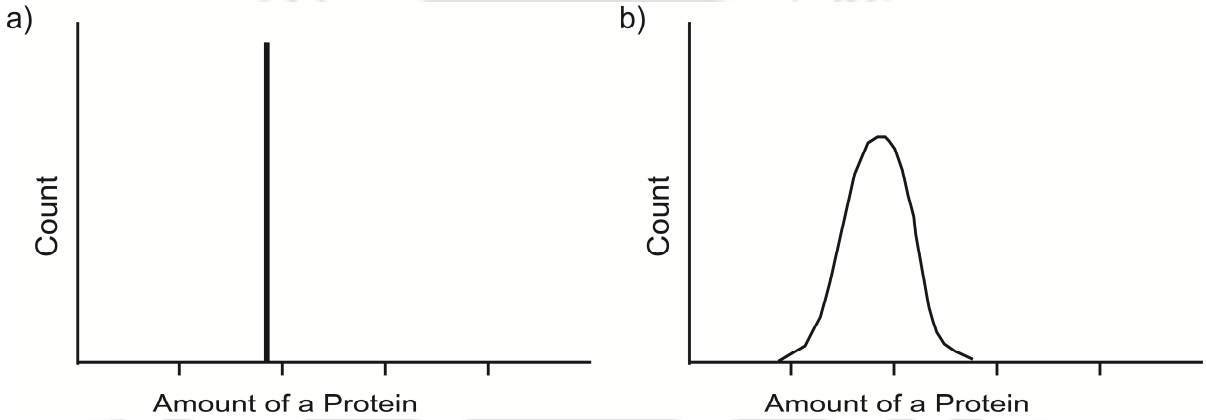

Figure 2.5: Noise or variability in protein distribution in a population of isogenic cells of same type. a) Histogram of distribution of a protein in absence of any noise. b) Histogram of distribution of the same protein in presence of noise.

Extensive theoretical and experimental works have been done to understand the stochastic nature of gene expression. One important component of stochastic gene expression is transcriptional bursting, where large number of mRNA is produced in successive random burst with intervening periods of no activity. McAdams and Arkin [100] first proposed stochastic burst in gene expression. Subsequently, such bursts were experimentally confirmed by various research groups [101-103]. It is now established that stochastic transition of the promoter between inactive (or OFF) state to active (or ON) state is responsible for such bursts [97]. Dynamic local structure of the chromatin, and binding-unbinding of transcription factors affect such ON-OFF transitions [101]. Other factors that affect fluctuation in gene expression are rate of transcription, translational efficiency and rate of protein degradation [97]. Translational efficiency is a measure of number of proteins produced per mRNA and depends upon relative rates of translation and mRNA degradation. The stochastic nature of gene expression is explained in Figure 2.6.

The cell-to-cell variability or noise in gene expression is usually measured in terms of coefficient of variation (CV = standard deviation/mean = σ/μ) [97]. Another measure is noise strength or Fano factor, which is the ratio of variance to mean ($F = \sigma^2/\mu$) [97]. For a Poisson process, variance is equal to mean. Therefore, if the variability in protein arises out of a Poisson process, noise would be equal to $1/\sqrt{\mu}$ and noise strength would be equal to one. In such a case, the noise decreases with increase in expression of the protein. Such inverse relation between noise and level of expression has been observed in several systems [92, 104, 105]. However, protein expression is not a pure Poisson process and the distribution of protein usually does not follow Poisson distribution. Several theoretical [94, 106] and experimental studies [93, 107] have shown that cell-to-cell variability in protein expression is well represented by Gamma distribution. In such systems, mean abundance of protein (μ) is directly proportional to standard deviation (σ) of cell-to-cell variation in protein level, as long as burst timing remains unchanged [108]. Burst timing depends on promoter transition rate and half-life of protein. In this situation, noise (σ/μ) remains constant. Therefore, if protein expression is induced through increase in rate of transcription, mean level of protein (μ) would increase without any change in noise (σ/μ).

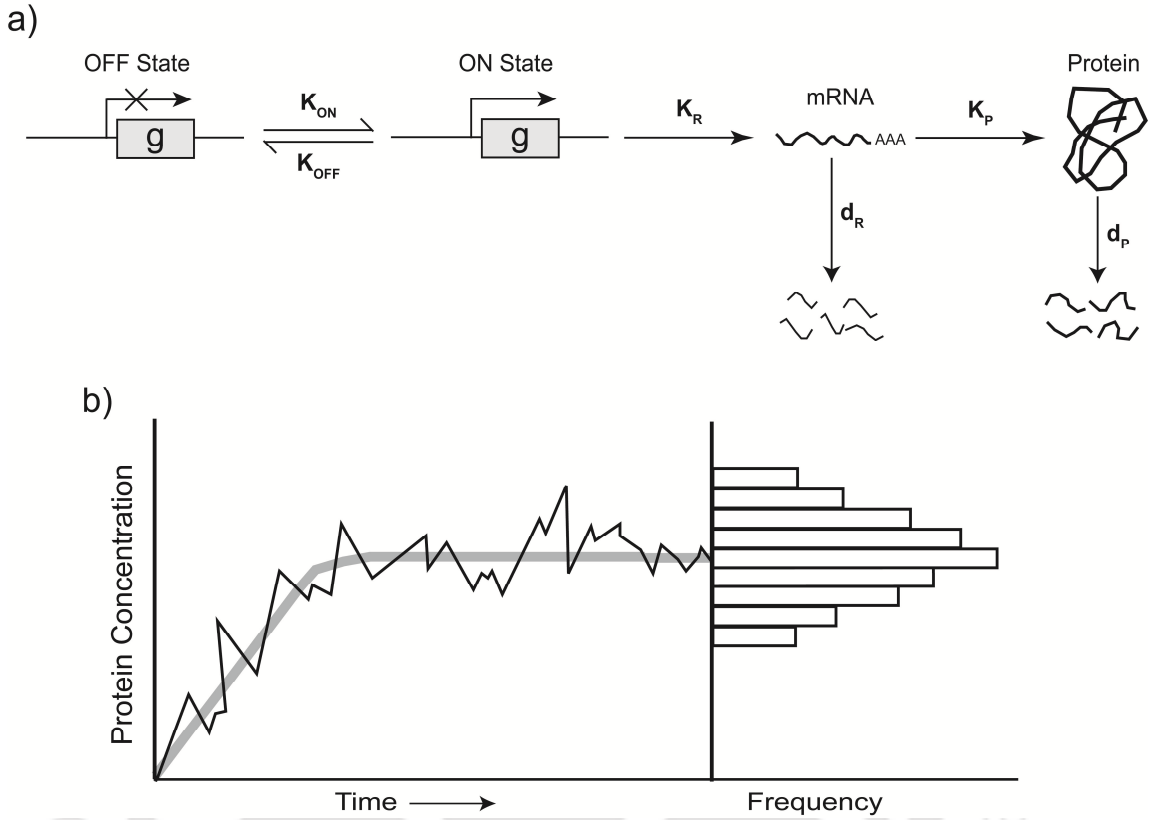

Figure 2.6: Stochasticity in gene expression. a) A simplified model of expression of a protein. The promoter transits reversibly between ON and OFF states. Transcription happens only when the promoter is in ON state. Other processes involved are translation, degradation of mRNA and the protein. Macroscopic rate constants for each step are shown. Each step is stochastic in nature and probabilities associated with each step can be calculated from the macroscopic rate consonants. b) Shows the effect of stochasticity in gene expression following the model shown above. For a deterministic system following the Law of Mass Action, concentration of the protein would increase with time and reach a steady-state value (as shown by the gray line). Similar observation would be made if protein expression is measured in a pool of large number of cells. However, due to stochasticity, amount of the protein in a single cell will fluctuate with time (shown by black line). Such fluctuation would give rise to cell-to-cell variability as shown in the associated histogram.

Experimental techniques to investigate heterogeneity in gene expression:

Estimating the noise in protein expression requires experiments with single cell resolution. Most of the experimental studies used fluorescent proteins or protein fused to fluorescent proteins as reporters. Subsequently epi-fluorescence microscopy [91, 93] or flow cytometry [109, 110] was used to measure cell-to-cell variability in protein abundance. Elowitz *et al.* [91] used two different fluorescence protein under the control of same promoter to measure intrinsic and extrinsic noise in gene expression in *E. coli*. Ozbudak *et al.* [109] systematically mutated the promoter and ribosome binding site (RBS) upstream to a fluorescent reporter gene in *Bacillus subtilis* and used flow cytometry to investigate the role of rate of transcription and translation in the noise in gene expression. Newman *et al.* [92] used large scale tagging to create a very large library of GFP-tagged proteins in yeast and subsequently, used flow cytometry to measure noise in protein expression across the whole proteome.

Conventional flow cytometry using protein specific fluorescent-tagged antibodies have also been used to investigate cellular heterogeneity in gene expression. Gupta *et al.* [111] used FACS to estimate heterogeneity in expression of certain stemness markers in breast cancer cells and isolated different subpopulations based on expression of these markers. Subsequently, they have showed that heterogeneity in gene expression is dynamic and cells stochastically transit between different phenotypic states. Mariani *et al.* [112] used flow cytometry to detect cytoplasmic IL-4 in T-helper cells. They observed that upon antigenic stimulation, only a fraction of cells expressed IL-4, resulting in a bimodal distribution of IL-4-producing and non-producing cells. They have used a stochastic model of gene expression to understand this phenomenon.

Quantitative single cell PCR has also been used to estimate cell-to-cell variability in gene expression. Bengtsson *et al.* [113] used single cell PCR and showed that transcript levels of the different genes are lognormally distributed in cells from the pancreatic islets of Langerhans. They also observed that variability in expression of two functionally related genes was highly correlated. Very recently, Narsinh *et al.* [114] used single-cell PCR to investigate heterogeneity in expression of key pluripotency associated molecules in human embryonic stem cells (hESCs) and in human induced pluripotent stem cells (hiPSCs). They observed that hiPSCs are considerably more heterogeneous at transcript expression levels in comparison to hESCs. Shalek *et al.* [115] used single-cell RNA sequencing for transcriptome analysis at single cell level in mouse bone-marrow-derived dendritic cells (BMDCs) stimulated with lipopolysaccharide. Interestingly, they

observed that large numbers of key immune-response related genes showed bimodal distribution of expression, with one subpopulation having lower expression than another subpopulation. Their observation proved that all cells in a population do not respond uniformly to the same stimulant.

The very stochastic nature of gene expression has been investigated using some innovative single cell experiments [101, 116]. Cai *et al.* [95] used a microfluidic based real-time monitoring system to measure expression of β-galactosidase in *E. coli* with single molecule sensitivity. Using this experimental system, they confirmed that protein expression happens in stochastic bursts and they were able to measure the frequency and size of such bursts. They observed that number of β-galactosidase produced per burst followed an exponential distribution. Similar stochastic burst in protein expression was documented and analyzed by Yu *et al.* [103] using a live-cell imaging system, where membrane localized fast-maturing yellow fluorescent protein was detected with single molecule sensitivity in *E. coli*. Raj *et al.* [101] used a very sensitive FISH based protocol to count individual mRNA molecules of a reporter gene in mammalian cells. They observed that the mRNA are synthesized in short stochastic bursts that originates from the stochastic transition of the promoter between active and inactive states. Golding *et al.* [102] have documented similar stochastic burst in transcription in *E. coli* using a very innovative technique. They engineered the target gene to transcribe an mRNA containing large number of copies of a specific RNA hairpin in its untranslated region. Each of these hairpins binds tightly to the coat protein of the bacteriophage MS2 fused to GFP expressed in the same cells. As multiple MS2-GFP proteins bind to an individual mRNA, enough spatially resolved fluorescence signal is generated that enables detection of each of the mRNA by live-cell fluorescence microscopy.

2.7: Transcriptional circuits affect cellular heterogeneity in gene expression:

Transcriptions of most of the genes are tightly controlled through specific molecular circuit involving multiple molecules. By a circuit, we mean a small network involving multiple molecules transferring information. Such circuits involve transcription factors, signal transduction molecules, receptors and their corresponding lignads. These circuits allow temporal and spatial control of gene expression based on specific signal. Very often, such circuits have non-linear components like feedbacks and feed-forwards [117]. The structure of the transcriptional circuit affects the dynamics of expression of the target gene [117, 118]. Eventually that also affect the heterogeneity in expression of a gene in an ensemble of cells [97, 119].

Effect of circuit architecture on cellular heterogeneity in gene expression has been extensively studied using synthetic genetic circuits. Becskei *et al*. [120] used tetracycline repressor (TetR) based synthetic circuits to show that autoregulation through negative feedback reduces cell-to-cell variability in expression of a reporter gene. Several theoretical [121] and experimental [122, 123] works have established that negative feedback can reduce noise in gene expression. This may explain the abundance of negative feedback in transcriptional circuits [124].

On the other hand, a positive feedback can amplify noise in gene expression [119]. Most of the inducible transcriptional systems show sigmoidal dose-response relation [125]. Such non-linear behavior is believed to arise out of the cooperativity in transcription factors and can give a switch like behavior. This non-linearity makes the system ultra-sensitive, where slight change in input can cause a drastic change in output [126]. In such a system, existence of a positive feedback can lead to bistability, where the system has two stable steady states [127]. Bistability allows a cell to be at one of the two stable steady states. For a transcriptional circuit with bistability, one stable steady-state, corresponds approximately to the basal or lower expression state, while the upper one reflects the higher expression state. At population level, this leads to a bimodal distribution, with two subpopulations cells having low and high expression of the target gene [120]. In absence of any induction the probability of being at the lower expression state would be higher and most of the cells will be in this state. However, any induction would increase the probability of transition to higher expression state and more and more cells will move to that state. Figure 2.7 explains the concept of bimodality that originates from positive feedback in transcriptional control.

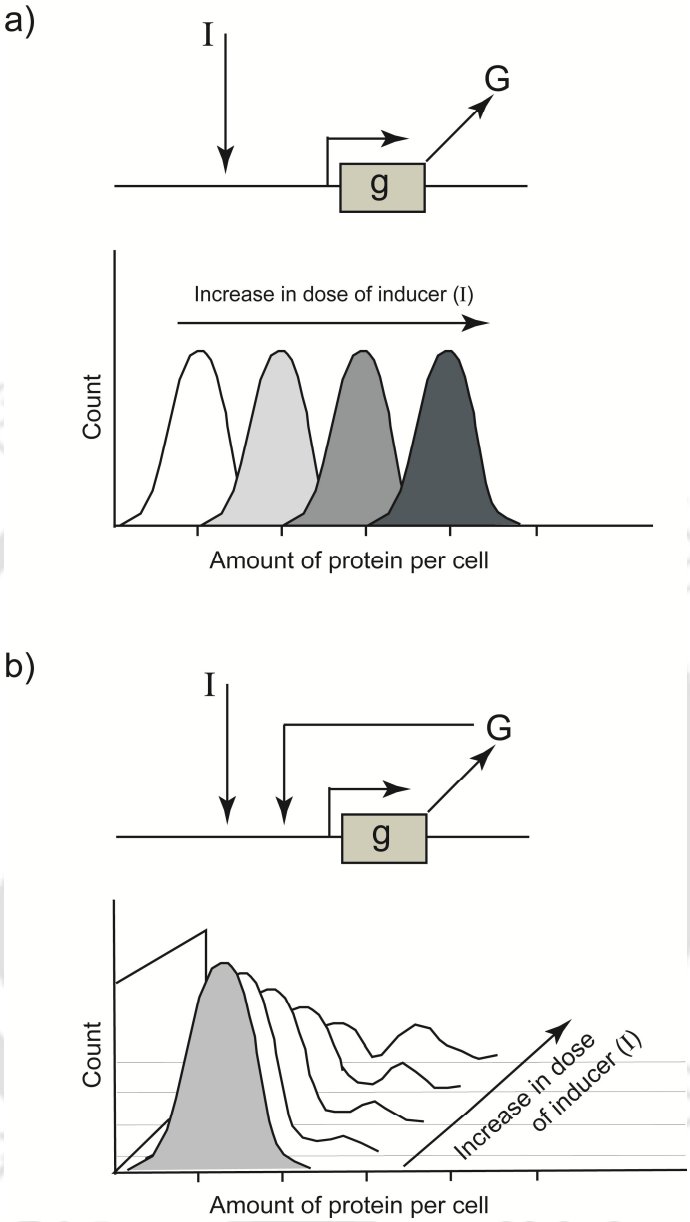

Figure 2.7: Positive feedback can give rise to bimodal gene expression. a) In a simple inducible system, increase in the dose of the inducer increases mean expression of the target gene. This shifts the population histogram for the expressed protein to the right side. However, the histogram remains unimodal. b) A positive feed-back can give rise to bimodal distribution. In absence of any inducer cells remain at lower expression level (gray unimodal histogram). With increase in induction, more and more cells transits to higher expression level, giving rise to two subpopulations.

Becskei *et al.* [120] used tetracycline-responsive transactivator based positive feedback system in yeast to show that positive feedback in transcription leads to bimodal cell population. System with positive feedback can show hysteresis, where the state of the cell would depend upon its past. May *et al.* [128] used a synthetic transcriptional circuit with positive feedback in a mammalian system to show that bistability can give rise to bimodal distribution and hysteresis. Similar observations have been made for several other synthetic positive feedback circuits [129, 130]. Bimodal gene expression in several natural cellular systems has been found to originate from positive feedbacks in the transcriptional circuit [131-133].

2.8: Importance of heterogeneity in gene expression:

Most of the molecular biology techniques obscure the heterogeneity in gene expression in clonally identical cells. Such heterogeneity in gene expression is also not adequately explored and appreciated in biological literatures. However, cell-to-cell variability in gene expression plays critical role in normal physiological process as well as in diseases.

Stochasticity in gene expression and associated cell-to-cell variability in gene expression can help a unicellular organism to survive through certain environmental conditions [134, 135]. Such heterogeneity would allow a population of cells to have multiple phenotypes without any genetic change. Some of those phenotypes may help the organism to ride through a particular stress. Acar *et al.* [136] engineered yeast to create a strain that transits faster between two phenotypes because of stochastic gene expression. They observed that strains that switch faster between different phenotypes survive better through rapidly fluctuating environment. Microbial persistence is a well-known phenomenon, where a small subpopulation exists that do not grow or grow very slowly in comparison to other isogenic cells and have drug resistance. Cells transit stochastically between persistent and non-persistent states. Sureka *et al.* [137] have shown that in *M. tuberculosis* such transition involves transcriptional positive feedback that leads to bimodal gene expression.

During embryonic development, clonally identical cells diverge and give rise to different cells types. Morphogen gradient and lateral inhibition, are well known molecular mechanisms that drive such diversification. Lateral inhibition requires stochastic fluctuation in expression of participating molecules to give rise to cellular patterns [138]. It has been observed that many key molecules that determine cell fate have heterogeneity in expression in embryonic cells and such variability correlates with differential fate of cells during development [139-141]. Nanog is key

molecule for maintenance of stem cell pluripotency. It has been shown that cultured mouse embryonic stem cells have heterogeneous expression of Nanog and differential expression of Nanog correlates with different phenotypic behaviors [142]. Raj *et al.* [143] have shown that incomplete penetrance of a mutation, in a gene related to development of *C. elegans*, originates from the increase in gene expression heterogeneity. Such increase was found to be the consequence of changes in transcriptional network caused by the mutation. In general it is now accepted that non-genetic heterogeneity originating from stochastic processes, including stochastic gene expression, plays crucial role in development of a multicellular organism from zygote along the Waddington's metaphoric 'epigenetic landscape' [98].

Heterogeneity is a hallmark of cancer cells. Cells in a tumor show extensive genetic heterogeneity [144]. Even genetically identical cancer cells shows cell-cell-variability in gene expression. Such heterogeneity can often lead to different phenotype, like higher tumorigenicity. Using a breast cancer cell line, Gupta *et al.* [111] have shown that a population of these cells had subpopulations of differing phenotype. Such subpopulations arise due to heterogeneity in gene expression and cells stochastically transit between different phenotypic states, thereby marinating a dynamic equilibrium. Roesch *et al.* [145] have shown that H3K4 demethylase JARID1B has heterogeneous expression in melanoma cells, with most of cells having very low or no expression of it. It was observed that cells that express JARID1B are more competent to sustain tumor growth. They separated the high-expressing subpopulation and have shown that these cells dynamically give rise to the heterogeneous population. Watanabe *et al.* [85] have observed that cultured human embryonal carcinoma cells have two subpopulations: one with high Cripto-1 expression and the other with low expression of Cripto-1. They further observed that cells having higher expression of CR-1 were more tumorigenic and have higher expression of some markers of pluripotent stem cells. The growth and progression of many cancers is believed to be driven by a small subpopulation of cancer stem cells that have the capability to self-renew and differentiate [146]. It has been shown that spontaneous noise driven heterogeneity in gene expression can dynamically transit cancer cells between stem cell phenotype and non-stem cell phenotype [147]. Even drug resistant phenotype can also emerge spontaneously through noise in gene expression [148]. Therefore it is now believed that apart from accumulation of oncogenic mutations, non-genetic heterogeneity in gene expression also plays significant role in development and progression of cancer [149]

3 Materials & Methods

Details of the common reagents used in this work along with their sources are given in appendix. List of buffers and solutions with compositions are given in Table A1 in the appendix.

3.1: Bacterial cell culture:

E. Coli strain and clones were stored in -70 ^{o}C as glycerol stock (15% glycerol) and were cultured in 2XTY media with suitable antibiotics. Media and other reagents used for bacterial culture, bacterial strains, and plasmids used are given in Table A2, Table A3 and Table A4 respectively in the appendix.

3.2: Treatment conditions and Growth factors:

In all experiments, U-87 MG cells were treated with various recombinant proteins in absence of serum unless otherwise it is mentioned. GST-tagged C-terminal truncated human CR-1 (CR1-GST; corresponding to 1st– 169th amino acid) was expressed in a bacterial system and purified, as reported earlier [24]. Recombinant GST was expressed and purified using similar expression system. Details of expression and purification methods are explained in this Chapter. Human recombinant CR-1 (corresponding to 31st– 172th amino acid) expressed in an insect expression system was purchased from R&D Systems. C-terminal truncated CR-1 (corresponding to 1st– 169th amino acid) was cloned in pCI-neo vector. This recombinant construct was used to overexpress CR-1 in soluble form, in stably transfected MCF-7 cells and conditioned media of these cells was used for experiments. Detail methods of transfection and generation of stably transfected clone are explained in this Chapter. Recombinant human TGF-β-1 was purchased from Gibco and used at 1 ng/ml as working concentration.

3.3: Expressions of GST tag CR-1(CR1-GST) in *E. Coli* Rosetta-gami-2 (DE3):

C-terminal truncated human Cripto-1 (corresponding to 1-169 amino acids) was cloned in pGE-4T2 expression vector (pGE-CR1-ΔC) as described by Das *et al.* [24]. *E.Coli* strain Rosetta Gami-2 (DE3), carrying the recombinant pGEX-CR-1-ΔC construct or pGEX-4T-2 only, was

inoculated in 5 ml 2xTY medium containing, ampicillin (50 µg/ml), chloramphenicol (25 µg/ml), tetracycline (12.5 µg/ml) and 1% glucose. Incubation was performed at 30° C overnight with shaking at 180 rpm. 1 ml of the overnight culture was sub-cultured to 100 ml 2xTY containing same concentration of ampicillin and chloramphenicol and incubated at the above condition till OD_{600} reached ~ 0.6. Expression of recombinant protein was induced by IPTG (0.5 mM) for 4 hrs in the same condition. Cells were harvested by centrifugation at 8,000 rpm for 10 min at 4°C and the pellet resuspended in ice cold PBS containing 1 mM EDTA. The resuspended cells were lysed with mechanical cell disruptor (Constant Systems, UK) at 18 kpsi. Immediately after disruption, PMSF (1 mM) was added to the cell lysate. The insoluble protein fraction was solubilized by adding 1% Triton-X-100 to the whole lysate and incubated on ice for 45 min with shaking at regular intervals. Cell lysate was clarified by centrifuging at 8,000 rpm for 10 min at 4°C. The supernatant was collected and stored at -20°C.

3.4: Purification of GST-tag CR-1(CR1-GST):

The clarified cell lysate containing recombinant fusion protein or GST only, was purified using Glutathione-Agarose beads (Sigma) as per manufacturer's protocol. The clarified cell lysate was passed through a 0.45 µm syringe filter (Millipore) and added to Glutathione-Agarose beads in a column and kept in shaking condition for 45 min. The flow through was drained out and the beads along with bound CR1-GST was washed with 5 volume of PBST (0.1% Tween20) and 2 volume of PBS. The bound protein was eluted by using 20 mM GSH in 50 mM Tris-HCl, pH 9.5. Purified protein was dialyzed against PBS for 8 hr at 4°C to remove residual GSH. Concentration of the recombinant protein was estimated by Bradford assay and purified protein was stored at -20°C.

3.5: Plasmid isolation:

Plasmid DNA was isolated from overnight cultures, 2xTY using Axyprep Plasmid Miniprep Kit (Axygen Biosciences) according to manufacturer's protocol. Isolated plasmids were stored in -20 °C for the subsequent use.

3.6: Mammalian cell culture:

Human glioblastoma cell line U-87 MG & U-373 MG, human cervical adenocarcinoma cell line HeLa, human liver hepatocellular carcinoma cell line HepG2, human colon adenocarcinoma cell line HT29 and human embryonic kidney cell line HEK were procured from National Center for Cell Science (NCCS), Pune, India. All the cells were maintained in DMEM (Gibco), with 10% Fetal Bovine Serum (PAA) and 1X antibiotic-antimycotic (Gibco) at 37^{o}C in a humidified atmosphere of 5% CO_2.

Sub-culturing of cells was carried out by trypsinization once the cells reached 80-90% confluences. The old saturated media was removed and the monolayer culture was washed with sterile PBS. After washing, appropriate volume of trypsin-EDTA was added and was kept at 37^{o}C for few minutes. Trypsin was deactivated by adding cell culture serum media (10% FBS) and was removed by centrifugation. The cell pellet was again resuspended in fresh media and approximately 30% of the cells were transferred to fresh culture flask and incubated in the above conditions. Medium was replenished at an interval of 3 days regularly. All the reagents and medium used for cell culture are given in Table A5 in the appendix.

3.7: Protein extraction from mammalian cells:

Total protein from mammalian cells was isolated by using RIPA (Radioimmunoprecipitation assay) buffer. Media was discarded from culture flask and residual media was removed by washing cells with ice cold PBS. RIPA buffer containing the protease inhibitor PMSF (1 mM), phosphatase inhibitor sodium fluride (50 mM) and sodium orthovanadate (1 mM) was added to cell and incubated for 5 min on ice. After 5 min, cells were scrapped out using cell scrapper and collected in an eppendorf tube. Cell lysate was sonicated at amplitude of 25 for 10 seconds and was clarified by centrifugation at 10,000 rpm for 10 min at 4^{o}C. The supernatant was collected and mixed with appropriate amount of SDS-PAGE sample loading buffer, boiled for 3 min at 100^{o}C and stored at -80^{o}C. Protein concentration was estimated by Lowry's method.

3.8: RNA isolation from mammalian cells:

Total RNA was isolated from mammalian cells by using TRI reagent (Sigma) as per manufacturer's protocol. All the materials used for RNA isolation were treated with 1% DEPC

for 2 hr at 37 ^{o}C and subsequently, DEPC was removed by autoclaving. 1 ml of TRI reagent was added to approximately 10^6 monolayer cells, cultured in 25 cm^2 culture flasks and lysate was transferred to eppendorf tube just after detachment. Lysate was passed through syringe for several times for proper homogenization and was allowed to stand for 5-15 min to ensure complete dissociation of nucleoprotein complex. Thereafter, 0.2 ml of chloroform per 1 ml TRI reagent was added to the homogenous cell lysate and mixed properly by vigorous shaking. The mixture was allowed to stand for 10 min at room temperature and centrifuged at 12,000 rpm for 15 min at 4 ^{o}C. The aqueous phase having RNA was transferred to a fresh eppendorf and 0.5 ml of isopropanol per 1 ml of RNA was added to precipitate the RNA. The precipitation was done for 10 min at room temperature with occasional mixing by inverting the tube. Thereafter, the RNA was pellet down by centrifuging at 12,000 rpm for 10 min at 4^{o}C. The supernatant was removed properly and the pellet was washed with chilled 75% ethanol and re-centrifuged at 12,000 rpm for 10 min at 4^{o}C. The ethanol was removed and the pellet was air dried and dissolved in suitable amount of water and stored at -20^{o}C for regular use. For long term storage, pellet was kept in 75% ethanol and stored at -80 ^{o}C.

3.9: Removal of Genomic DNA contamination from RNA:

Contaminated genomic DNA from isolated RNA samples was removed by treating with RNase free DNase (Promega) as per manufacturer's protocol with little modifications. The composition of reaction mixture was as follows:

RNA	5 µg
RNase free DNase Buffer (10X)	5 µl
RNase free DNase (1,000 U/ml)	5 µl
Nuclease free water to final volume	50 µl

The reaction mixture was incubated at 37 ^{o}C for 45 min, followed by re-extraction of RNA from the mixture by TRI-reagent following the same protocol as described earlier. DNase free RNA samples were dissolved in desired volume of nuclease free water and subsequently used for cDNA synthesis and stored at -20 ^{o}C for regular use. For long term storage, RNA samples were kept in 75% alcohol and stored in -80 ^{o}C.

3.10: Reverse transcription for cDNA synthesis:

cDNA was prepared with 1 µg of total RNA using H Minus Reverse Transcriptase (RT) (Thermo Scientific) and Random Hexamer (Fermantus) as primer. Total volume of 20 µl reaction mixture was prepared and reverse transcribed as per the protocol mentioned below:

The RNA mixture was prepared as:

RNA	1 µg
Random Hexamer (100 pmol/µl)	1 µl
Nuclease free water to final volume	10 µl

The RNA mixture was heated at 65 ^{o}C for 5 min to break secondary structures and was snap frozen on ice. To heat treated RNA mixture, 10 µl of reaction mix was added and mixed properly, subsequently incubated at 25 ^{o}C for 10 min followed by 42 ^{o}C for 60 min and was snap frozen on ice. The reaction mix was prepared as:

5X Reaction Buffer	4.00 µl
dNTP mix (10 mM each) (1mM final concentration)	2.00 µl
H Minus Reverse Transcriptase (200 U/µl)	1.00 µl
Nuclease Free water	3.00 µl

Final cDNA product was checked by PCR using suitable housekeeping gene and stored at -20 ^{o}C for regular use and stored at -80 ^{o}C for long term use.

3.11: Quantification of DNA and RNA:

Amount of RNA and DNA samples were measured by using NanoVue (GE Healthcare life Sciences). 1 µl of sample was used to measure the absorbance of RNA and DNA at 260 nm. Concentration of RNA and DNA were calculated by considering the factors as 1 O.D. at 260 nm

is equal to 40 µg/ml of RNA and 50 µg/ml is equal to double stranded DNA. Concentration was calculated as:

$$\text{Concentration} = A_{260} \text{ X Factor}$$

The ratio of absorbance at 260 nm and 280 nm is used to assess the purity of DNA and RNA. A ratio of ≥1.7 is generally accepted as 'pure' for DNA, whereas a ratio of ≥2.0 is generally accepted as 'pure' for RNA. If the ratio is appreciably lower in either case, it may indicate the presence of protein, phenol or other contaminants that absorb strongly at or near 280 nm.

3.12: Semi-quantitative Reverse Transcriptase–Polymerase Chain Reaction (RT-PCR):

Readymade master mix (Bioline) was used for RT-PCR. Final amount of 50 ng of RNA equivalent cDNA was used as a template and 200 nM of final primer concentration was used in 20 µl of reaction mix. The composition of reaction mix was as:

BioMix Red (2X)	10 µl
Forward primer (4 µM)	1 µl
Reverse primer (4 µM)	1 µl
DNA template	1 µl
Nuclease free water to final volume	20 µl

PCR amplification was performed in Palm-Cycler thermal cycler (Genetix Biotech Asia Pvt. Ltd., India). The Cycle number and PCR conditions were standardized for different primer sets and reactions were performed accordingly. Primer sequences used for different PCR reactions are given in the Table A6 in the appendix.

3.13: Agarose gel electrophoresis:

DNA samples and PCR products were resolved in agarose gel electrophoresis using agarose gel (0.5-1.5%), prepared in 1X TAE buffer. The gel was pre-stained in 0.5 µg/ml of Ethidium Bromide. Resolving was performed in 1X TAE running buffer at 80 V until the proper resolution

was achieved and was visualized in trans-illuminator. The image was captured in ChemiDoc imaging system (Biorad).

3.14: Quantitative real-time PCR (qPCR):

Expression of mRNA was quantified by real-time PCR (Applied Biosystem, 7500). SYBR Green (Power SYBR PCR Master Mix, Applied Biosystem) was used as a reporter dye. All the real-time PCR reactions were performed in a 25 µl of reaction mixture containing 12.5 µl of SYBR Green with 1 µL of cDNA (~50 ng of RNA equivalent) and 200 nM final concentration of each primer at 60^{o}C annealing and extension. The reaction mix was prepared as:

2X SYBR Green PCR Master Mix	12.5 µl
Forward primer (4 µM)	1.25 µl
Reverse primer (4 µM)	1.25 µl
cDNA (50 ng/µl)	1.00 µl
Nuclease free water	9.00 µl

All the primer sets used for real-time PCR are listed in Table A6 in the appendix. Non-specific amplification of each primer sets was checked by melting curve using Applied Biosystem real-time PCR system software. Melting curve profile of all the primers is shown in Figure A1 in the appendix. Cyclophilin was used as endogenous control for each reaction. Data from Applied Biosystem real-time PCR system software was extracted to excel sheet and PCR efficiency was calculated by using LinRegPCR software. Fold change in expression of target gene in comparison with endogenous control gene was calculated by ΔΔCt method as used in REST [150].

3.15: Sodium Dodecyl Sulfate polyacrelamide gel electrophoresis (SDS-PAGE):

SDS-PAGE was performed to analyze the expression of recombinant protein by western blot. Protein samples were separated and visualized by using SDS-PAGE following the method of Laemmli [151]. Required amount of protein samples or cell lysates was mixed with 4X SDS-PAGE gels loading buffer with reducing agent (2-mercaptoethanol) and heated in boiling water bath for 3 min. The denatured protein along with standard protein marker was stacked in 5%

stacking gel and was separated using 12% separating gel of thickness 0.75 mm. The electrophoresis was performed by using 1X SDS-PAGE running buffer at 120 V in a MiniVE vertical electrophoresis system (GE Healthcare). After completion of the electrophoresis, the gels were stained with the coomassie brilliant blue or silver staining method. The compositions of all the buffers used for SDS-PAGE was mentioned in Table A7 in appendix.

3.16: Protein estimation by Bradford assay:

The protein sample dissolved in PBS was estimated by Bradford assay using Bradford reagent (Sigma) as per the manufacturer protocol. BSA dissolved in PBS was used as standard and estimation was carried out in 96 well assay formats. Standards and protein samples were diluted to a final volume of 200 µl of PBS, was mixed with 200 µl Bradford Reagent and incubated at room temperature for 15 min. After incubation, 200 µl of the reaction mixture of each sample was transferred to the 96 well plates and the optical density was measured at 595 nm.

3.17: Protein estimation by Lowry's method:

The protein sample that was in RIPA buffer was estimated according to the Lowry's method. BSA dissolved in RIPA buffer was used as standard and estimation was carried out in 96 well assay formats. Diluted crude protein sample of 100 µl or standards was mixed with 500 µl of freshly prepared complex forming reagent (2% Na_2CO_3 in 0.1 N NaOH: 1.0% $CuSO_4.5H_2O$: 2% potassium sodium tartarate in a ratio of 100:1:1). The reaction mixture was mixed properly and incubated at room temperature for 10 min. Fresh Folin reagent diluted with distilled water (1:1) in a volume of 50 µl was added to the reaction mixture and vortexed for 5 s. This reaction mixture was incubated in the dark at room temperature for 30 min. After 30 min of incubation, 200 µl of the reaction mixture was transferred to 96 well plates and the optical density was measured at 660 nm.

3.18: Western blot:

Protein samples along with standard protein marker that were resolved in 12% SDS-PAGE were transferred to PVDF membrane (Millipore) for 4 hrs using semi-dry transfer blot apparatus (G.E. Healthcare) using Towbin buffer. Proper transfer of protein was confirmed by Ponceau S staining. Membrane was washed properly to remove Ponceau S with 0.1% of TBS-Tween20 (TBST)

buffer and thereafter, blocked with 3% BSA-TBST for 2 hrs at room temperature. After blocking, membrane was incubated with primary antibody in an appropriate dilution overnight at 4 ^{0}C. Next day, membrane was washed three times with TBST for 10 minutes, followed by incubation with HRP-conjugated secondary antibody for 2 hours at room temperature .Blot was developed using chemoluminescence (Super signal West Dura, Thermo Scientific) and imaged ChemiDoc imaging system (Biorad). Three separate experiments were done and average fold change has been calculated by densitometry analysis using ImageJ software. Details of reagent used for western blot and antibodies used for western blot are given in Table A8 and Table A9 in appendix respectively.

3.19: Inhibitors assays:

All the inhibitors are used 30 min prior to the treatment unless it is mentioned. Alk4 inhibitor (SB-431542), PI3K inhibitor (LY294002) and MEK inhibitor (U0126) are used in final concentration of 10 µM, 1.5 µM and 6 µM respectively. Sub-optimal dose of these inhibitors were determined by MTT assay. List of inhibitors used for various experiments are given in Table A10 in appendix.

3.20: MTT Assay:

To measure viability of cells in different experimental conditions, MTT assay was performed. MTT is a colorimetric assay that is based on the cleavage of tetrazolium salt 3-[4, 5-dimethylthiazol-2-yl]-2, 5-diphenyltetrazolium bromide or MTT to formazan by mitochondrial dehydrogenase in viable cells. Briefly, cells were seeded at 1 x 10^4 cells per well in 96 well plate and cultured for 24 hrs and subsequently, cells were treated as per experimental design. At specific time, 10 µl of MTT (5 mg/ml in PBS, Himedia) was added to each well and incubated for an additional 4 hrs at 37ºC in a 5% humidified incubator. The purple-blue MTT formazan precipitate was dissolved in 100 µl of MTT solvent (DMSO). The activity of mitochondria, reflecting cell growth and viability, was evaluated by measuring optical density at 570 nm and the background subtraction was done at 650 nm. Percentage of cell viability was estimated by dividing the measurements of treated cells by that of untreated cells.

Cell viability= Treated cells/Untreated cells X 100

3.21: mRNA stability assay:

Actinomycin-D (Act-D), a global transcription inhibitor used to study mRNA stability [152]. We have decided the sub-optimal concentration of Act-D by MTT assay, as it is a global transcription inhibitor and higher concentration may hinder the normal physiology of the cells. We have used a method similar to that reported by Hennes *et al.* [153]. U-87 MG cells were treated with CR1-GST (200 ng/ml) or equivalent amount of PBS. After 16 hr of treatment, cells were treated with 5 μg/ml of actinomycin D (Himedia) to block transcription and incubated for different time points (0, 3, 6 and 9 hr) in presence or absence of CR1-GST. Total RNA was isolated at these specific time points and subsequent to synthesis of cDNA, real-time PCR was used to measure CR-1 transcript as described earlier.

3.22: Transfection and generation of stably transfected clones:

All the transfections in this study were done by Electroporation using ElectroSquarePorator ECM 830 (BTX, Harvard Apparatus) electroporator. Mammalian cells were detached by trypsinization and washed with DMEM containing 10% FBS. Cells were again washed with DMEM containing 2.5% FBS (without antibiotic) and resuspended in a density of 1 X 10^7 cells/ml. 400 μl of cell suspensions and 20 μg of purified recombinant plasmid were mixed and kept at room temperature for 5 min. Electroporation was done at 140 volt for 70 ms. After electroporation, cells were resuspended in complete culture media (DMM/10% FBS/antibiotic) and seeded in six well plates. Cells were incubated in CO_2 incubator at 37 ^oC for another 48 hr. transfected cells were selected for stable transfectomas using G418 as selection marker. After 48 hr of transfection, culture media was aspirated off and cells were replenished with DMEM containing 10% FBS having G418 with final concentration of 800 μg/ml. Culture media was replenished after 72 hr intervals with fresh G418. About 9-12 days after transfection, majority of cells started dying and drug resistant clones formed distinct colonies. The drug resistant clones were maintained in DMEM/10% serum containing G418 with working concentration (400 μg/ml).

Full-length CR-1 cloned in pCI-neo vector [63] was transfected to MCF-7, to generate full length CR-1 overexpressing stable clone. However, the C-terminal end of CR-1 (170-188 amino acids residue) is essential for membrane anchorage by a glycosylphosphatidylinositol (GPI). So, to generate soluble CR-1, C-terminal truncated CR-1 (corresponding to 1^{st}– 169^{th} amino acid) was

amplified by PCR using the full-length CR-1 clone and was cloned in pCI-neo vector to generate pCI-CR1ΔC construct. Cloning primer sequence with restriction site is shown in Table A6 in appendix. pCI-CR1ΔC construct was transfected to MCF-7. Soluble CR1ΔC proteins were subsequently collected from serum free culture media.

3.23: Overton histogram subtraction:

Overton histogram subtraction [154] is a method to identify percentage of positive cells and is useful when the positive population is very close to the control. In this particular method, isotype control is subtracted from cells stained with desired antibody to measure positive percentage (Figure 3.1). We have used this method to measure percentage of CR-1 positive cells using FCS Express 4 (De Novo Software). Cells treated stained with mouse anti-human Cripto-1-PE were sample and cells stained with isotype control antibody were used as control. Here, isotype control cells were subtracted from CR1-GST treated cells and thereby, CR-1 positive population was estimated.

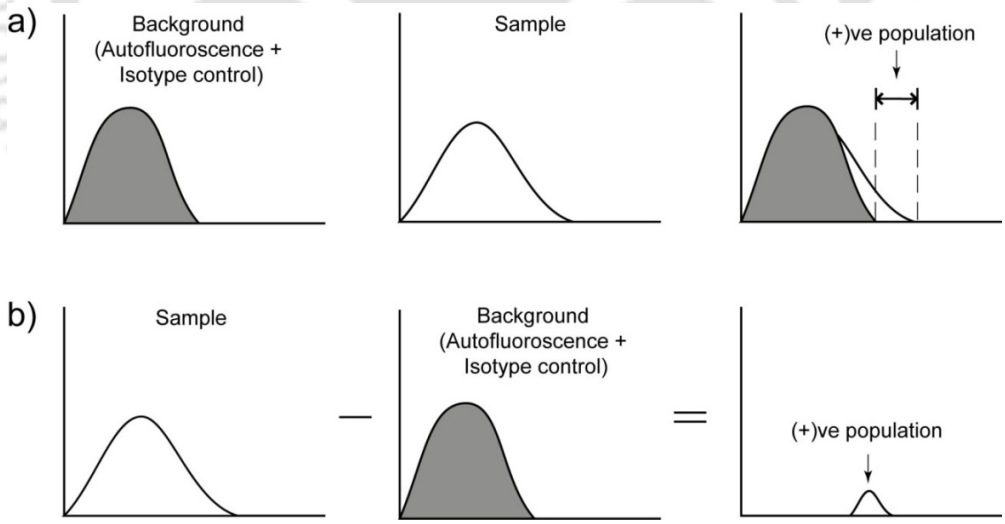

Figure 3.1: Histogram subtraction to identify positive population. a) Conventional gating in histogram to identify positive population. This method depends upon visual perception of individual. It is difficult to use for cases where sample reading is close to background reading. b) Histogram subtraction where bin-to-bin subtraction is used to calculate positive population. It is independent of analyzer's perception and more robust than any other methods.

3.24: Flow Cytometry experiments:

Cells were treated with different concentrations of CR1-GST for 24 hr in serum free condition. Treated cells were detached using enzyme free dissociation buffer (Invitrogen) and washed with FACS buffer (PBS with 0.1% BSA). Non-specific blocking was performed by incubating cells with blocking buffer (2% BSA in PBS) for 15 min at room temperature. Subsequently, 1 X 10^5 cells in 25 µl volume of FACS buffer were stained for cell surface CR-1 using mouse anti-human Cripto-1-PE (10 µl, R&D system) as per the manufacturer's protocol. Cell surface CR-1 was detected in FL2-H in log mode. Cells were further treated with maximum concentration of CR1-GST (400 ng/ml) and processed as mentioned above. Cells were dual stained for cell surface CR-1 and MDR1 using mouse anti-human Cripto-1-PE (R&D system) and mouse anti-human P Glycoprotein-FITC (2 µl, Abcam) respectively. As required, cells were also stained by corresponding isotype control antibodies. For dual stain, CR-1 and MDR1 were detected in FL2-H and FL1-H respectively, both in log mode. Single or double stained cells were analyzed in FACSCalibur flow cytometer (BD Biosciences) and data was collected using CellQuest Pro software (BD Biosciences). For each sample, data for 20,000 cells were collected. Data was analyzed using FCS Express 4 (De Novo Software). For analysis of CR-1 expression, data of each sample was gated first in FSC-SSC dot plot and then in the histogram for FL2-H to remove debris, and extreme data points. In general, more than 97% cells were retained after gating for further analysis. Arithmetic mean (µ), standard deviation (σ) and geometric mean (MFI) were calculated.

3.25: Cell sorting:

For cell sorting, U-87 MG cells were treated with maximum concentration of CR1-GST (400 ng/ml) for 24 hr and stained with mouse anti-human Cripto-1-PE mAb or Isotype control antibody as discussed above. CR-1-positive and CR-1-negative populations were sorted out using FACSAria III (BD Biosciences) equipped with BD FACSDiva 6.0 software. Immediately post sorting, total RNA was isolated using TRI reagent and gene expression was checked by RT-PCR.

3.26: Simulation of behavior of noise is a population of cells:

We have simulated a mixed population of cells. This population has two subpopulations. One subpopulation, called "Low cells" and the other is called "High cells". Each member of this

population have a assigned random number that represent expression level of a protein of that cell. This value is taken from a log-normal distribution, with specific mean and variance. Relative size of these two subpopulation was varied. Parameter values were changed and mean and CV of the whole population were calculated for different combinations of the parameters. The simulation was performed using MATLAB R2013b (MathWorks). The steps involved in the simulation are:

Step 1: Input μ_L, μ_H, σ^2_L, σ^2_H, N, f_H

Here,

μ_L = mean of the subpopulation of Low Cells

μ_H = mean of the subpopulation of High Cells

σ^2_L = variance of the subpopulation of Low Cells

σ^2_H = variance of the subpopulation of High Cells

N = Total size of the population (= 20,000 in our simulation)

f_H = fraction of cells in High Cells subpopulation

$\mu_L < \mu_H$; $\sigma^2_L < \sigma^2_H$; $0 \leq f_H \leq 1$;

Step 2: Generate the population P:

Generate N.(1-f_H) number of random numbers having log-normal distribution with mean = μ_L and variance = σ^2_L.

Generate N.f_H number of random numbers having log-normal distribution with mean = μ_H and variance = σ^2_H.

Together, these N number of random numbers represent population P.

Step 3: Calculate Statistical parameters of population P, like mean, μ and CV, σ/μ

Step 4: Repeat step 2 to step 3, M times (M is usually 1000)

Step 5: Calculate average population mean, μ and CV, σ/μ

Step 6: Report the data

Parameters used in our simulations were:

Population size, N = 20,000

Number of repetition of each simulation, M = 1000

Parameters for Low cells subpopulation were kept constant in all simulations:

$\mu_L = 5$; $\sigma^2_L = 50$;

Parameters for High cells populations were varied as given in the table:

f_H	μ_H	σ^2_H when $\gamma = \sigma^2/\mu = 10$	σ^2_H when $\gamma = \sigma^2/\mu = 100$	σ^2_H when $\gamma = \sigma^2/\mu = 1000$
0	0	0	0	0
0.05	10	100	1000	10000
0.1	27	270	2700	27000
0.2	57	570	5700	57000
0.3	75	750	7500	75000
0.4	85	850	8500	85000
0.5	90	900	9000	90000
0.6	94	940	9400	94000
0.7	96	960	9600	96000
0.8	98	980	9800	98000
0.9	99	990	9900	99000
1	100	1000	10000	100000

3.27: Data analysis:

Two-way ANOVA or one-way ANOVA was used depending upon the type of experiment. Mann-Whitney Rank Sum Test was used for data derived from real-time PCR experiments. SigmaPlot was used to generate graphs, for data fitting and statistical analysis. Means of multiple data points were plotted, as mentioned in figure legends. Error bars represent standard deviations.

4 Results & Discussion

Human Cripto-1 (CR-1) is an oncofetal protein that participates in various functions during embryonic development and cancer. It is involved in multiple signaling pathways, which are essential for cellular transformation, metastasis and angiogenesis [12]. Extensive work has been done to elucidate CR-1 signaling and it's functional importance, both in embryonic development and in cancer. Being a crucial molecule during embryonic development, it is expected that transcriptional circuit of CR-1 will have tight regulatory control. The current work investigates the regulatory circuit of CR-1 expression.

TGF-β binds to its receptor TβRI/TβRII and phosphorylates SMAD2/3 that forms complex with SMAD4. This complex translocates to the nucleus and activates expression of target genes by binding to binds to SMAD binding elements (SBEs) [155] . Mancino *et al.* [76] have shown that CR-1 promoter has three SBEs. We have also analyzed an extended region of CR-1 promoter corresponding to 6000 bp upstream from exon 1, using JASPAR [156]. The analysis indicated that there are thirteen putative SBEs (Figure 4.1). Mancino *et al.* [76] have further shown that treatment with TGF-β induces CR-1 expression in colon cancer cell line. CR-1 also activates SMAD2/3 pathway through Nodal-dependent activation of Alk4/ActRII. Therefore, we hypothesized that CR-1 can induce its own expression through Alk4/SMAD2/3 pathway (Figure 4.2a). CR-1 expressed inside the cell would eventually go the cell surface and would activate the same pathway. This would create an autoregulatory positive feedback as shown in figure 4.2b.

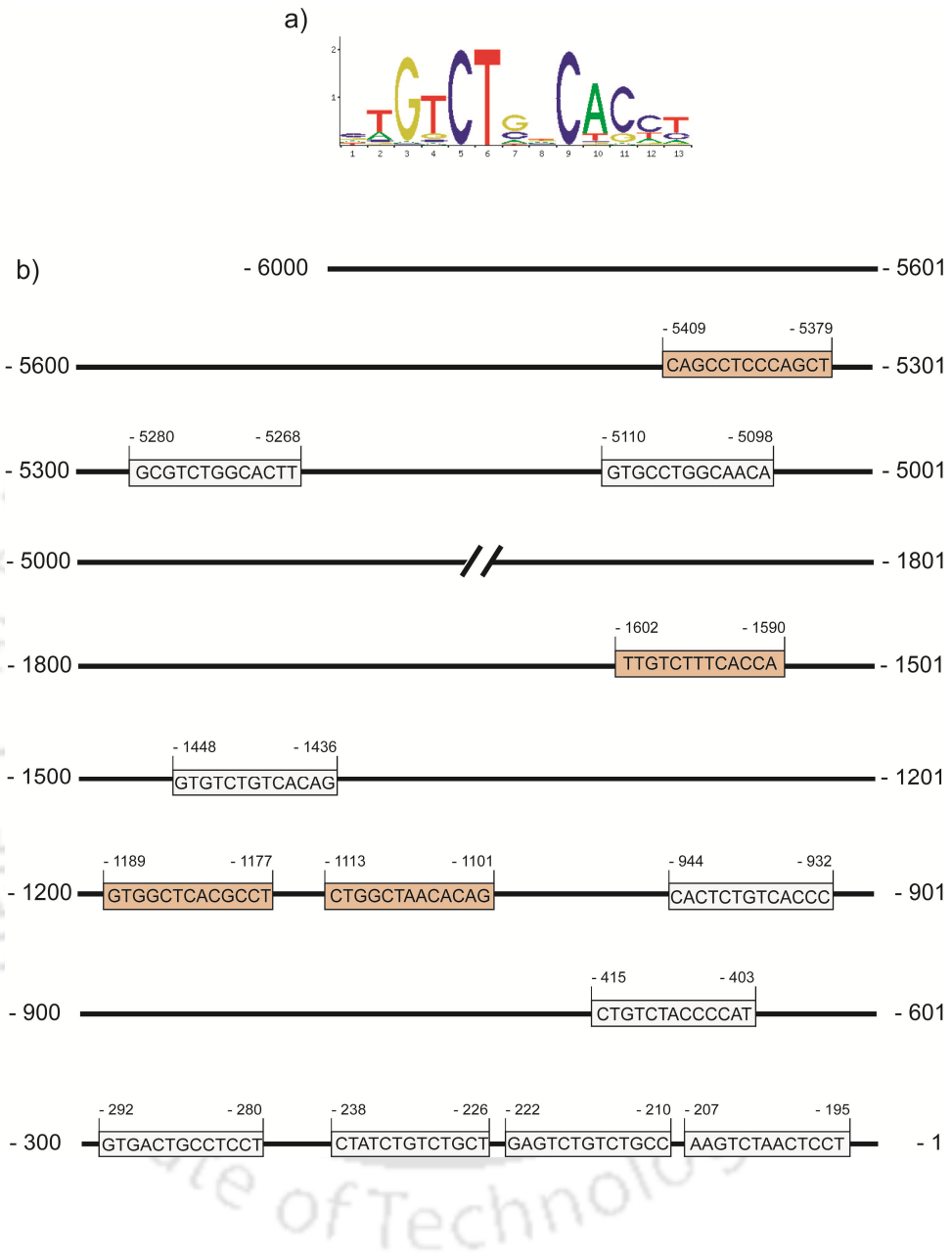

Figure 4.1: SMAD Binding Elements (SBEs) in CR-1 promoter. a) Conserved sequence for SBE as provided in JASPAR CORE databases. b) Positions of thirteen putative SBEs in the promoter of CR-1 (6,000 bp upstream to the first exon of CR-1). Unfilled box represents SBEs in sense strand and colored box represents SBEs in anti-sense strands. Human genome sequence of genomic assembly GRCh37/hg/9 was used.

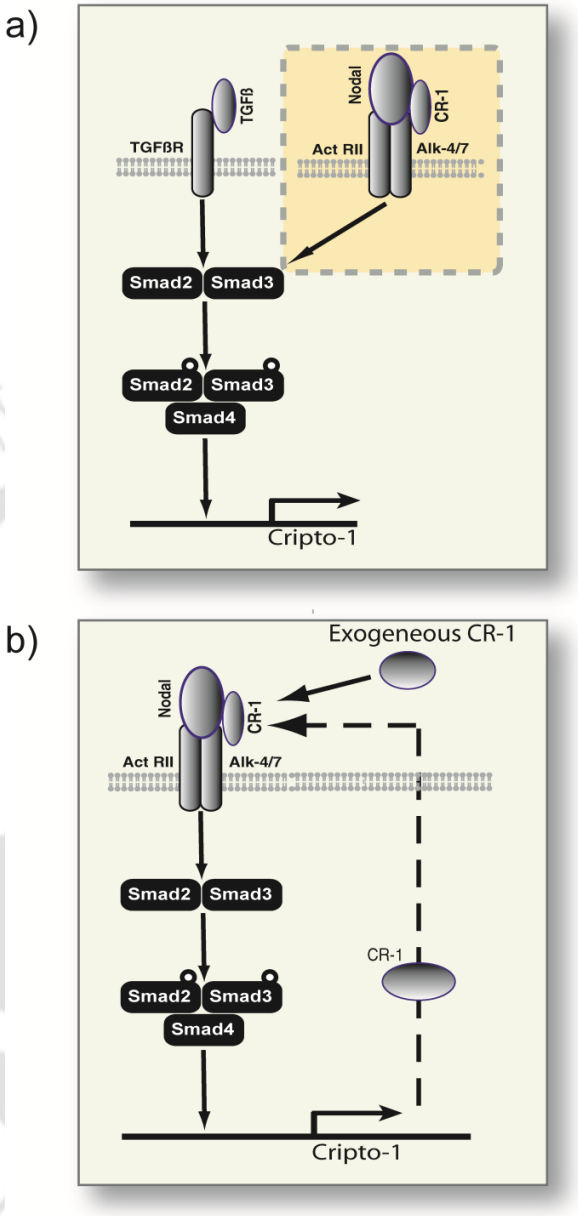

Figure 4.2: A possible positive feedback pathway for CR-1 expression. a) Shows existing information. TGF-β induces the expression of CR-1 via phosphorylation of SMAD2/3. CR-1 forms complex with Nodal/Alk4 and phosphorylates SMAD2/3. b) A hypothetical positive feedback where CR-1 phosphorylates SMAD2/3 and induces its own expression via Alk4/SMAD2/3 pathway. Exogenous CR-1 and endogenous CR-1 would be able to activate this pathway.

4.1: Selection of suitable cellular assay system:

Expression profiling of CR-1 in different cell lines:

Human Cripto-1 (CR-1) is an oncofetal protein known to be expressed in various types of cell lines [21, 72, 74, 76, 157]. To study our proposed hypothesis *in vitro*, we looked into several cell lines that were suitable for our study. We have checked the expression of endogenous CR-1 in six different cell lines, namely human glioblastoma cells U-87 MG & U-373 MG, human hepatocarcinoma cells HepG2, human embryonic kidney cells HEK-293, human colon carcinoma cells HT-29 and human cervical adenocarcinoma cells HeLa using RT-PCR. Expression of CR-1 was detected in U-87 MG, HepG2, HEK-293 and HT-29; however we could not detect the expression in U-373 MG and HeLa (Figure 4.3a). We intended to investigate induction in expression of CR-1. A cell line having lower but detectable level of basal expression of CR-1 would be suitable for our experiments. Therefore, U-87 MG cells were used for further studies.

Expression of Nodal/Alk4/SMAD2/3 pathway molecules in U-87 MG cells:

Signaling molecules associated with the hypothesized positive feedback loop are Nodal, Alk4, ActRIIB, SMAD2, SMAD3 and SMAD4. We checked the expression of these molecules in U-87 MG cells using RT-PCR. It was observed that, all these molecules are expressed in U-87 MG cells (Figure 4.3b). This further confirmed that U-87 MG cells are suitable for our investigation.

TGF-β induces expression of CR-1 in U-87 MG cells:

TGF-β is known to induce expression of CR-1 via SMAD2/3 pathway. We treated the U-87 MG cells with TGF-β (1 ng/ml) for 24 hr in absence of serum. Expression of CR-1 was checked by RT-PCR. As expected, treatment with TGF-β increased CR-1 expression in these cells (Figure 4.4). This confirmed that the molecular pathway through which CR-1 can activates its own expression is present and functional in U-87 MG cells. All the subsequent studies were performed in this cell line.

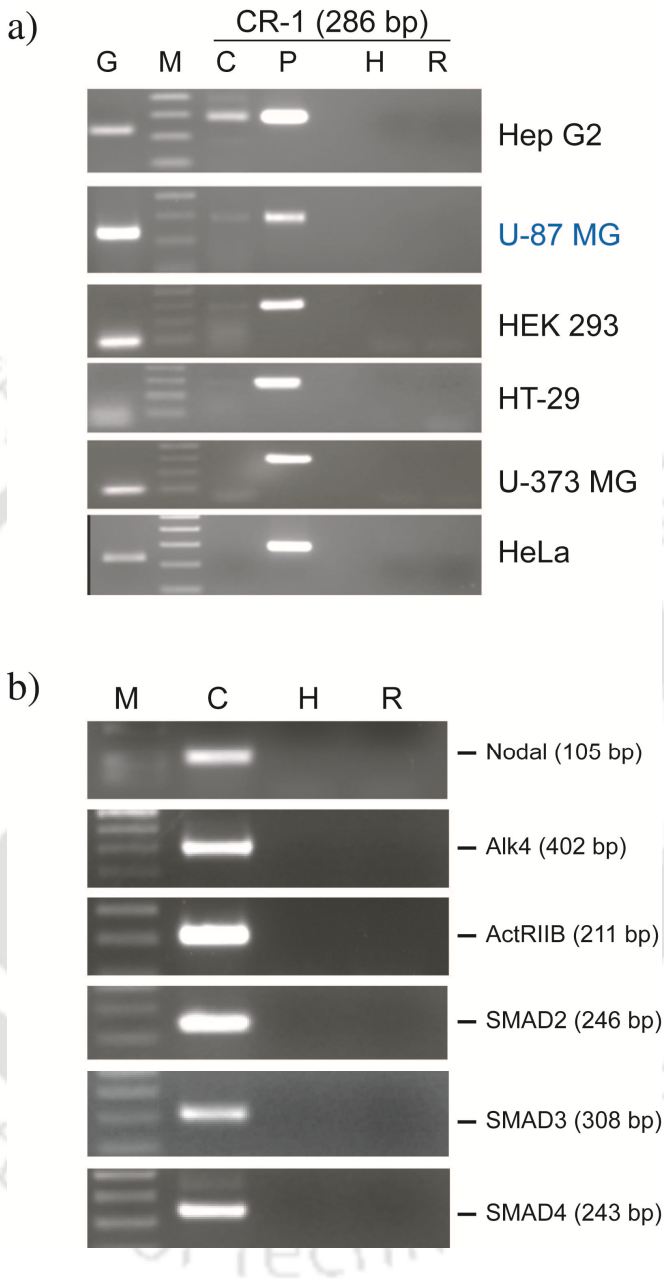

Figure 4.3: Selection of suitable cell line a) RT-PCR to check the expression of CR-1 in different human cell lines. G: GAPDH or Cyclophilin, as endogenous control, C: cDNA, P: full-length CR-1 cloned in a plasmid, H: water, R: RNA. b) RT-PCR to check expression of different molecules of Nodal/Alk4/SMAD2/3 pathway in U-87 MG cells. C: cDNA, R: RNA, H: water, M: DNA marker.

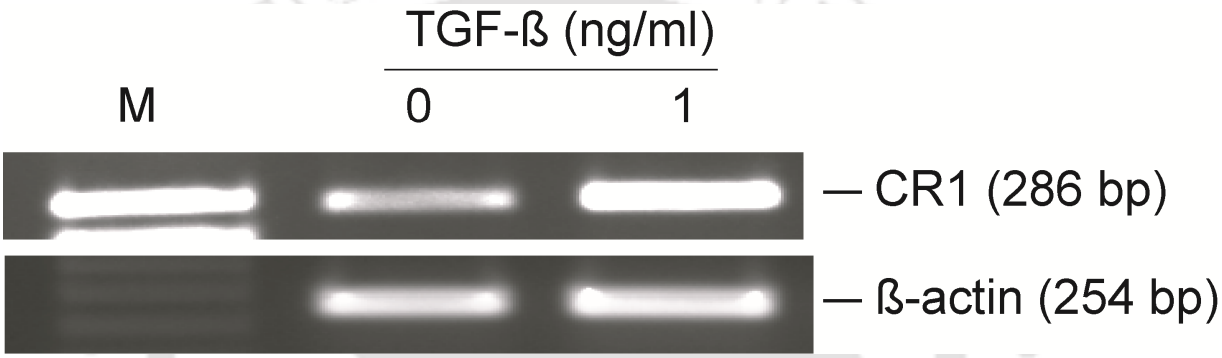

Figure 4.4: TGF-β induces expression of CR-1 in U-87 MG cells. Cells were treated with TGF-β (1 ng/ml) for 24 hr in serum free condition. Expression of CR-1 was checked by RT-PCR. β-actin was used as endogenous control. M: DNA marker.

4.2: Expression of different recombinant CR-1:

To investigate the proposed autoregulatory pathway, we have treated U-87 MG cells with exogenous CR-1. Three different types of CR-1 were used in these experiments (Figure 4.5). Most of the experiments were performed using recombinant C-terminal truncated CR-1 fused to GST (CR1-GST). This was expressed using a bacterial expression system. We have also used recombinant CR-1 expressed in mammalian and insect expression systems in two experiments.

Das A.B. *et al.* [24] had earlier cloned C-terminal truncated human CR-1 (corresponding to 1st-169th amino acid residues) in pGEX-4T2 vector and expressed it in *E.Coli* Rosetta-gami-2 (DE3). The GST-tagged CR-1 has purified and functionally characterized [24]. We have used the same clone to prepare purified recombinant GST-tagged CR-1 (CR1-GST). The recombinant constructs used for the expression of CR1-GST and purified CR1-GST protein was analyzed by SDS-PAGE (Figure 4.6).

To express CR-1 in soluble form in mammalian system, C-terminal truncated CR-1 was cloned in pCI-neo vector and the resulting construct, pCI-CR1ΔC, was used to create stably transfected MCF-7 cells. C-terminal truncation removed the GPI-anchor domain from the protein. The recombinant construct is shown in Figure 4.7a. Stably transfected cells were selected by treating with G418 and maintained with the same drug. Being C-terminal truncated, CR-1 expressed by these cells was secreted out of the cells and accumulate in the culture media. Three days old serum free condition media (CM) of these cells was used as a source of CR-1. Presence of CR-1 in the CM was confirmed by Western Blot (Figure 4.7b).

Subsequently, we performed functional assay for CR-1 using this CM. CR-1 is known to induce cell proliferation in U-87 MG cells [24]. We treated U-87 MG cells with different dilutions of CM containing CR1ΔC, for 48 hr in serum free condition. Subsequently, MTT assay was performed to measure the cell viability. As shown in Figure 4.8, treatment with different dilutions of the CM having CR1ΔC increased cell viability in a dose-dependent fashion. However, no such effect was seen in the cells treated with the CM of MCF-7 cells stably transfected with pCI-neo vector alone (Figure 4.8). This confirmed that the C-terminal truncated CR-1 expressed in the CM of the stably transfected MCF-7 cells is functional.

We have also used commercially available human recombinant CR-1 (rCR-1) (R&D systems) in one experiment. This was expressed in insect expression system. This rCR-1 corresponds to 31st - 172nd amino acids of human CR-1.

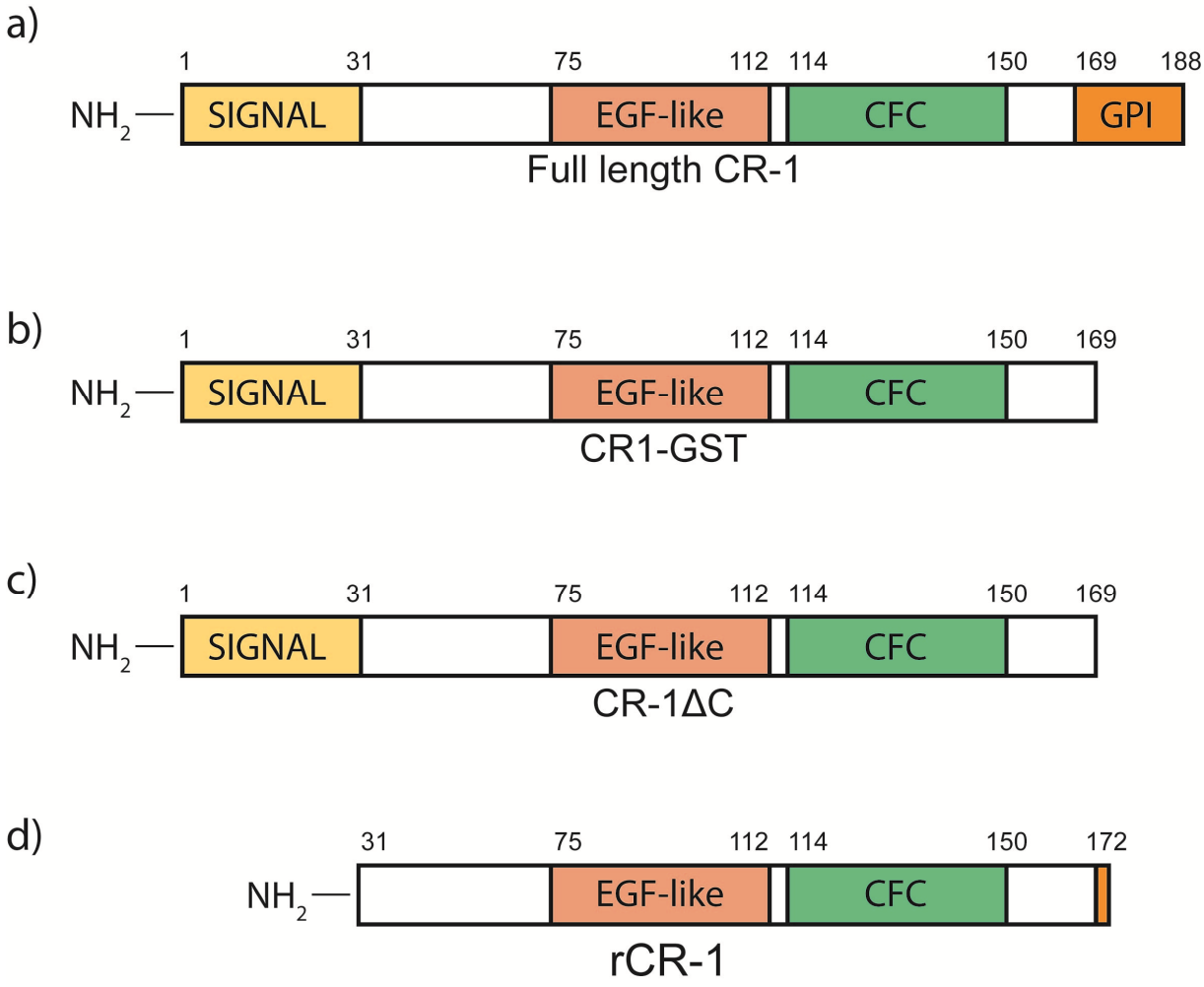

Figure 4.5: Different forms of CR-1 used in different experiments in this work. a) Full length human CR-1, shown here as reference. b) C-terminal truncated GST-tagged recombinant CR-1 (CR1-GST) expressed in bacterial system. GST tag is present at the N-terminal of CR-1 and is not shown here. c) C-terminal truncated CR-1 (CR1ΔC) expressed using mammalian expression system in MCF-7 cells. d) Commercially available recombinant CR-1 expressed in insect expression system (R&D Systems). Numbers written above the boxes represent residue numbers in the full-length CR-1.

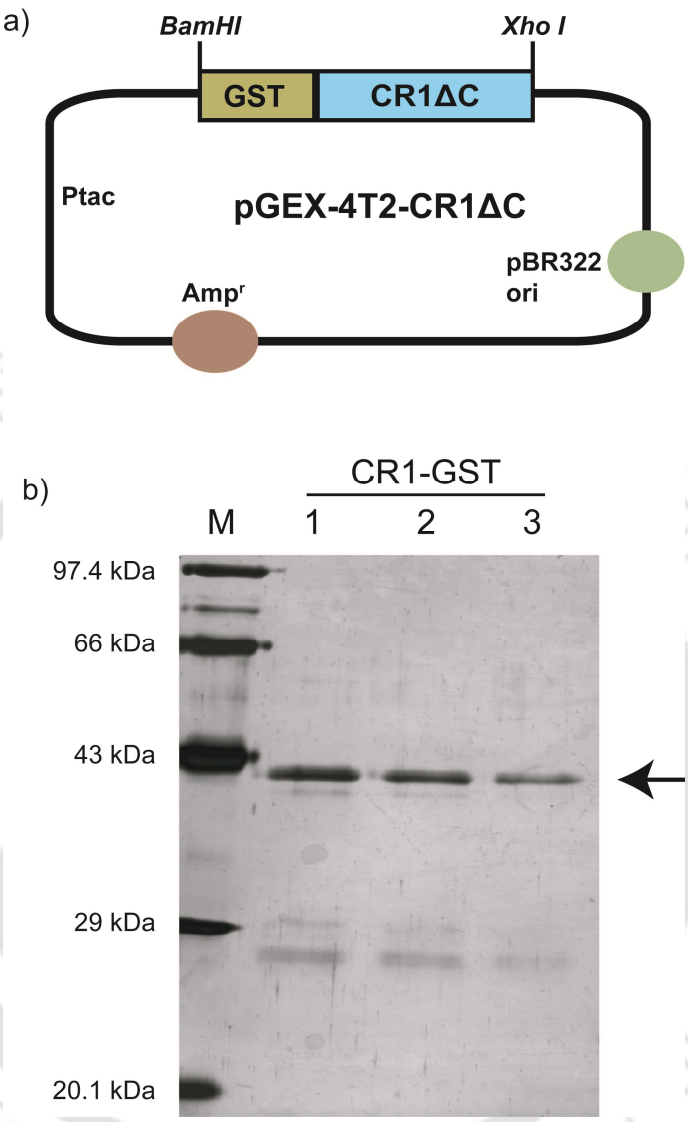

Figure 4.6: Expression of CR1-GST in bacterial system. a) Recombinant construct of GST-tagged C-terminal truncated CR-1 in pGEX-4T2 bacterial expression vector. Amp^r is the ampicillin resistant gene. b) SDS-PAGE to detect purified CR1-GST. 12% polyacrelamide gel was used and was silver stained. *Lane*-1, *Lane*-2 & *Lane*-3 are three eluted fractions from the same lysate.

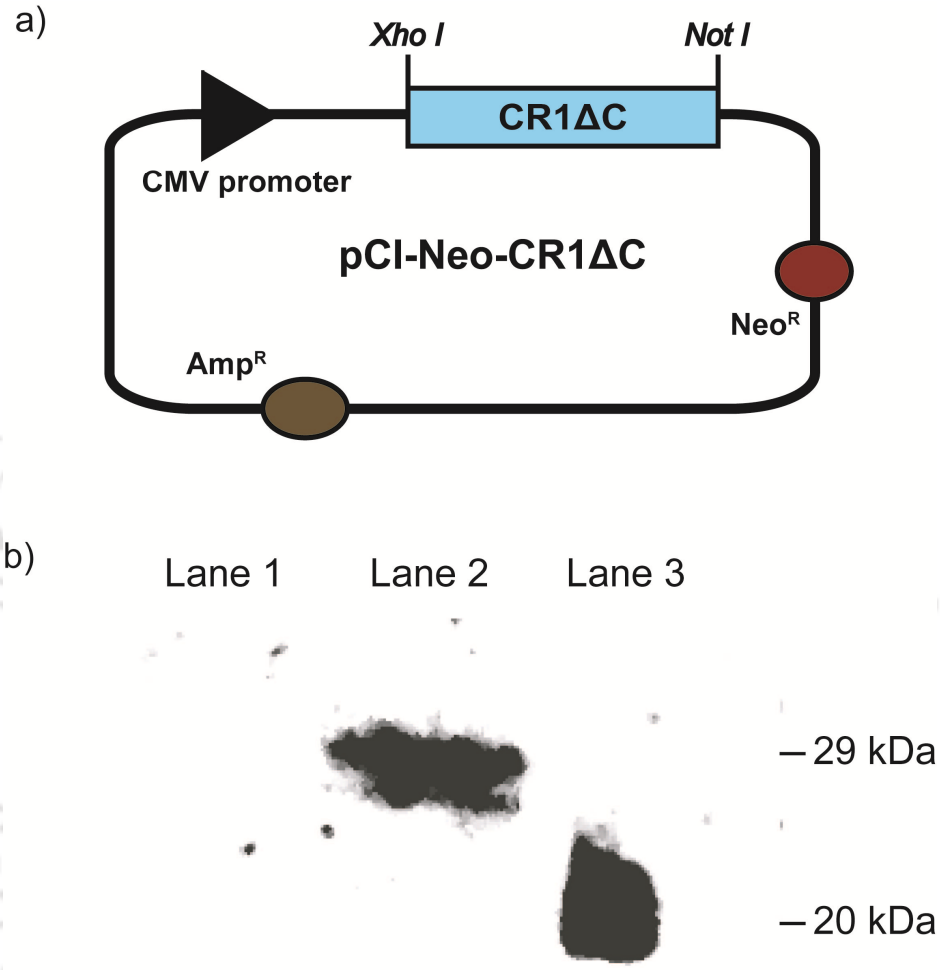

Figure 4.7: Expression of recombinant human CR-1 using mammalian expression system. a) Recombinant construct pCI-Neo-CR1ΔC used for creating stably transfected to MCF-7 Cells. Neo^r and Amp^r represent neomycin and ampicillin resistant gene respectively. b) Western blot to detect CR1ΔC (29 kDa) in the conditioned media (CM) of stably transfected MCF-7 cells. Lane 1: CM of MCF-7 cells transfected with pCI-neo vector only, lane 2: CM of MCF-7 cells transfected with pCI-Neo-CR1ΔC, lane 3: commercially available recombinant human CR-1 (rCR-1) expressed in insect cell line (R&D systems).

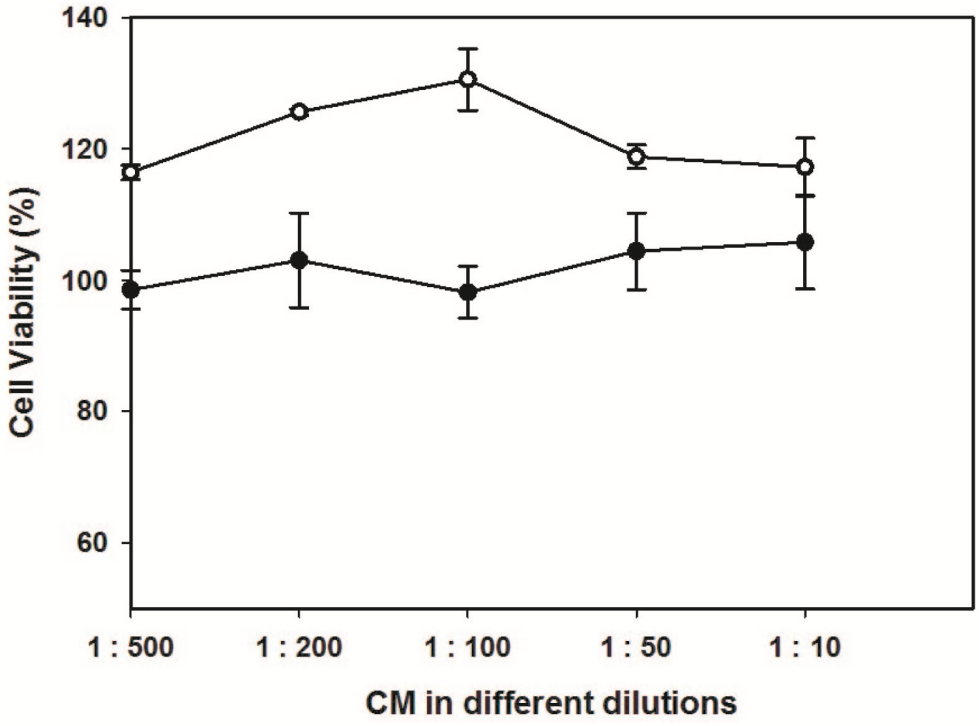

Figure 4.8: Functional assay of the conditioned-media having CR1ΔC. U-87 MG cells were treated with different dilutions of either the CM of MCF-7 cells expressing CR1ΔC or the CM of MCF-7 cells transfected with pCI-Neo vector alone, for 48 hr in serum free condition. MTT assay was performed to determine cell viability. Each data point's represents mean of four different wells. Two-way ANOVA with pair-wise comparison showed that the CM of CR1ΔC has dose dependent effect ($p < 0.01$) but CM of vector transected cells does not affect cell viability ($p > 0.05$).

4.3: Treatment with CR-1 induces expression of CR-1 in U-87 MG cells:

To test our hypothesis, we have treated U-87 MG cells with different concentrations of CR1-GST for 24 hr in absence of serum and measured the expression of CR-1 in these cells by RT-PCR. It was observed that CR1-GST induced the expression of CR-1 in a dose dependent fashion (Figure 4.9a). However, no such induction was observed in the cells treated with GST only. Real-time PCR was used to further confirm induction of CR-1 expression. As shown in Figure 4.9b, treatment with exogenous CR-1 increased CR-1 transcript in a non-linear dose dependant fashion.

Inducible gene expression systems often have sigmoidal dose-response behavior, represented by Hill function [125]. Such non-linear nature of induction is crucial in modulating the population heterogeneity in expression of a gene [158]. The data shown in Figure 4.9b is sigmoidal in nature and fits well with Hill function having Hill coefficient 2.37. A Hill coefficient > 1 indicates cooperativity in the transcriptional circuit [125]. Transcription in mammalian system involves multiple transcription factors interacting with each other. Even the same transcription factor may bind to multiple sites in the same promoter and interact with each other. Such interactions lead to cooperativity in transcriptional circuits. SMADs are known to have such cooperativity [159, 160]. The promoter region of CR-1 has multiple SMAD-binding elements and one can expect binding of multiple, interacting SMAD complexes at those sites.

We have also performed time-dependant experiments to understand the temporal behavior of CR-1 induction. U-87 MG cells were treated with 200 ng/ml of CR1-GST for different durations in absence of serum. Subsequently, the expression of CR-1 was checked by real-time PCR (Figure 4.10). We have observed that up to 8 hr of treatment, induction in CR-1 was not detectable. Subsequently the level of induction increased and reached a peak at 24 hr. However, by 48 hr of treatment, expression level of CR-1 returns back to the basal level. Such temporal behavior with a peak has been earlier observed for TGF-β induced system and is believed to be associated with time-dependent depletion of the ligand [161]. Similar depletion of CR-1, after long period of incubation, can be a reason in decrease in level of induction at 48 hr. As maximum induction was observed after 24 hr of treatment, all subsequent experiments were performed at that time point.

CR1ΔC from CM and rCR-1 also induces CR-1 expression:

Further, we investigated whether two other recombinant CR-1, expressed in mammalian and insect expression systems, induce expression of CR-1 in U-87 MG. We treated U-87 MG cells with different dilutions of the conditioned media of the stably transfected MCF-7 cells that expresses CR1ΔC. Expression of CR-1 was checked by RT-PCR. As shown in Figure 11a, the conditioned media induced expression of CR-1 in a dose dependent fashion. No such induction was seen in the cells treated with CM from the cells having pCI-Neo vector alone (Figure 11a).

Such induction was also observed by using commercially available human recombinant CR-1 (rCR-1) that is expressed in an insect expression system. U-87 MG cells were treated with 200 ng/ml of rCR-1 for 24 hr in serum free condition. RNA was isolated and expression of CR-1 was detected using RT-PCR. We observed that rCR-1 also induced the expression of CR-1 in U-87 MG cells (Figure 4.11b).

Such consistent inducing effect of various recombinant CR-1 confirmed that CR-1 mediated induction of CR-1 expression was not an artifact arising out of using the recombinant CR-1 expressed in *E. coli*. Subsequently, we used CR1-GST for our experiments.

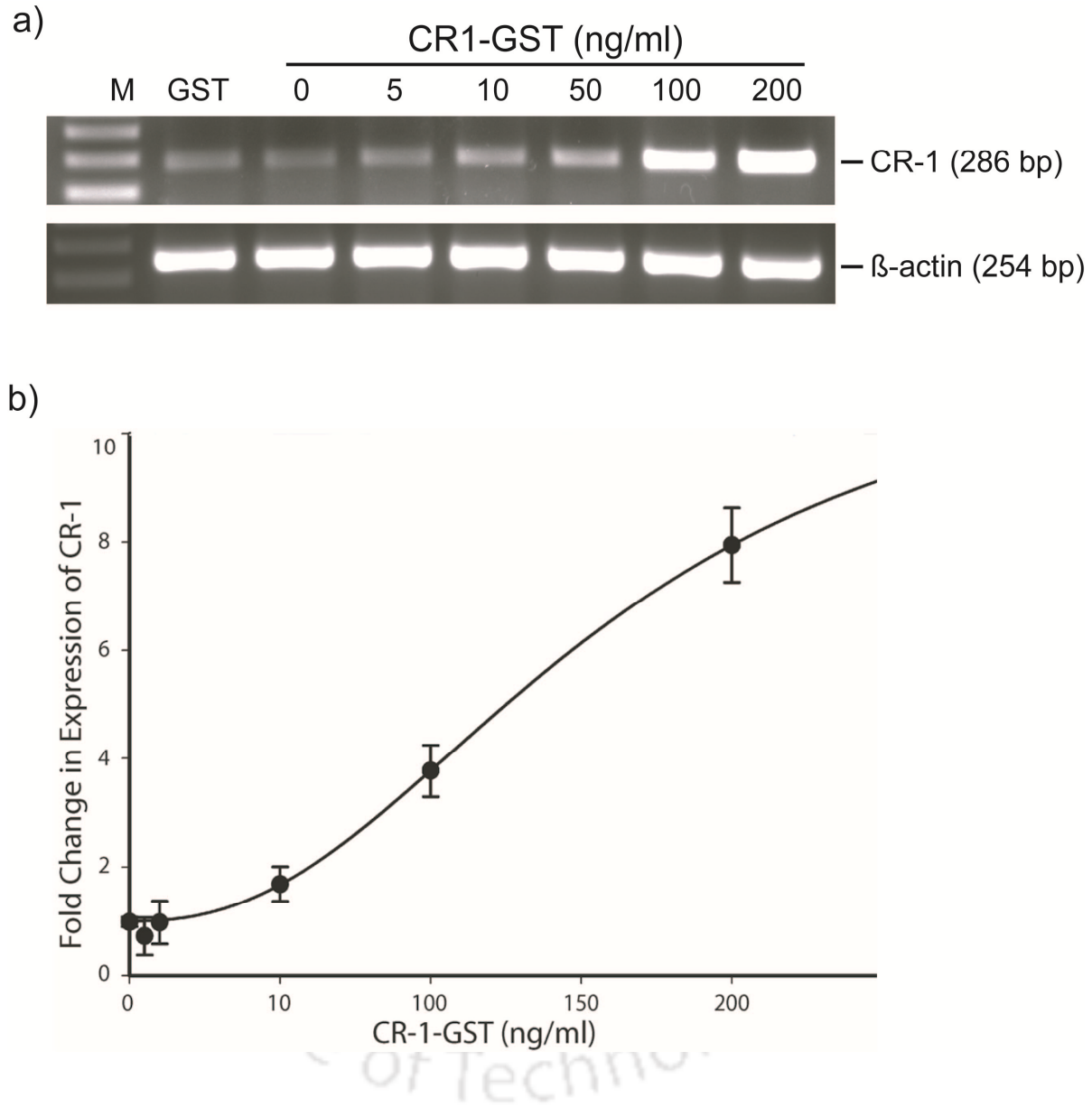

Figure 4.9: Treatment with recombinant CR-1 induces CR-1 expression. U-87 MG cells were treated with different doses of CR1-GST or GST (200 ng/ml) for 24 hr in serum free condition. Expression of CR-1 was measured by (a) RT-PCR and (b) Real-time PCR. Data of real-time PCR was fitted to Hill function (fold change = 1+ 10.85 × $dose^{2.37}$/(156.99$^{2.37}$+ $dose^{2.37}$); R^2 = 0.98). Each data point represents average of four independent experiments. For RT-PCR β-actin was used as endogenous control.

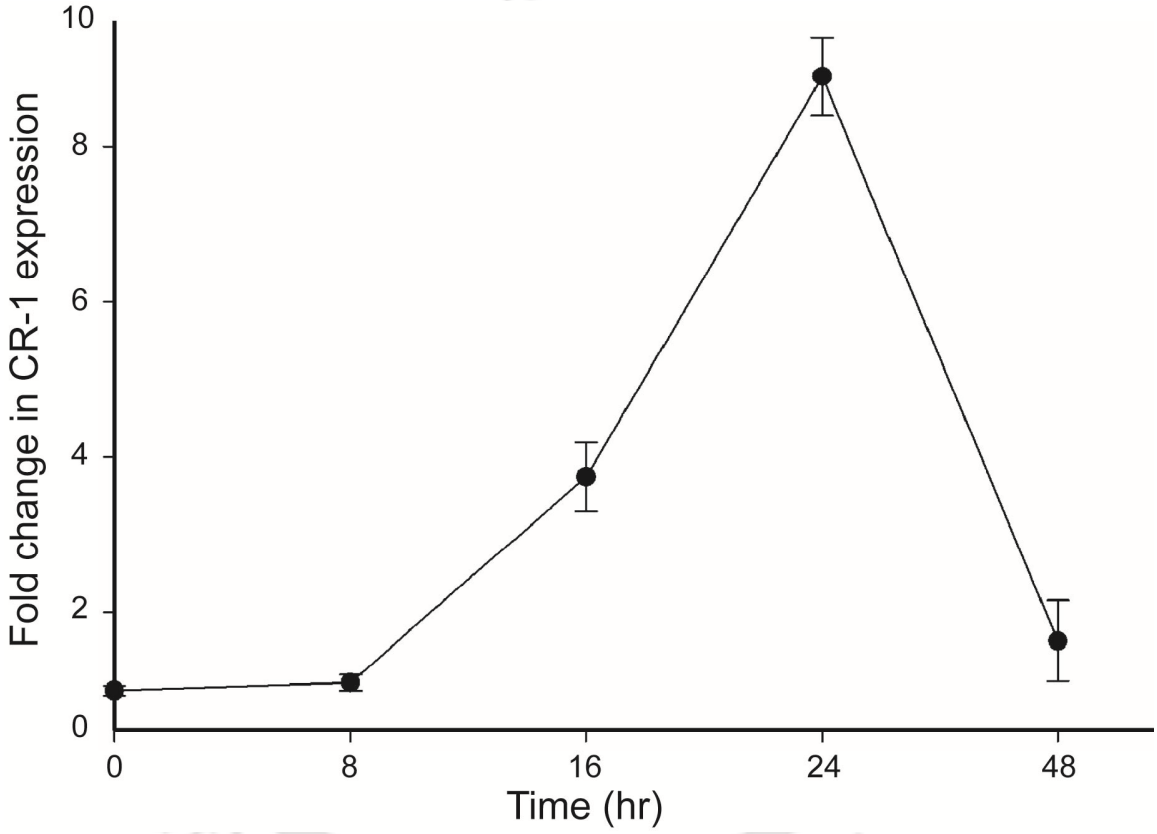

Figure 4.10: Time course of induction of CR-1. U-87 MG cells were treated with CR1-GST (200 ng/ml) in serum free condition for specific durations. Expression of CR-1 was measured by real-time PCR. Each data point represents average of four independent experiments.

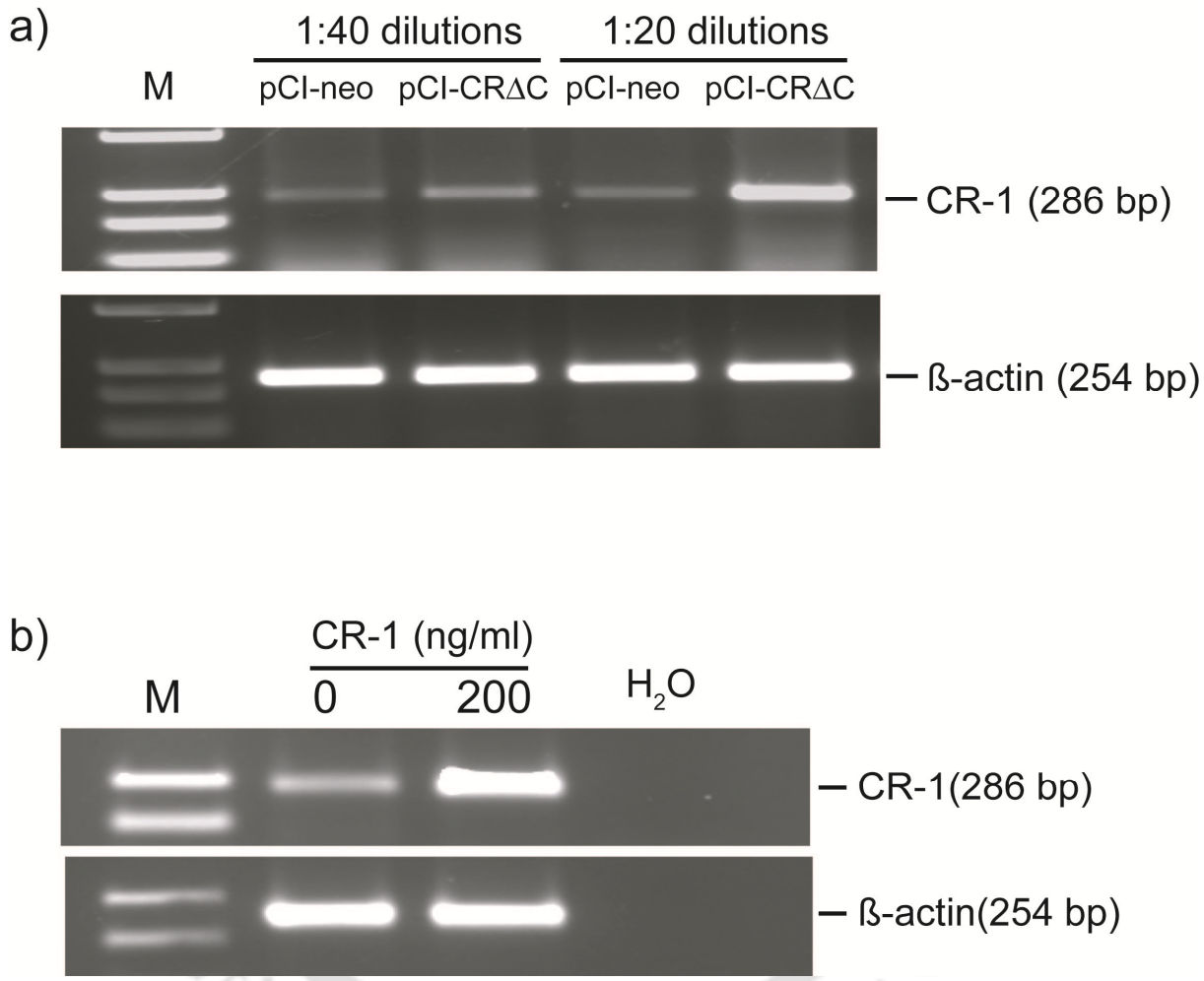

Figure 4.11: RT-PCR to check induction of CR-1 expression in U-87 MG cells by two different recombinant CR-1. a) Cells were treated with two dilutions (1:40 and 1:20) of conditioned media (CM) of MCF-7 cells overexpressing soluble CR1ΔC or having transfected with the vector only. b) Cells were treated with recombinant CR-1 (R&D systems) expressed using an insect expression system. In both the experiments, cells were treated for 24 hr in serum free condition. β-actin was used as endogenous control. M: Marker.

4.4: Issue of CR-1 transcript variants:

There are three transcripts variant of CR-1 [21, 87, 157]. These variants are shown in Figure 4.12a. Transcript variant-1 codes for the full-length CR-1 protein. The primer pair (FCR286 and RCR286) used in our experiments amplifies a region between exon-4 and exon-7 of CR-1 and cannot discriminate among these three different transcripts. Therefore, one can ask which transcript variant of CR-1 is induced by the treatment with recombinant CR-1. To address this question, we have used another primer pair, CF and RCR114, to amplify a region between Exon-2 and Exon-4 (Figure 4.12a). This primer pair will amplify only the transcript variant-1.

U-87 MG cells were treated with 200 ng/ml of CR1-GST for 24 hr in absence of serum. RT-PCR was performed to check the expression of CR-1 using primer pair CF and RCR114. As shown in Figure 4.12b, this primer pair was able to amplify CR-1 in both CR1-GST treated and untreated samples and the band intensity was much higher in the CR1-GST treated sample. This confirmed that U-87 MG expresses transcript variant-1 of CR-1 and treatment with exogenous CR-1 induces this transcript variant.

4.5: Issue of CR-1 pseudogene Cripto-3:

Cripto-1 has several pseudogenes, namely CR-2, CR-3, CR-4, CR-5 and CR-6 (also called TDGF-2, TDGF-3, TDGF-4, TDGF-5 and TDGF-6) [5]. Sun *et al.* [68] have shown that CR-3, a pseudogene of CR-1, is expressed in some cancer cell lines. CR-3 does not have any intron and its sequence is almost identical with the mRNA of CR-1, with only seven single bases difference in coding region that results in six amino acid changes [68]. Therefore, we need to check whether the transcript expressed in U-87 MG cells is of CR-1 or CR-3. We have used the same primer pair used by Sun *et al.* [68] to differentiate CR-1 and CR-3 (CRF3 and CRR3). This primer pair will amplify only CR-3 transcript. U-87 MG cells were treated with CR1-GST (200 ng/ml) for 24 hr in absence of serum and RT-PCR was used to detect expression of CR-3. Genomic DNA of U-87 MG and full-length CR-1 cloned in a plasmid were taken as positive and negative control respectively. As shown in Figure 4.13, we have not observed any amplification for CR-3 in cases where cDNAs from CR-GST treated and untreated U-87 MG cells were used in the PCR. However as expected, a product of correct size was observed when genomic DNA of U-87 MG was used as template. This confirmed that U-87 MG does not express CR-3 and CR-3 is not induced by treatment with exogenous CR-1.

4.6: Treatment with recombinant CR-1 increases CR-1 protein:

Treatment with exogenous CR-1 induces expression of CR-1 transcript. To check whether such induction leads to increase in CR-1 protein, we had used Western blot experiment. U-87 MG cells were treated with different concentration of CR1-GST for 24 hr in serum free condition. The expression of CR-1 was checked by western blot. As shown in Figure 4.14a, treatment with recombinant CR-1 increased the level of CR-1 protein in U-87 MG cells in a dose dependent fashion. The experiment was repeated and average fold change of CR-1 protein at various doses of recombinant CR-1 is shown in Figure 4.14b.

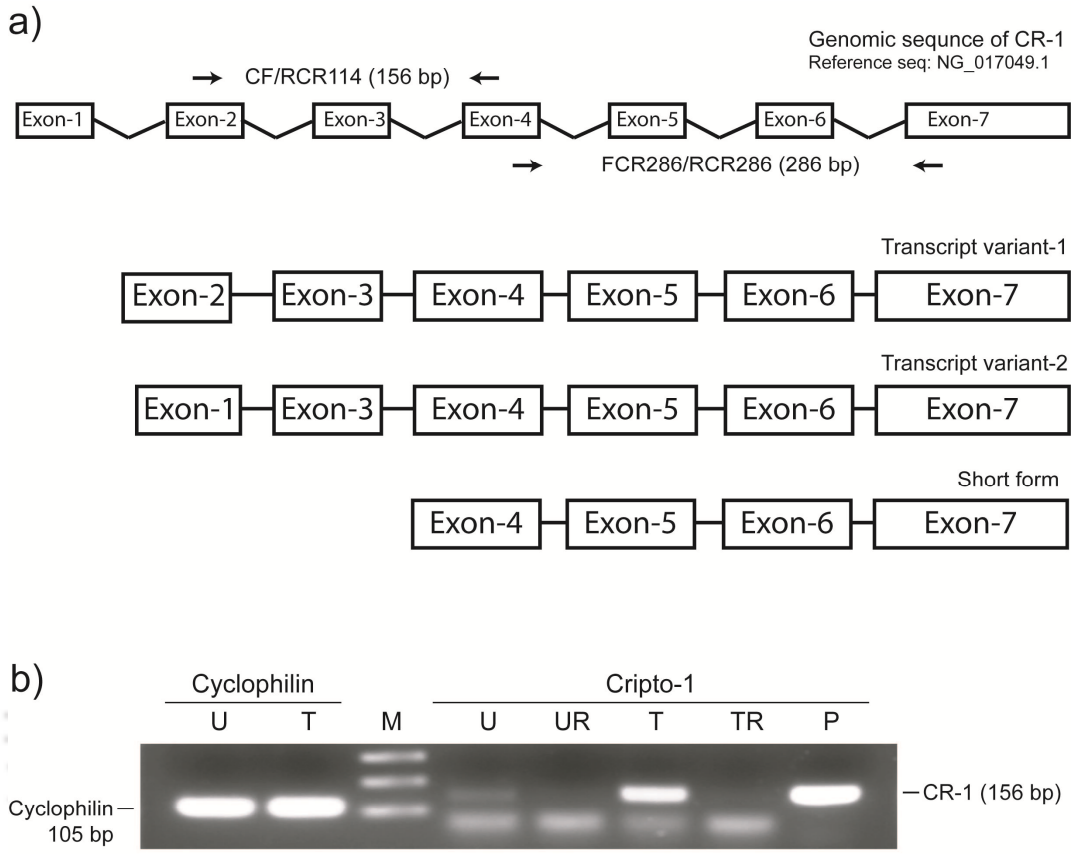

Figure 4.12: Expression of CR-1 transcript variants. a) Different transcript variants of CR-1 and position of primers used in our experiments. Primer pair FCR286 and RCR286 detects all the three CR-1 transcript variants. Primer pair CF and RCR114 detects only transcript variant-1. b) Only transcript variant-1 is expressed and induced in U-87 MG cells. U-87 MG cells were treated with CR1-GST (200 ng/ml) for 24 hr in serum free conditions. Expression of CR-1 was measured by RT-PCR using the primer pair CF and RCR114. Cyclophilin was used as endogenous control. U: untreated cDNA, T: treated cDNA, UR: untreated RNA, TR: treated RNA, P: CR-1 plasmid as positive control. M: Marker.

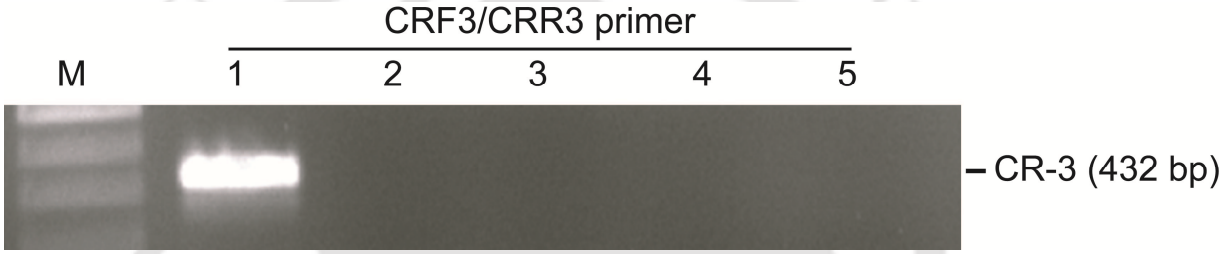

Figure 4.13: U-87 MG does not express the pseudogene CR-3. U-87 MG cells were treated with CR1-GST for 24 hr in serum free condition. Expression of CR-3 was measured by RT-PCR. 1: U-87 MG genomic DNA as positive control, 2: CR-1 plasmid as negative control, 3. cDNA of CR1-GST treated U-87 MG, 4: cDNA of untreated U-87 MG and 5: water.

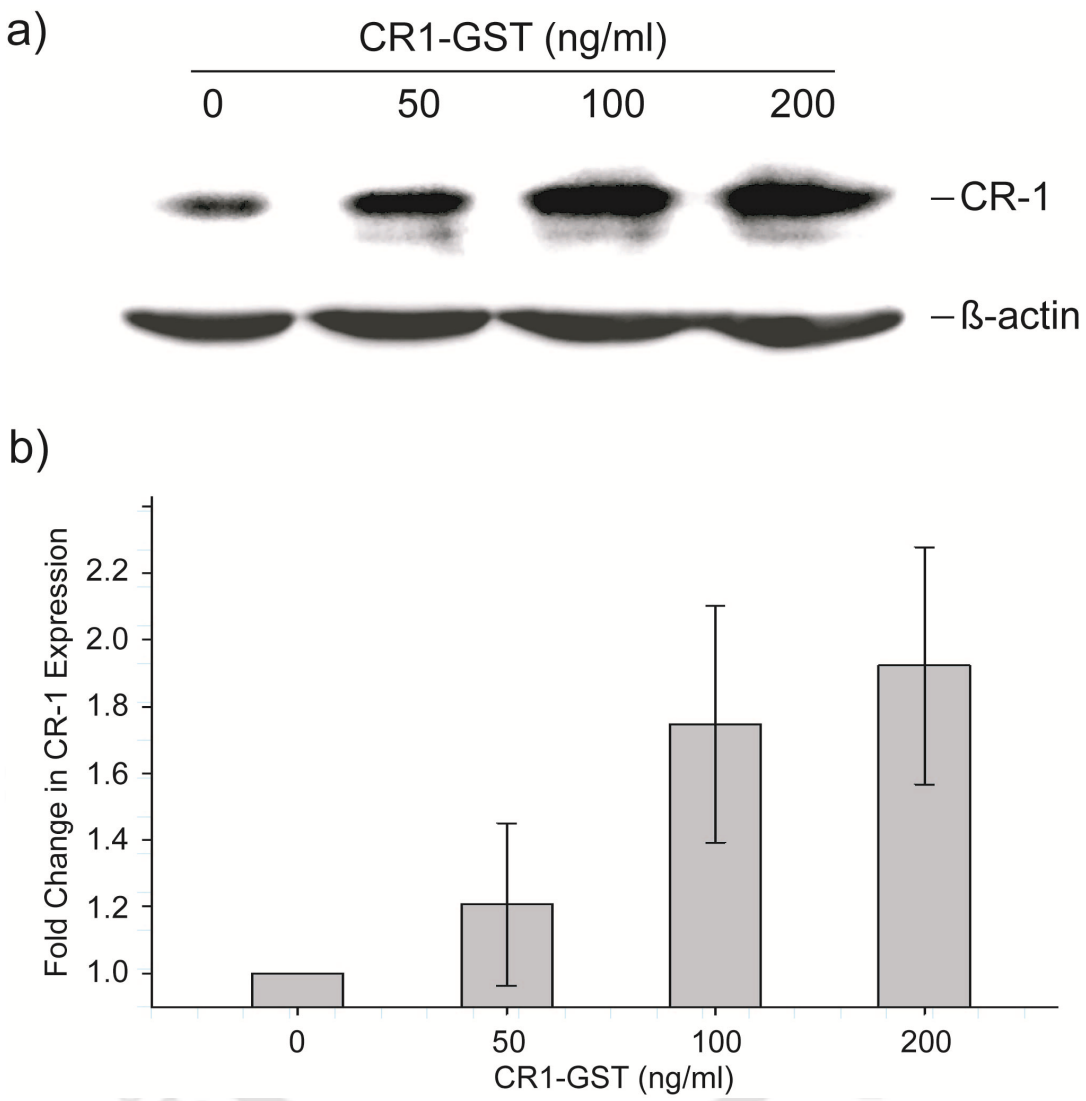

Figure 4.14: Treatment with exogenous CR-1 increases CR-1 protein. a) Western blots to detect the increase in CR-1 protein in U-87 MG cells. Cells were treated with different doses of CR-1 GST, for 24 hr in serum free condition. CR-1 was detected using anti-human CR-1 antibody. β-actin was used as loading control. b) Western blot experiments were repeated for three times and densitometry analysis was performed. Relative fold change was calculated relative to β-actin expression in each sample. Each data point represents the mean of three independent experiments. One-way ANOVA with pair wise comparison indicates that there was significant dose dependent change in expression of CR-1 ($P<0.011$).

4.7: Treatment with recombinant CR-1 does not affect mRNA stability:

The increase in the transcript of CR-1, recombinant CR-1 treated cells, may arise due to two possible reasons: (a) treatment with CR-1 increases rate of transcription of CR-1 and b) treatment with CR-1 increases stability of the CR-1 mRNA.

Therefore, we designed an experiment to check the effect of CR-1 treatment on the degradation of CR-1 mRNA. The method is similar to that reported by Hennes *et al.* [153]. Actiomycin D (Act-D), an antibiotic, is as global transcription inhibitor. It binds to the transcription initiation complex of double stranded DNA and prevents the initiation of RNA chain by RNA polymerase [152]. Experimental strategy of studying the stability of CR-1 mRNA is given in (Figure 4.15a). As Act-D is a global transcription inhibitor, it can affect the viability of cells. Therefore, one needs to use a dose of Act-D that would not drastically affect the cell viability at least during the period of experiment. An MTT assay was carried out to decide suitable concentration of Act-D. U-87 MG cells were treated with different concentration of Act-D for 24 hr in serum free condition. The percentage of cell viability was measured by MTT assay (Figure 4.15b). Based on the MTT, we used 5 μg/ml of Act-D in subsequent experiment.

U-87 MG cells were treated with 200 ng/ml of recombinant CR-1 or left untreated, for 16 hr in serum free condition. Subsequently, cells were treated with Act-D (5 μg/ml) and RNA samples were collected at different time points (0, 3, 6 and 9 hr). As shown in Figure 4.10, by 16 hr of treatment, considerable increase in CR-1 would happen in CR1-GST treated U-87 MG cells. Subsequent treatment with Act-D would stop further expression of CR-1. Real-time PCR was used to estimate the time dependent change in level of CR-1 transcript in CR-1 treated and untreated cells after Act-D treatment. As shown in Figure 4.16b, subsequent to Act-D treatment, amount of CR-1 transcript, in untreated U-87 MG cells, reduced in a time dependent fashion typical of first order degradation of mRNA. The decay of CR-1 mRNA was not significantly different in CR-1 treated cells. This indicates that treatment with CR-1 does not affect the stability of CR-1 mRNA. Based on these experiments we concluded that treatment with CR-1 increases transcription of CR-1 in U-87 MG cells.

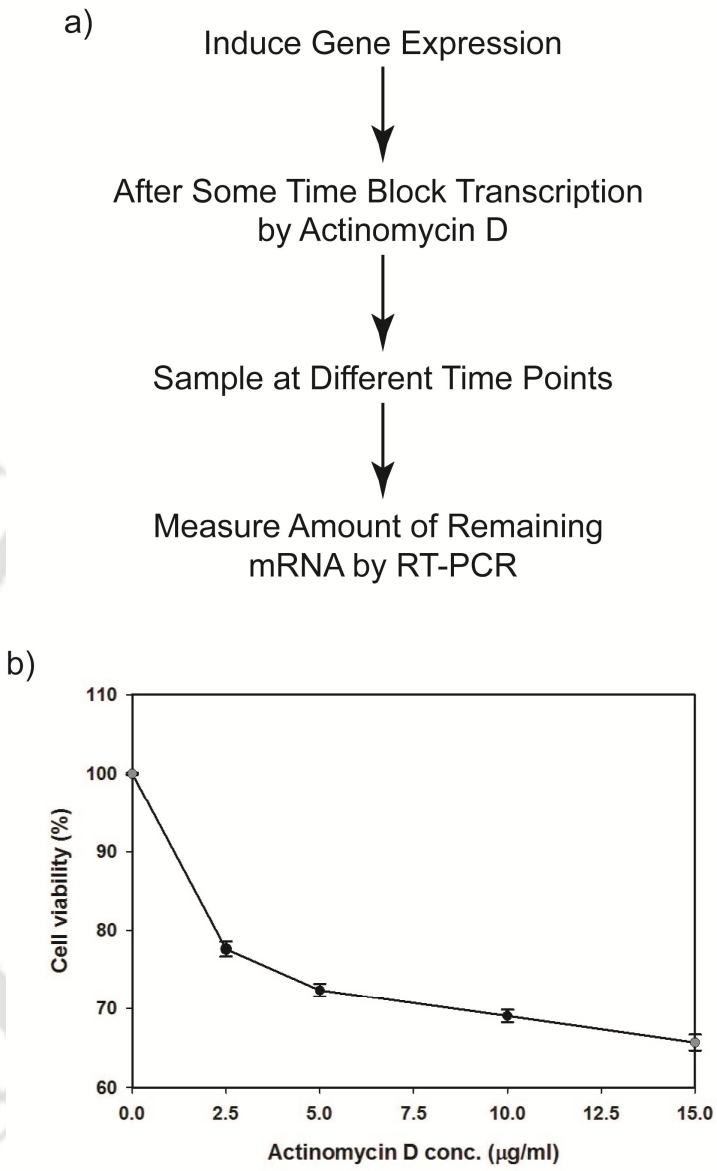

Figure 4.15: a) Schematic representation of experimental strategy to study mRNA stability. b) MTT assay was carried out to determine the suitable dose of Actinomycin D (Act-D). U-87 MG cells were treated with different concentration of Act-D for 24 hr. Percentage cell viability was estimated by dividing the measurement for treated cells by that of untreated cells. Each data point's represents mean of four different wells.

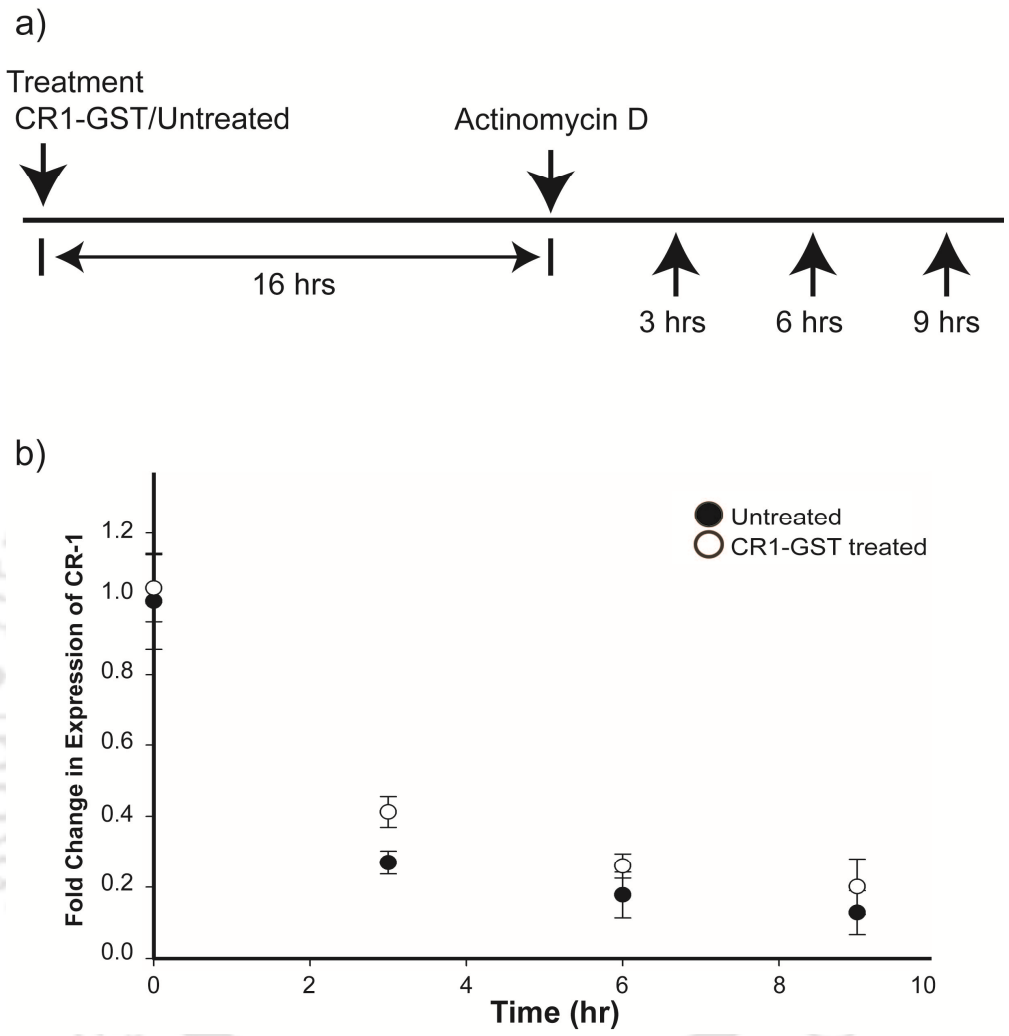

Figure 4.16: Treatment with CR-1 does not affect stability of CR-1 mRNA. a) Schematic representation of treatment strategy for mRNA stability assay b) Fold change in CR-1 transcript at different time points after treatment with Actinomycin D in presence and absence of recombinant CR-1. No significant difference between treated and untreated cells (Rank Sum Test, $p = 0.127$). Each data point represents average of four independent experiments.

4.8: CR-1 induces its own expression through Alk4/SMAD2/3 pathway:

Earlier, we have proposed that, CR-1 induces its own expression via Alk4/SMAD2/3 pathway. To investigate this, we have used SB-431542, a small molecule inhibitor of Alk4 [162]. Figure 4.17a, shows the pathway and the point of inhibition by SB-431542.

An experiment was performed to check the dose of SB-431542 that would not drastically affect the viability of U-87 MG cells. U-87 MG cells were treated with different concentration of SB-431542 for 24 hr in serum free condition and the percentage of cell viability was estimated by MTT assay. The result of this experiment is shown Figure 4.17b. Based on this result, 10 μM of SB-431542 was subsequently used for other assays. .

An experiment was performed to check whether treatment with CR-1 activates Alk4/SMAD2/3 pathway. U-87 MG cells were serum starved for 24 hr and treated with CR1-GST (200 ng/ml) for different durations. Subsequently, phosphorylation of SMAD2 was determined by Western blot. As shown in Figure 4.18a, treatment with recombinant CR-1 induced phosphorylation of SMAD2 and maximum phosphorylation was observed after 15 minutes of treatment.

Subsequently, we performed a similar experiment but in presence and absence of the Alk4 inhibitor. U-87 MG cells were serum starved for 24 hr and then treated with 200 ng/ml of CR1-GST in absence or presence of the Alk4 inhibitor, SB-431542. SB-431542 (10 μM) was added to cells 30 min prior to the treatment with CR1-GST. After 15 minutes of treatment with recombinant CR-1, samples were collected and western blot was performed to detect phosphorylated SMAD2 and total SMAD2. We observed that recombinant CR-1 induced SMAD2 phosphorylation and such phosphorylation was inhibited by SB-431542 (Figure 4.18b). This experiment confirmed that recombinant CR-1 induces phosphorylation of SMAD2 via Alk4 pathway.

Our hypothesis was that CR-1 would activate Alk4/SMAD2/3 pathway and that in turn would induce expression of CR-1. Therefore, we investigated the effect of the Alk4 inhibitor on induction of CR-1 expression in U-87 MG cells treated with recombinant CR-1. U-87 MG cells were treated with recombinant CR-1 (200 ng/ml) in absence or presence of the inhibitor, SB-431542, for 24 hr in serum free condition. SB-431542 (10 μM) was added 30 min prior to the CR-1 treatment. RT-PCR was performed to check the expression of CR-1 in these cells. As expected, we observed that inhibition of Alk4 blocked CR-1 mediated induction of CR-1

expression (Figure 4.19). Taken together, these observations confirm that CR-1 induces its own expression through Alk4/SMAD2/3 pathway.

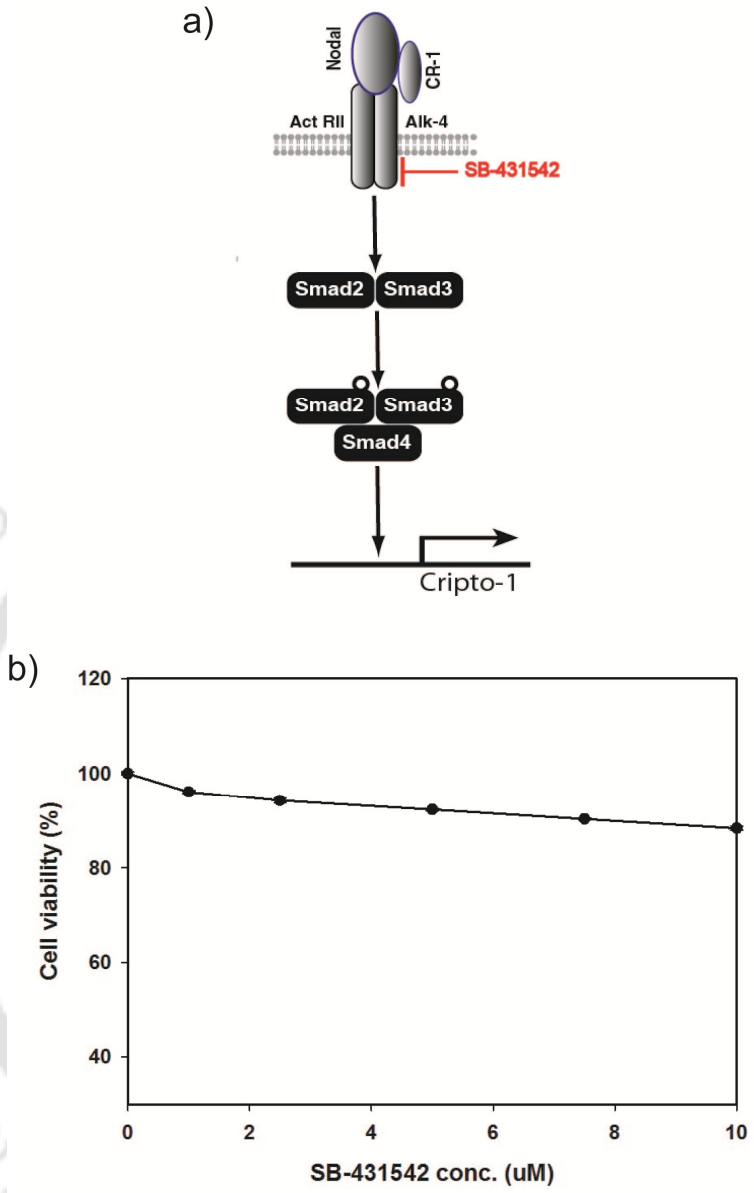

Figure 17: Blocking of Alk4 by SB-431542 to study involvement of Alk4/SMAD2/3 pathway. a) Schematic representation of blocking of Alk4 by SB-431542 in Alk4/SMAD2/3 pathway. b) MTT assay was carried out to determine the suitable dose of SB-431542. U-87 MG cells were treated with different concentrations of SB-431542 for 24 hr. Percentage cell viability was estimated by MTT assay. Each data point's represents mean of four different wells. 10 μM of SB-431542 was used for subsequent experiments.

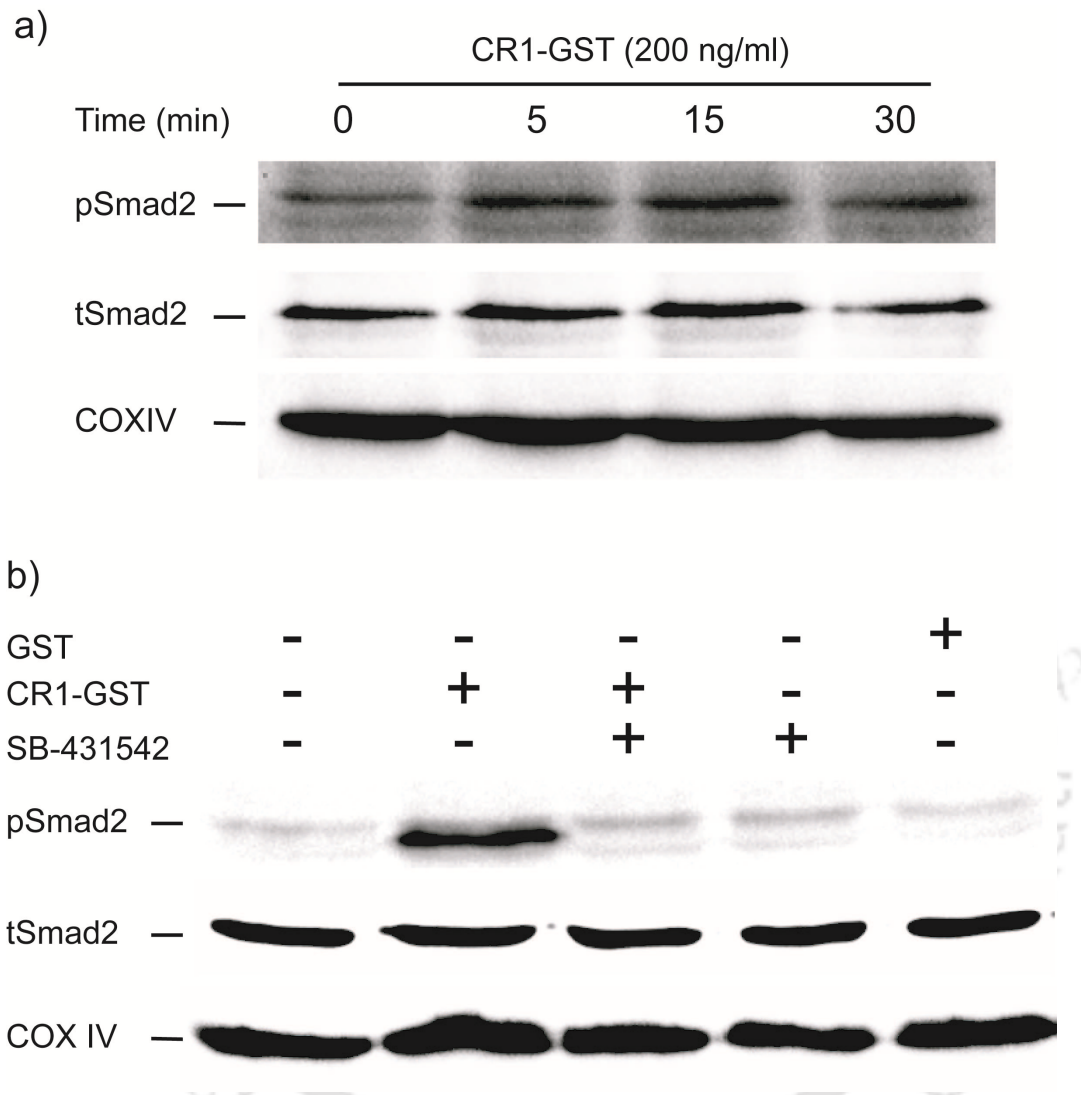

Figure 18: CR-1 activates Alk4/SMAD2/3 pathway in U-87 MG cells. a) Western blot to detect phosphorylation of SMAD2 in U-87 MG cells treated with recombinant CR-1 (200 ng/ml) for different durations. b) Western blot to detect phosphorylation of SMAD2 in U-87 MG cells treated with different combinations of CR1-GST, GST and Alk4 inhibitor (SB-431542) for 15 min. For (a) and b), primary antibodies: rabbit anti-phospho-SMAD2 (Ser465/467) (1:1000 dilutions), rabbit anti-total-SMAD2 (1:3000 dilutions) & rabbit anti COX IV (1:3000 dilutions). Goat anti-rabbit HRP-conjugate (1:6000 dilutions) was used as secondary antibody.

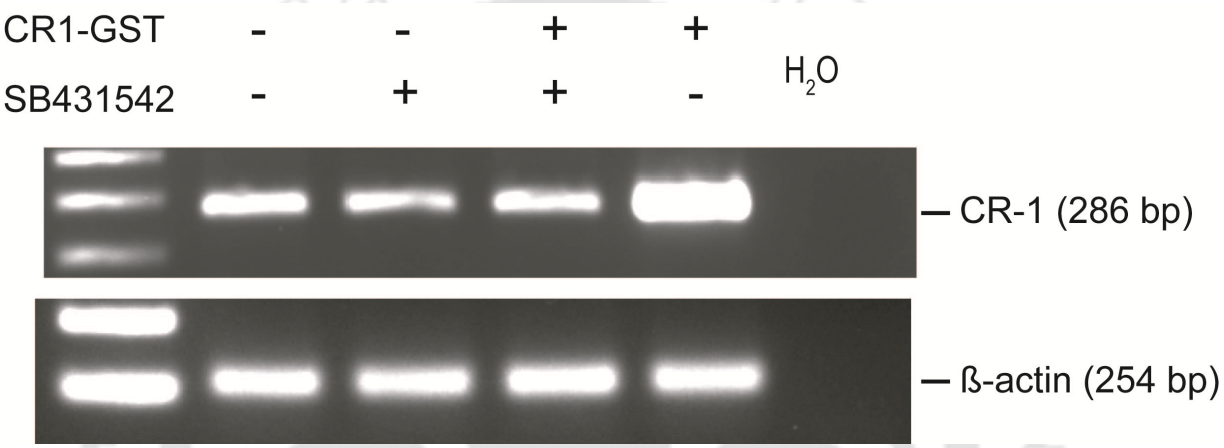

Figure 19: Effect of Alk4 inhibitor on CR-1 mediated induction of CR-1. U-87 MG cells were treated with different combinations of recombinant CR-1 (200 ng/ml) and SB-431542 in serum free condition for 24 hr. RT-PCR was used to check expression of CR-1. β-Actin was used as endogenous control.

4.9: Cellular heterogeneity in CR-1 expression:

Gene expression is stochastic and such stochasticity leads to heterogeneity in expression [97]. The design of the transcriptional circuit often affects such heterogeneity [119]. A transcriptional circuit with positive feedback results in bistability and it leads to the emergence of bimodality with two subpopulations having low and high expression [120, 163]. Due to the stochasticity in gene expression, bimodality can appear in a positive feedback circuit even without bistability [164].

Heterogeneity in gene expression is crucial in embryonic development [165] and many genes involved in embryonic development show bimodal expression [166, 167]. Expression of Nanog, a key embryonic regulator, is controlled by a positive feedback circuit. Expression of Nanog in embryonic stem cells is bimodal [167].

Treatment with recombinant CR-1 induces expression of CR-1 through Nodal/Alk-4/SMAD2/3 pathway. This would increase endogenous CR-1 on the cell surface. These cell surface CR-1 molecules will also induce the same pathway, thereby creating a positive feedback. Therefore, one can expect that the autoregulatory pathway of CR-1 may lead to emergence of two subpopulations. We used flow cytometry to investigate such heterogeneity in expression of CR-1 in U-87 MG cells.

4.10: Heterogeneous Expression of CR-1 in U87 MG cells:

To investigate the expression of CR-1, we have used PE-tagged antibody against human CR-1. At the very beginning, we have checked the ability of this antibody to detect CR-1. MCF-7 cells do not have expression of CR-1 (Figure 4.20). These cells were stably transfected with mammalian expression vector pCI-Neo having full-length CR-1 cloned in it [63]. Stably transfected clones were selected using G418. Being full-length, CR-1 overexpressed in these cells was expected to be present on the cell surface as a membrane-anchored protein. These cells were stained with anti-CR1-PE antibody and analyzed by flow cytometry. MCF-7 cells were transfected with the empty vector and stained with in the same fashion was used as negative control. As shown in Figure 4.21, one can clearly distinguish between cells expressing CR-1 from those not expressing the same. The stably transfected MCF-7 cells, overeexpressing CR-1, were not monoclonal. Rather, transfected clones selected for drug resistance were pooled and used for this experiment. Therefore, we have a mixed population of cells as evident in the fluorescence histogram.

Subsequently, we moved to analyze expression of CR-1 in U-87 MG cells using this anti-CR1-PE antibody. U-87 MG cells were stained either with anti-CR1-PE or with PE-tagged isotype-control antibody. Flow cytometry was performed to detect level of expression of CR-1 in these cells. We observed that there was no visual difference between cells stained with isotype-control antibody and anti-CR1-PE (Figure 22). Therefore, we used histogram subtraction to identify percentage of cells that are positive for CR-1. It was found that only an extremely minor subpopulation of cells (~7%) had detectable level of CR-1 expression. We call these cells CR-1-positive. Rest of the cells, where CR-1 was not detected by flow cytometry are called CR-1-negative. Strizzi *et al.* [168] also detected very low CR-1-positive population in human melanoma cells using the same antibody that we have used. They had observed that ~5% and ~2% of C8161 and ROS184 cells were CR-1-positive, respectively.

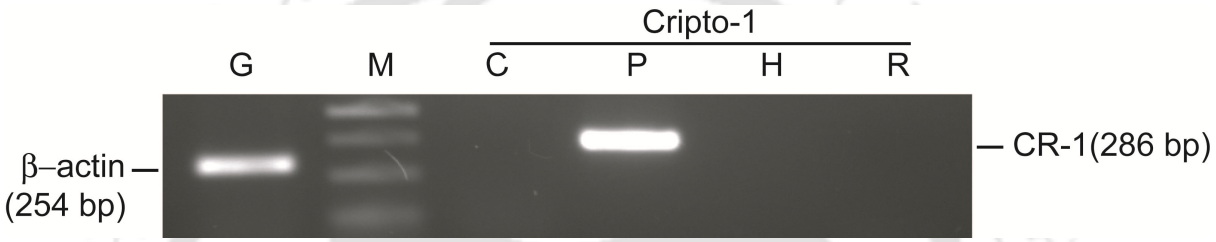

Figure 4.20: Expression of CR-1 in MCF-7 cells. RT-PCR was carried out to check the expression of CR-1 in MCF-7 cell line. G: β-actin, as endogenous control, C: cDNA of MCF-7, P: full-length CR-1 cloned in a plasmid, H: water, R: RNA of MCF-7.

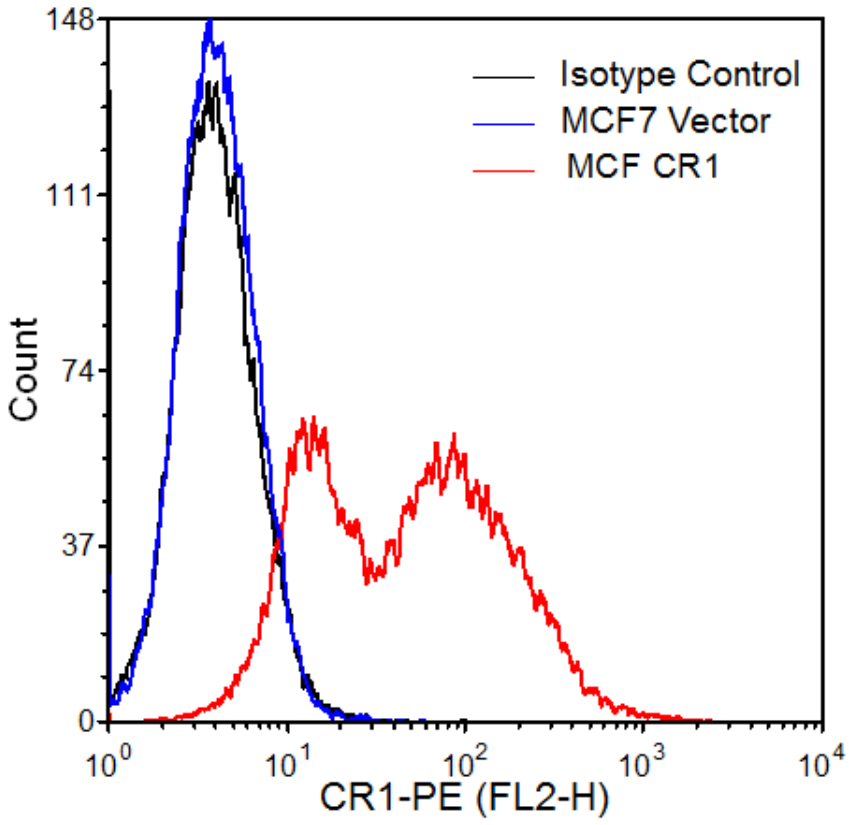

Figure 4.21: Flow cytometry to check activity of the anti-human CR-1-PE conjugated antibody. MCF CR1: MCF-7 cells overexpressing full-length CR-1 and stained with the anti-CR-1 antibody PE conjugate; MCF7 vector: MCF-7 cells transfected with empty vector and stained with the anti-CR-1 antibody PE conjugate; Isotype control: MCF-7 cells overexpressing full-length CR-1 and stained with isotype control antibody.

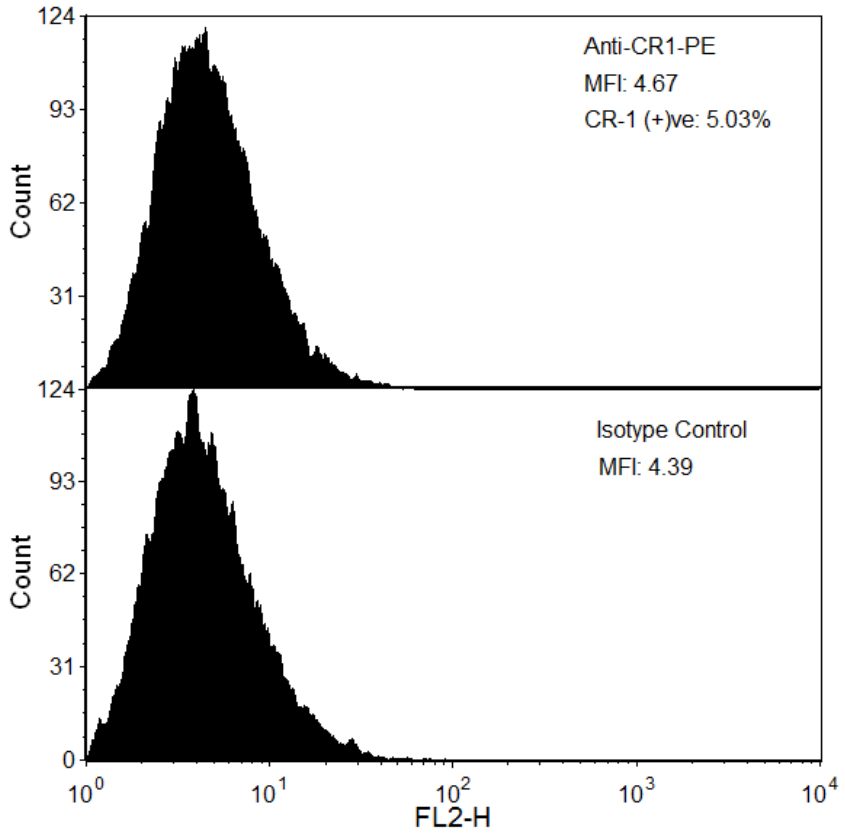

Figure 4.22: Flow cytometry to detect **e**xpression of CR-1. a) U-87 MG cells were stained either with anti-human CR1-PE or isotype control antibody. Flow cytometry was performed and CR-1 expression was measured in FL2-H. Percentage of CR-1-positive cells was determined by subtracting the histogram of Isotype control sample from the histogram of the sample stained with anti-CR-1-PE. The experiment was repeated and data of one representative experiment is shown here.

4.11: Heterogeneity in induction of CR-1 expression:

In RT-PCR and Western Blot experiments, we had observed dose-dependent increase in expression of CR-1. If such induction happens in all cells, the fluorescence histogram for CR-1, in the flow cytometry experiment, should shift to the right in a dose dependent fashion. We treated U-87 MG cells with different doses of recombinant CR-1 and checked the expression of CR-1 by flow cytometry. The data of one such experiment is shown in Figure 4.23. Interestingly, the fluorescence histogram for CR-1 did not shift entirely to the right side. It was observed that most of the cells had fluorescence signal similar to cells stained with isotype control antibody. Only a minority subpopulation had detectably higher expression of CR-1. As defined earlier these cells were called CR-1-positive. The size of the CR-1-positive subpopulation increased with the dose of CR1-GST (Figure 4.23).

Further, we looked into the dose-dependent behavior of the CR-1-positive subpopulation. We observed that with increase in dose of the recombinant CR-1, the size of the CR-1-positive subpopulation also increases (Figure 4.24a). However, size of this subpopulation was always smaller than CR-1-negative subpopulation. Even at the highest dose (400 ng/ml), majority of the cells do not have detectable level of CR-1 (i.e. CR-1-negative). Note that as per the sigmoidal dose-response curve shown earlier in Figure 4.9, at a dose of 400 ng/ml of CR1-GST, the level of induction of CR-1 would reach the saturation. Our flow cytometry data suggest that such high saturating level of induction was achieved only in a minority subpopulation. We have also measured the MFI of CR-1-positive cells. It was observed that level of expression in those CR-1 positive cells increased with increase in the dose of recombinant CR-1(Figure 4.24b). These observations confirmed that treatment with exogenous CR-1 leads to induction in CR-1 expression only in a minority subpopulation. Size of this subpopulation and the level of induction in these cells increases with increase in inducing signal. Similar behavior has been earlier observed in transcriptional circuit with positive feedback [120].

However, cell size can affect the variability in flow cytometry data [92]. Increase in cell size can also increase the MFI of cells. Recently, Scheidenhelm *et al.* [169] demonstrated that higher expression of AMOG, a cell adhesion molecule increases the cell size in human and mouse gliomas through selective activation of the Akt/mTOR/S6K signaling pathway. Therefore, we checked the correlation between FSC (an approximate measure of cell size) and FL2-H (measurement of CR-1) in cells treated with different doses of recombinant CR-1. We have not

observed any such correlation in our data (Figure 4.25). This indicates that increase in the dose of recombinant CR-1 increases level of expression of CR-1 but not cell size.

One can argue that probably majority of U-87 MG cells did not have the machinery required for induction of CR-1 through Alk4/SMAD2/3 pathway. Therefore, treatment with recombinant CR-1 failed to induce CR-1 expression in those cells. We have treated U-87 MG cells with recombinant CR-1 (400 ng/ml) for 24 hr in serum free conditions. Subsequently, we have sorted out CR-1-positive and CR-1-negative cells by FACS. RNA was isolated from both the subpopulations and expression of molecules involved in Alk4/SMAD2/3 pathway was checked by RT-PCR. As shown in Figure 4.26, these molecules were expressed at similar levels in both the subpopulations. This confirmed that two subpopulations in CR-1 treated cells have not originated due to differences in expression of pathway molecules among two groups of cells. The size of the CR-1-positive subpopulation increases with treatment dose. This observation also negates the possibility of the emergence of two subpopulations due to existence of two groups of cells having high and low expression of pathway molecules.

Based on flow cytometry data, we have named two subpopulations of U-87 MG cells as CR-1-positive and CR-1-negative. However, this does not mean that CR-1-negative cells did not express CR-1 at all. RT-PCR with RNA isolated from this subpopulation showed presence of CR-1 transcript, albeit at low, basal level (Figure 4.26). This level of expression was so low that one cannot differentiate these cells from isotype control cells in flow cytometry. The other subpopulation, called CR-1 positive, showed expression of CR-1 at higher level. RT-PCR also confirmed higher level of transcription in these cells (Figure 4.26).

Interestingly, this CR-1-positive subpopulation, though miniscule in size, is present even in uninduced cells (Figure 4.24a). With increase in inducing signal, the size of this population increased. This strengthens our claim for the autoregulatory positive feedback in CR-1 expression. There is a basal level of expression of CR-1 in U-87 MG cells, even in absence of externally added CR-1. The endogenous CR-1 would be present on cell surface and would activate the Nodal/Alk4/SMAD2/3 pathway, creating the positive feedback. Due to this positive feedback and inherent stochasticity, two subpopulations, with lower and higher expression, would emerge. Cells transits between these two populations (or states) probabilistically and the probability of such transition would depend upon the level of induction in each cell. In absence of any external perturbation, these two populations would be in equilibrium. Treatment with external

CR-1 would increase the strength of induction, thereby increasing the probability of transition from low expressing to high expressing state. This leads to increase in the size of CR-1 positive subpopulation.

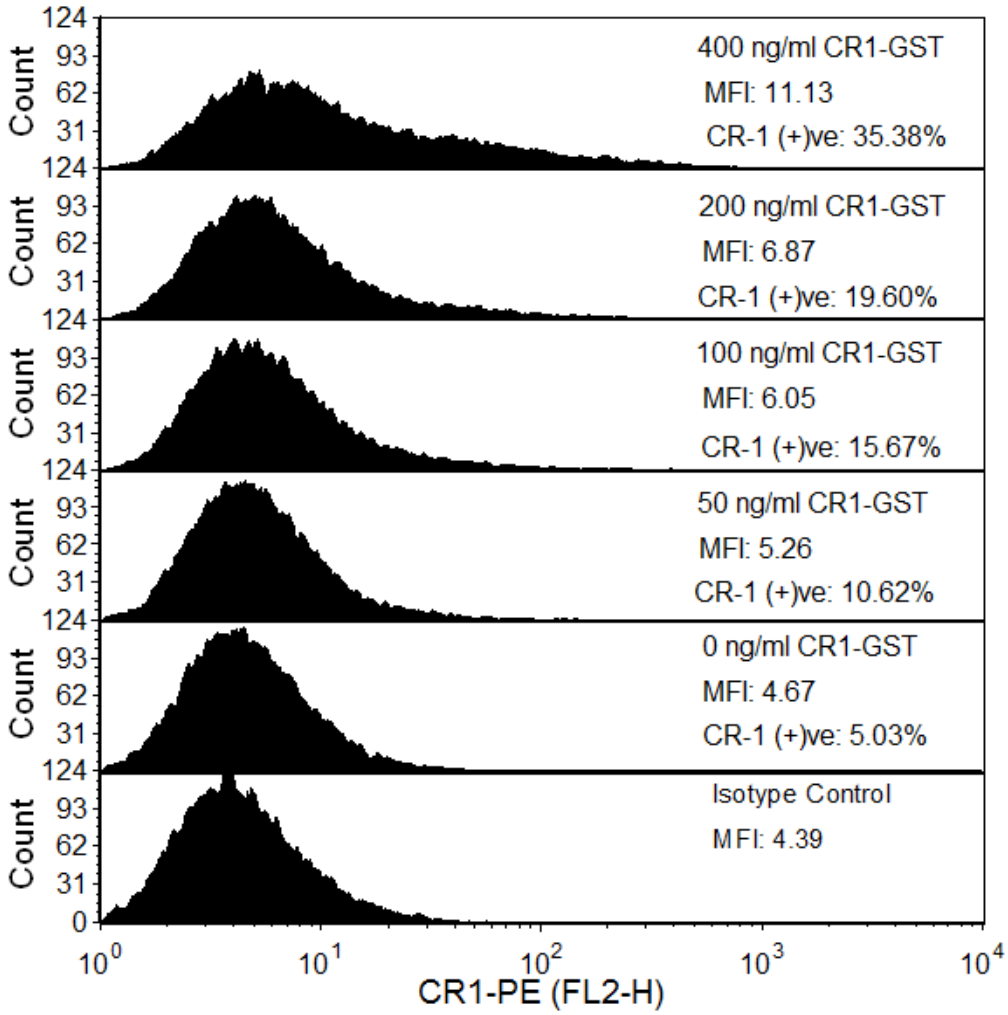

Figure 4.23: Flow cytometry to detect heterogeneity in induction of CR-1. U-87 MG cells were treated with different doses of CR1-GST for 24 hr and expression of CR-1 was measured. Cells treated with CR1-GST (400 ng/ml) but stained with isotype control antibody was used as negative control. This experiment has been repeated and one representative data is shown here.

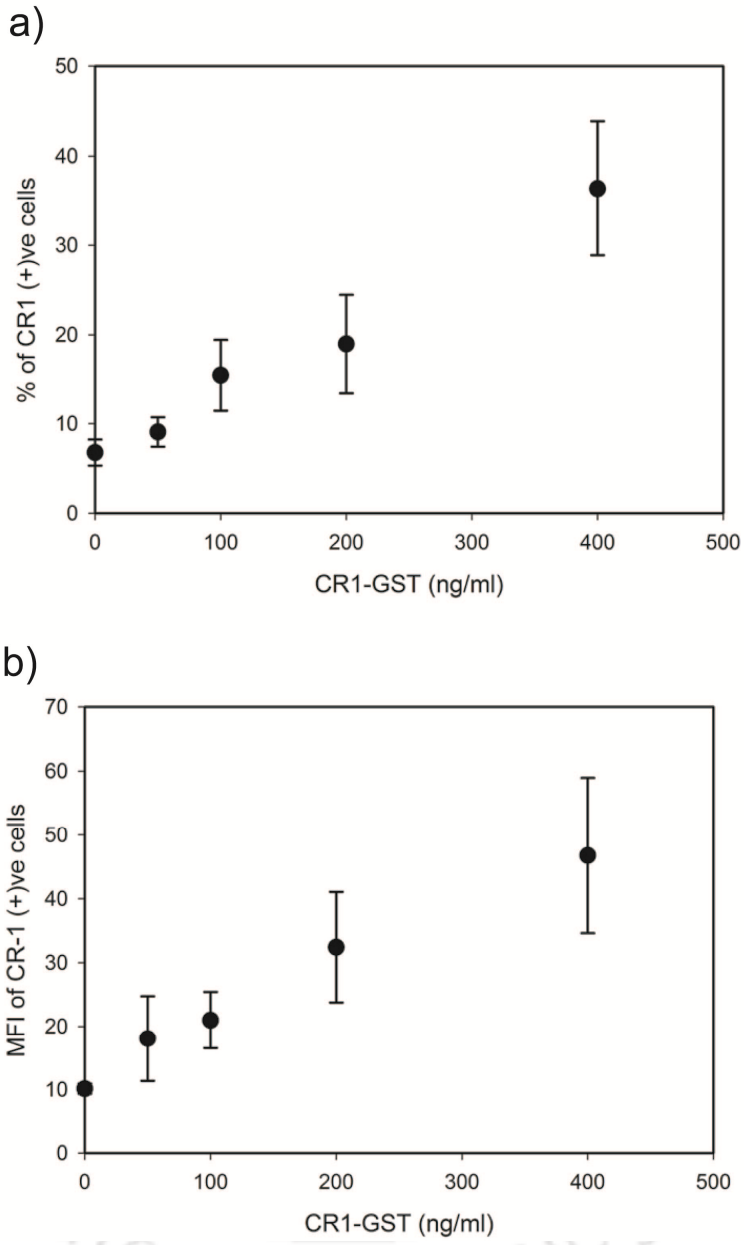

Figure 4.24: Dose dependent behavior of CR-1 positive subpopulation. U-87 MG cells were treated with different doses of CR1-GST for 24 hr and expression of CR-1 was measured by flow cytometry. (a) Percentage of cells in CR-1 positive subpopulation and (b) level of CR-1 expression, measured in terms of MFI, in cells of CR-1 positive subpopulation. Each data point represents mean of three independent experiments.

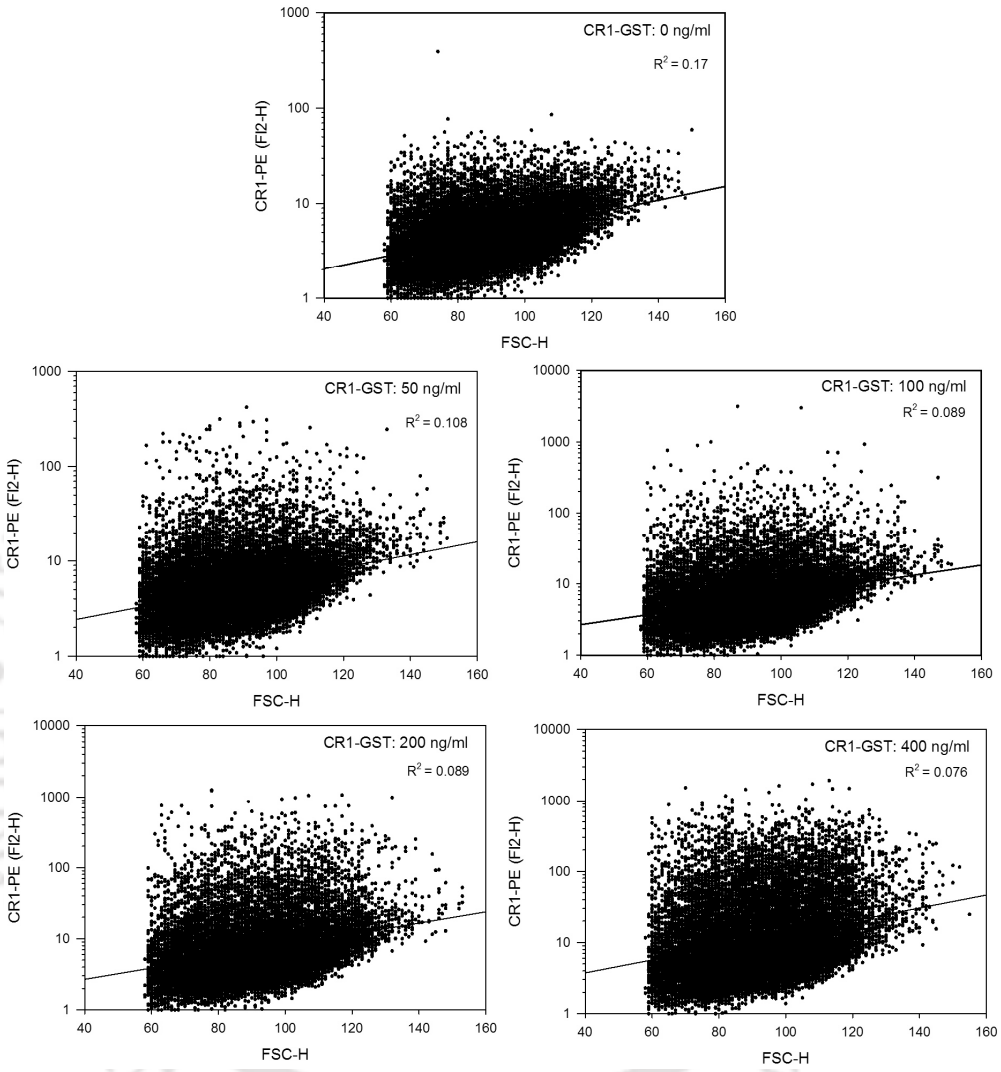

Figure 4.25: Dot-plot to show absence of any correlation between cells size (measured by FSC-H) and readings for CR1-PE in FL2-H. Data of a typical experiment with different treatment group is shown here. The straight line in each plot was obtained by linear regression. R^2: correlation coefficient.

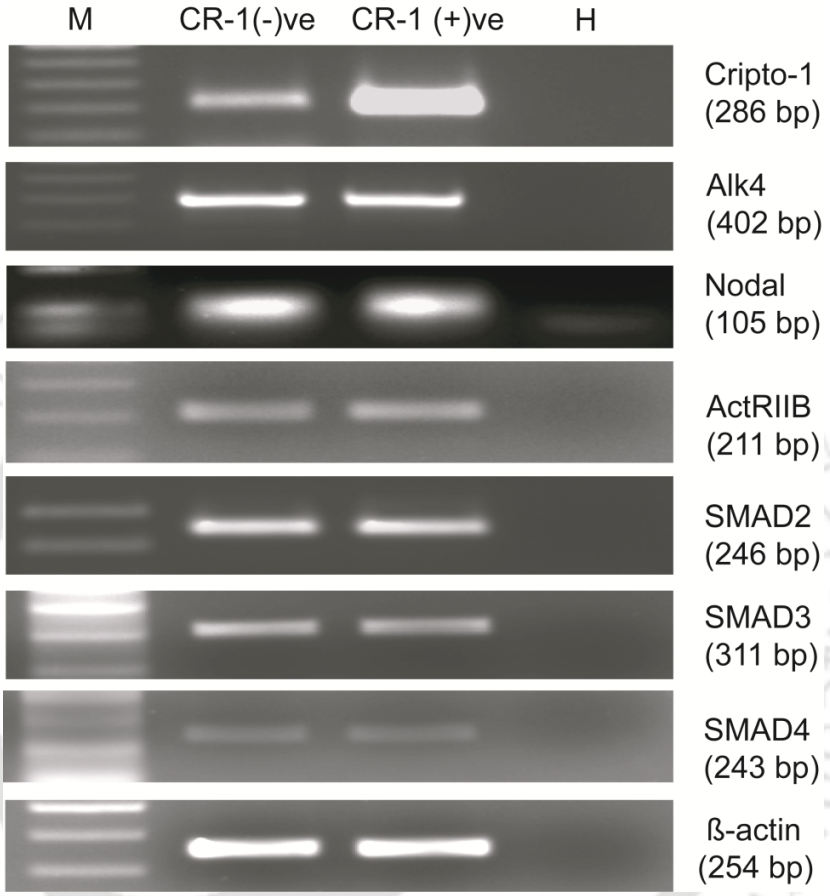

Figure 4.26: Expression of different pathway molecules in CR-1 positive and negative subpopulations. U-87 MG cells treated with CR1-GST (400 ng/ml) for 24 hr in serum free condition. CR-1 positive and CR-1 negative cells were sorted out and RT-PCR was used to measure gene expression. CR-1 (-)ve : CR-1 negative cells and CR-1 (+)ve : CR-1 positive cells. M is the marker and H is the water control.

4.12: Signature of Bimodality in CR-1 Induction:

Several groups have shown that positive feedback in transcriptional circuit gives rise to bimodal distribution in gene expression [119, 120]. A bimodal distribution will have two different modes. In flow cytometry experiments such distribution generates a fluorescence histogram with two distinct peaks. Though we have observed two subpopulations of CR-1 upon induction, we have not observed clear bimodal distribution with two distinct peaks in our flow cytometry data. Bimodality in a population is not clearly visible when both the populations are very close to each other [170], as it happened in our experiments. In our experiments, bimodality was further obscured as the background reading (measured in terms of the isotype control) was very high and had a long tail. We looked into the noise in the flow cytometry data to identify signature of bimodality. Noise in gene expression is usually measured in terms of coefficient of variation (CV), which is the ratio of standard deviation to mean [119]. We calculated mean and CV of FL2-H (i.e. CR1-PE) data in different treatment groups.

In our experiments, treatment with CR-1 increased mRNA of CR-1 without changing its stability. That means induction by exogenous CR-1 increases the rate of transcription of CR-1. Distribution of a protein in a population of cells usually follows unimodal distribution, like gamma, log-normal and Weibull distributions [108]. In such systems, increase in the rate of transcription increases mean level of the protein without changing the noise (CV) [108]. In our experiments, mean expression of CR-1 increased with the dose of recombinant CR-1 (Figure 4.27a). However, the noise in CR-1 expression was not constant but changed non-monotonically with increase in expression of CR-1 (Figure 4.27b). Initially, noise rises with increase in the inducing signal and reaches a maximum. Further increase in dose of recombinant CR-1 leads to increase in mean expression of CR-1 but decrease in noise.

This type of noise pattern can arise due to bimodal population distribution and have been observed earlier [158, 171]. In a mixed cell population, mean and CV are decided by the relative sizes and the statistical parameters of each subpopulation. In untreated cells, CR-1 positive subpopulation was miniscule. Statistical parameters of the whole population were decided primarily by the CR-1 negative subpopulation. With increase in the inducing signal, size of the CR-1 positive subpopulation increased and it affected the statistics of the whole population. This population had higher mean and variance. This led to increase in CV of the whole population. After a threshold, effect of the CR-1 positive subpopulation became dominant. With further

increase in this population, the CV of the whole population decreased and moved towards that of the CR-1 positive population.

Further, we took help of mathematical simulation to understand this type of noise behavior. We simulated a mixed population of cells with two subpopulations. One subpopulation has higher mean and variance than the other. Size of these subpopulations were varied and simulations were performed to show the effect of relative population sizes on the mean and CV of the whole population. We observed that in certain parameter regime, the CV of the whole population behaves similar to our observation (Figure 4.28).

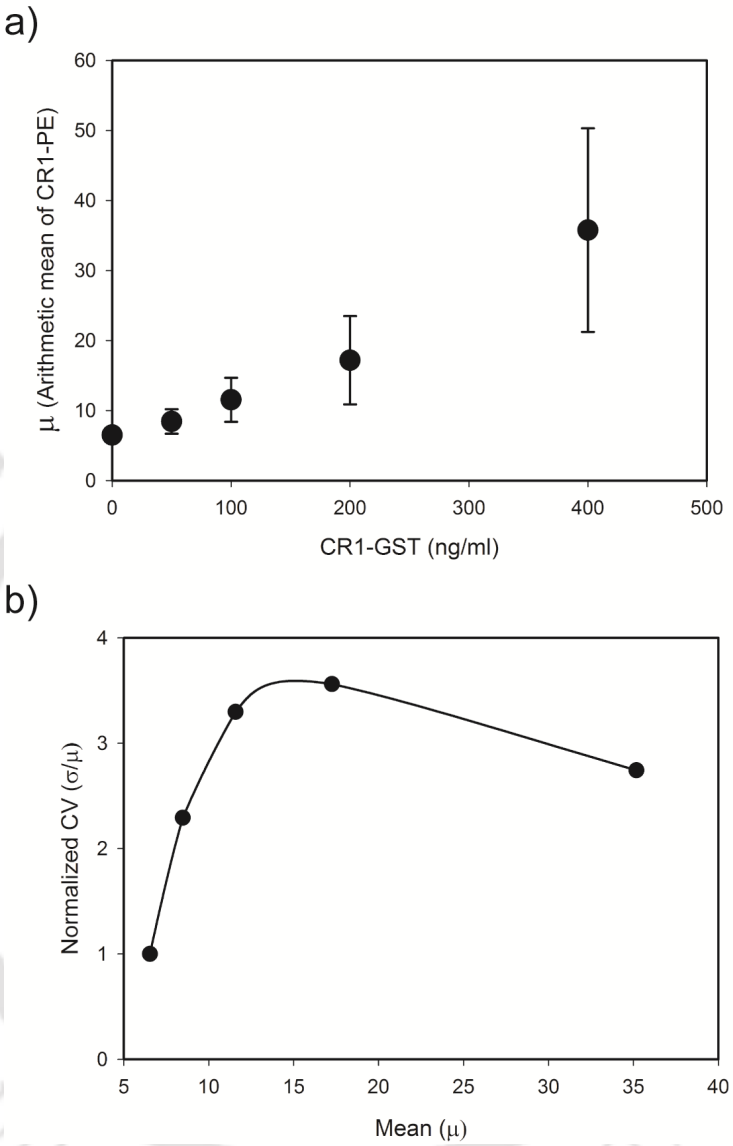

Figure 4.27: Noise in CR-1 induced expression of CR-1 in U-87 MG cells. Expression of CR-1 was measured by flow cytometry. a) Shows the change in mean of CR1-PE (FL2-H) reading for the whole population of cells with dose of recombinant CR-1. b) Shows the relation between mean and noise in CR-1 expression. Noise is represented in terms of normalized CV. CV of CR1-PE (FL2-H) of each treated sample was normalized by dividing with that of untreated cells. Average results of three independent experiments are shown here.

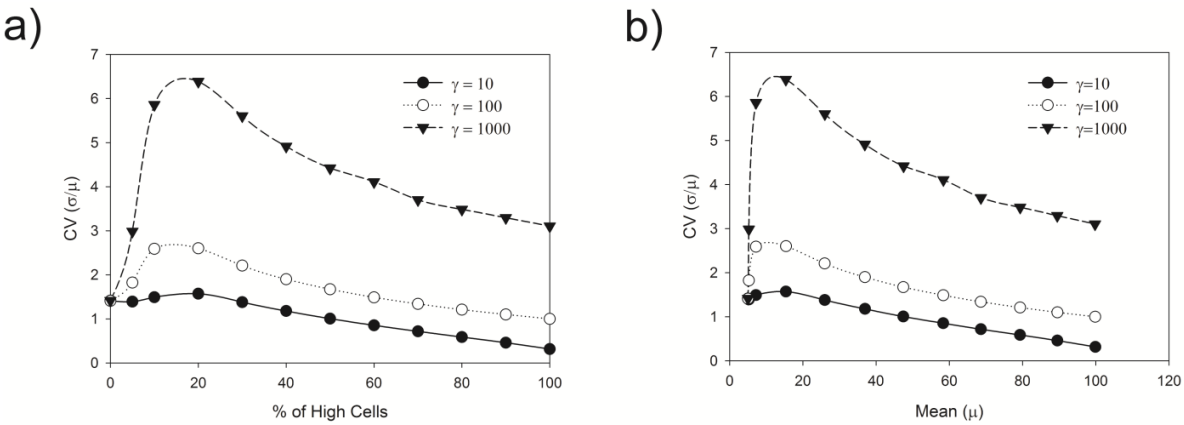

Figure 4.28: Simulated noise behavior of an ensemble of cells having two subpopulations. Both the subpopulations have lognormal distribution. One subpopulation has lower mean and variance than the other, and is called "Low cells". It is equivalent to CR-1 negative population in our experiments. Mean and variance of the other subpopulation (called High cells) is higher and equivalent to CR-1 positive subpopulation in our experiment. The size of this subpopulation was varied from 0 to 100 % of the whole population. Similar to our experimental observation, the mean and variance of this subpopulation was increased with increase in its size. We have simulated 20000 cells in one run with a particular set of parameter values. Each run was repeated 1000 times and the average result is shown here. For Low cells: $\mu = 5$ and $\sigma^2 = 50$. For High cells: μ varied from 10 to 100 and $\gamma = \sigma^2/\mu = 10$, 100, and 1000. Parameters were not obtained by any fitting with experimental data. Rather those have been chosen to achieve a trend in noise similar to our observation. Simulations were performed using MATLAB. a) Shows change in CV of the whole population with increase in percentage of High cells. b) Shows relation between mean and CV, as the percentage of High cells increases.

4.13: Significance of CR-1 positive cells:

Heterogeneity in expression of CR-1 has been observed earlier too [85, 168]. Watanabe *et al.* [85] have observed that human embryonal carcinoma, NTERA2/D1, cells have two populations, CR-1 high and low. The heterogeneous expression of CR-1 observed by Watanabe *et al.* [89] and Strizzi *et al.* [168] can also be explained in terms of autoregulatory positive feedback proposed in the present work. Interestingly, Watanabe *e. al.* [85] observed that markers of pluripotent stem cells, NANOG, Oct4, and Sox2 had higher expression in CR-1 high population. Similarly, Strizzi *et al.* [172] have observed that only a small subpopulation of melanoma cell line C8161 is CR-1 positive and these cells expresses higher amount of Oct4, NANOG and MDR1. It has been suggested that such CR-1 positive subpopulation of cells may be potential cancer stem cells [172, 173]. Cancer stem cells (CSCs) are minority subpopulation of tumor cells that are tumorigenic and have stem cell properties of self-renewal and differentiation [174]. CSCs have been implicated in development of drug resistance and it often found to overexpress drug efflux proteins like MDR1 [175].

CR-1-positive cells have high MDR1:

MDR1 is a member of ABC transporter family of membrane pumps that use ATP hydrolysis to efflux various drugs from a cell. Strizzi *et al.* [168] have earlier reported that CR-1 positive melanoma cells have higher expression of the multidrug resistance protein MDR1. Hu *et al.* [176] have shown that Doxorubicin selected drug resistant leukaemia cell line has higher expression of CR-1 and MDR1. Nakai *et al.* [177] established a cell line derived from spheroid culture of U-87 MG cells that showed drug resistance and higher expression of MDR1.

To investigate the relation of CR-1-positive cells with MDR1, we have treated U-87 MG cells with recombinant CR-1 (400 ng/ml) for 24 hr in serum free condition. Subsequently, CR-1-positive and CR-1-negative cells were sorted out and expression of MDR1 in these subpopulations was checked using RT-PCR. Interestingly, we have observed that expression of MDR1 is higher in CR-1-positive cells (Figure 4.29a). Further, we used flow cytometry to characterize MDR1 expression with respect to CR-1 expression. U-87 MG cells were treated with recombinant CR-1 (400 ng/ml) for 24 hr in serum free conditions. Flow cytometry was performed to detect CR-1 (FL2-H) using anti-CR1-PE and MDR1 (FL1-H) using anti-P-Glycoprotein-FITC. We have observed that, like CR-1, MDR1 is expressed at detectable level only in a minor subpopulation (~13%) of U-87 MG cells. Treatment with CR-1 (400 ng/ml) increased MDR1

positive population to ~37%. As shown in Figure 4.29b, most of these induced cells are positive for both CR-1 and MDR1. Therefore, CR-1 co-induced expression of CR-1 and MDR1 in a minority subpopulation of U-87 MG cells.

There exists similarity in transcriptional control of expression of CR-1 and MDR1. Like CR-1, MDR1 is also a target of HIF [178] and β-catenin [179]. TGF-β also induces expression of MDR1 [180, 181] and there exist crosstalks between TGF-β/SMAD2/3 and β-catenin pathways [182, 183]. Further, AP-1 also controls expression of MDR1 [184] and it is also known that SMAD interacts with AP-1 [185]. Interestingly, Hu *et al.* [176] have shown that treatment of a multidrug resistant leukemia cell line with an anti-CR-1 antibody led to slight decrease in expression of MDR-1. Therefore, one can speculate that induction in MDR1 expression in U-87 MG cells by CR-1 may be happening through crosstalk between transcription factors controlling MDR1 expression and Alk4/SMAD2/3 pathway. Such crosstalk would lead to correlated population dynamics of expression of CR-1 and MDR-1, as we have observed.

CR-1-positive U-87 MG cells may not be Cancer Stem Cells (CSCs):

Watanabe *et al.* [85] and Strizzi *et al.* [172] have suggested that CR-1 positive cells have higher expression of markers of pluripotent stem cells, NANOG, Oct4 and Sox2. To investigate this, we have treated U-87 MG cells with recombinant CR-1 (400 ng/ml) and subsequently separated out CR-1 positive cells and CR-1 negative cells. Subsequently, we have checked the expression of stem cell markers CD133, Oct-4, NANOG, and Sox2 in CR-1-positive and negative subpopulations of CR-1 treated U-87 MG cells (Figure 4.30). We have not observed any increase in expression of these molecules in CR-1 positive subpopulation. These observations make us believe that the CR-1 positive population in U-87 MG cells may not have stem cell like characteristics as observed in other cellular systems.

Our experiments indicate that a CR-1 positive subpopulation may emerge spontaneously due to the autoregulatory positive feedback in its transcriptional control. This will happen even in absence of expression of other molecules of embryonic stem cells. Simultaneous but independent activation of other molecular events may lead to expression of key molecules of embryonic stem cells like NANOG and Oct-4. Some of these molecules may further activate expression of CR-1. Additionally, many of those molecules may show heterogeneous expression. Coupling of all these processes may lead to emergence of two subpopulations of CR-1 expressing cell: one with higher expression of CR-1, MDR-1 and other markers of pluripotency and the other with lower

expression of these molecules. Though small in size, such CR-1 high subpopulation may eventually play crucial role in progression of cancer.

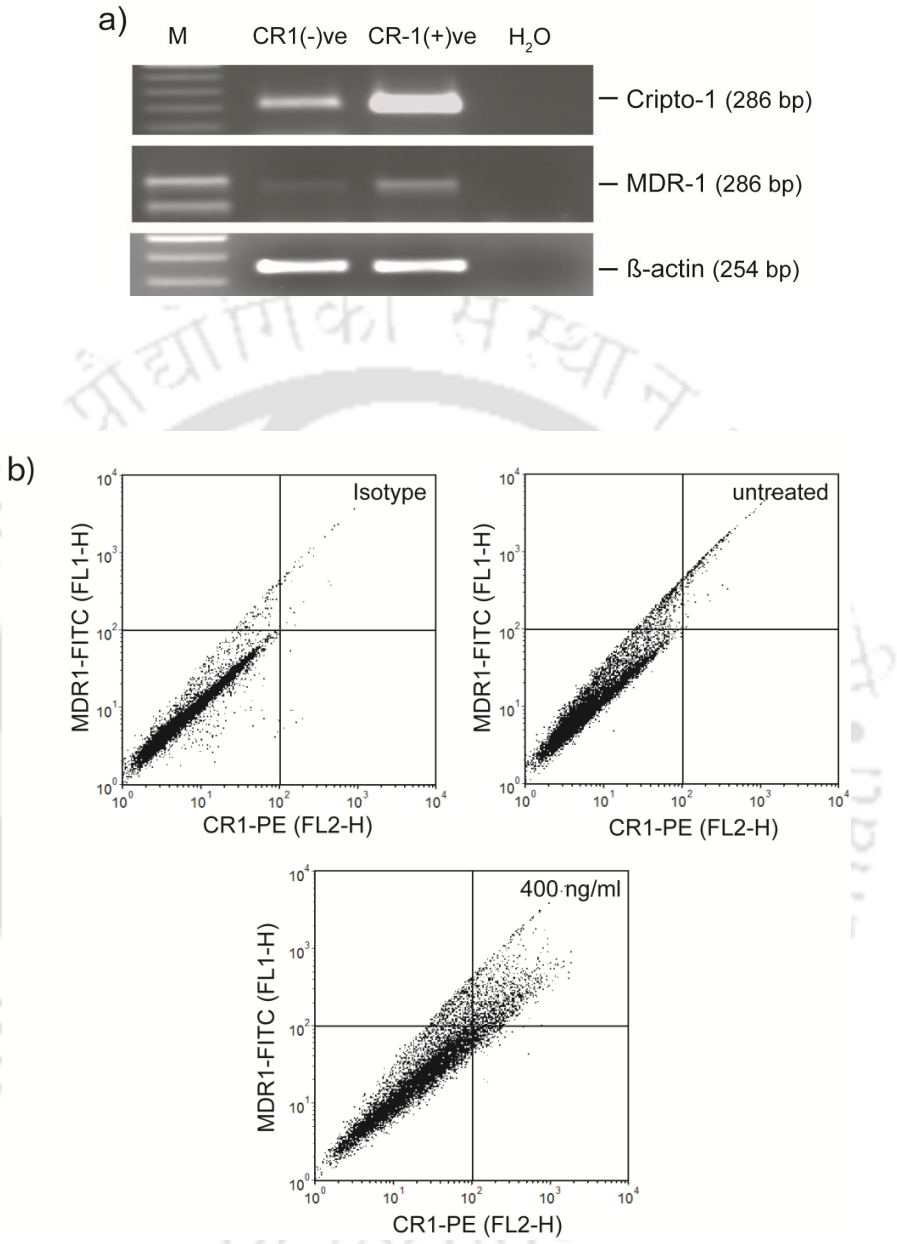

Figure 4.29: CR-1 positive subpopulations have higher expression of MDR-1. a) U-87 MG cells treated with CR1-GST (400 ng/ml) for 24 hr were sorted in two subpopulations and RT-PCR was used to measure gene expression. CR1(-)ve : CR-1 negative cells and CR(+)ve: CR-1 positive cells. b) Cells were treated with CR1-GST (400 ng/ml) or left untreated for 24 hr and expression of CR-1 and MDR-1 was measured by flow cytometry. Cells treated with CR1-GST (400 ng/ml) but stained with isotype control antibodies was used as negative control.

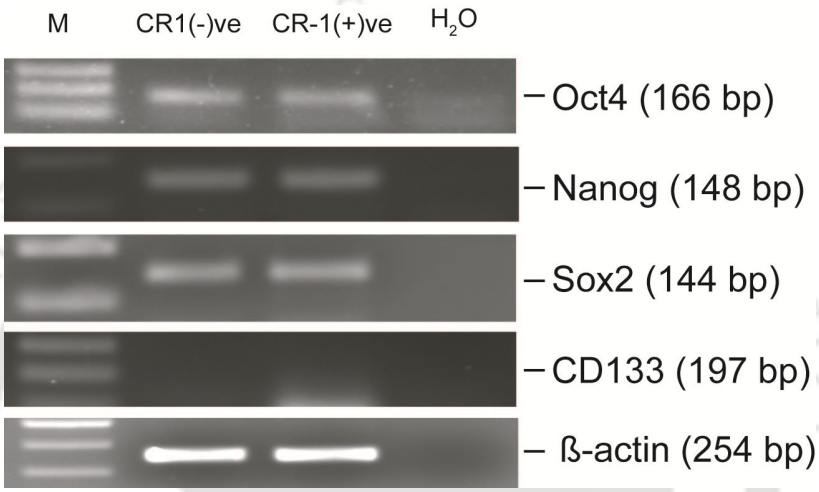

Figure 4.30: Expression of different markers for pluripotency in CR-1 positive and negative subpopulations. U-87 MG cells treated with CR1-GST (400 ng/ml) for 24 hr in serum free condition. CR-1 positive and CR-1 negative cells were sorted out and RT-PCR was used to measure gene expression. CR-1(-)ve : CR-1 negative cells and CR-1(+)ve : CR-1 positive cells.

4.14: Effects of growth factors on CR-1 expression:

So far, we have discussed about the autoregulatory control of CR-1 expression through Alk4/SMAD2/3 pathway. We have also observed that such induction is heterogeneous, with two subpopulations having low and high expression of CR-1. Subsequently, we looked into the roles of other cardinal signaling pathways in expression of CR-1. Several growth factors, involved in embryonic development and cancer, signals through PI3K/Akt and MAPK/Erk pathways [186, 187]. However, role of these two cardinal pathways in CR-1 expression have not been investigated.

All of our experiments, discussed so far, were performed using cells treated in absence of serum. Serum contains several growth factors that can trigger multiple pathways, particularly SMAD2/3, PI3K/Akt and MAPK/Erk pathways. To check the probable role of PI3K/Akt and MAPK/Erk pathways, we treated U-87 MG cells with 200 ng/ml of recombinant CR-1 for 24 hrs in presence and absence of serum. We used 10% FBS in this experiment. Interestingly, we have observed that, treatment with exogenous CR-1 failed to induce CR-1 expression in presence of serum (Figure 4.31). This indicated that some growth factors present in serum may be negatively regulating CR-1 expression.

To investigate this further, we used inhibitors of PI3K/Akt and MAPK/Erk pathways in our experiments. We have used LY294002 and U0126, potent inhibitors of PI3K and MAPK pathways respectively as shown in Figure 4.32a [188, 189]. However, complete blockage of these pathways may hinder the normal physiology of cells. Therefore, it was necessary to decide the suitable doses of these inhibitors for our experiments.

U-87 MG cells were treated with different concentration of these inhibitors and MTT assay was performed to measure the effect of LY294002 (Figure 4.32b) and U0126 (Figure 4.32c) on cell viability. Based on these data, 1.5 μM of LY294002 and 6 μM U0126 was used in our subsequent experiments. Inhibitors at these doses did not have considerable deleterious effect on the cell viability.

U-87 MG cells were treated with LY294002 (1.5 μM) in presence 10% FBS for 24 hr and expression of CR-1 was checked by RT-PCR. As shown in figure 4.33a, inhibition of PI3k pathway led to induction in expression of CR-1 in these cells. Such increase in CR-1 expression

was also observed in U-87 MG cells treated with MAPK inhibitor (Figure 4.33b). These observations indicated that both the pathways negatively regulate the expression of CR-1.

Further, real-time PCR was used to investigate the crosstalk between PI3K pathway and Alk4/SMAD2/3 pathway in control of CR-1 expression. U-87 MG cells were treated with different combinations of LY294002, and SB-431542 in presence and absence of serum (10%) for 24 hr. Expression of CR-1 was measured by real-time PCR (Figure 4.34a). Similar to our earlier observation in RT-PCR, inhibition of PI3K pathway, by LY294002, in U-87 MG cells, maintained in 10% serum, led to six-fold increase in expression of CR-1. However, such inhibition did not have considerable effect on CR-1 expression in cells maintained without serum. Similar experiments were performed in presence of Alk4 inhibitor SB-431542. As shown in Figure 4.34a, inhibition of PI3k pathway does not have considerable effect on CR-1 expression in cells treated with SB-431542. These observations indicate that the induction in CR-1 expression in U-87 MG cells involves Alk4/SMAD2/3 pathway and activation of PI3K pathway negatively regulate Alk4/SMAD2/3 mediated expression of CR-1. Serum would have components to activate both PI3K/Akt and Alk4/SMAd2/3 pathways. In presence of serum, PI3K pathway gets activated and opposes Alk4/SMAD2/3 mediated expression of CR-1. Inhibition of PI3K by LY294002, removes such negative effect and CR-1 expression is induced.

Subsequently we induced expression of CR-1 by treating U-87 MG cells with recombinant CR-1, in presence and absence of LY294002. This treatment was performed in absence of serum. We expected that recombinant CR-1 would activate the Alk4/SMAD2/3 pathway and LY294002 would inhibit any basal level activity of PI3k/Akt pathway. As shown in Figure 4.34b, in presence of PI3K inhibitor, treatment with exogenous CR-1 leads to an enormous increase (~42 fold) in CR-1 expression. Such increase in CR-1 expression was not achieved when cells were co-treated with Alk4 inhibitor.

These observations confirmed our proposal that the PI3k/Akt pathway negatively regulate Alk4/SMAD2/3 mediated expression of CR-1. However, we are not being able to investigate further molecular details of these opposing activities. Such crosstalk between SMAD2/3 pathway and PI3K/Akt pathway has been observed earlier. Several studies have shown that MAPKs and Akt controls intracellular distribution and transcriptional activities of R-SMADs [190]. Both these pathways also regulate a variety of SMAD binding molecules, thereby indirectly affecting transcriptional control by SMADs [190]. Such crosstalk is very crucial in embryonic cells. Singh *et al.* [142] have shown that PI3k/Akt pathway modulates SMAD2/3 pathway in pluripotent cells.

They have shown that activation of PI3K/Akt pathway suppresses Wnt signaling, allowing SMAD2/3 to activate specific genes, like NANOG, required for self-renewal. On the other hand, when PI3K/akt pathway is blocked, activation of Wnt pathways leads to SMAD2/3 mediated cellular differentiation.

Though the molecular mechanism is not known, our observations on the crosstalk between Alk4/SMAD2/3 and PI3K/Akt and MAPK pathways leads to certain questions that are very relevant in cancer therapy. Various drugs, like Erlotinib, are currently used in clinic to block overactive PI3K/Akt and MAPK pathways in cancer cells. Based on our observation, one may expect that use of such inhibitors may lead to enhanced expression of CR-1. CR-1 is known to help cell proliferation, angiogenesis and metastasis. Such drug induced increase in CR-1 expression, would eventually counteract the effects of the drug, and would reduce its efficacy.

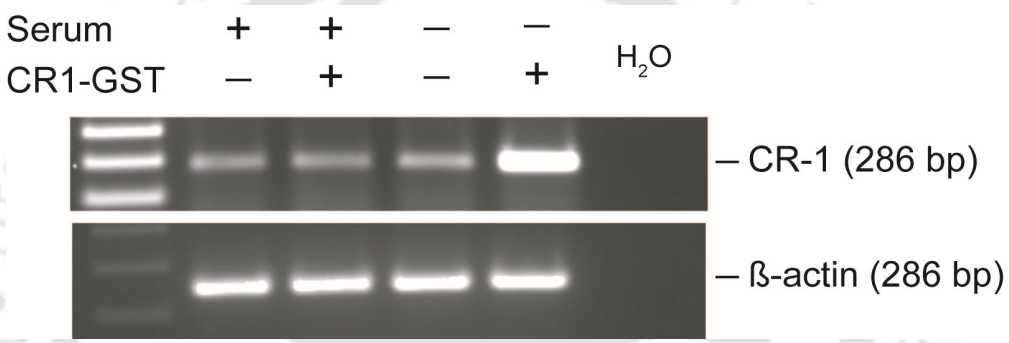

Figure 4.31: Induction of CR-1 expression fails in presence of serum. U-87 MG cells were treated CR1-GST (200 ng/ml) for 24 hr in absence or presence of FBS (10%). FBS was used as a source growth factors. Expression of CR-1 was checked by RT-PCR.

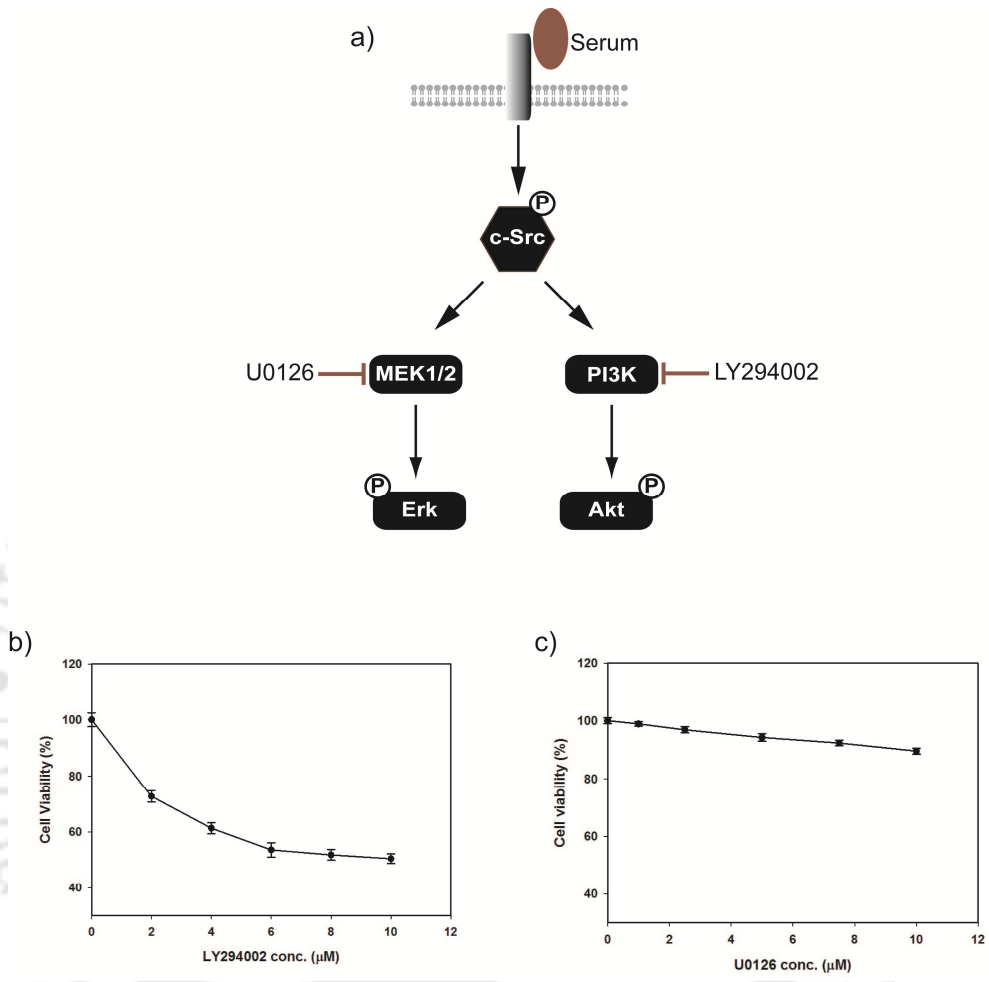

Figure 4.32: PI3K and MAPK inhibitors. a) Schematic representation of using PI3K inhibitor, LY294002 and MAPK inhibitor, U0126 in the respective pathways. MTT assay to decide suitable concentration of b) LY294002 and c) U0126. For both b) & c), U-87 MG cells were treated with different concentrations of inhibitors for 24 hr. Cell viability was measured by MTT assay. Each data point's represents mean of four different wells. 1.5 μM LY294002 and 6 μM U0126 were used in subsequent experiments.

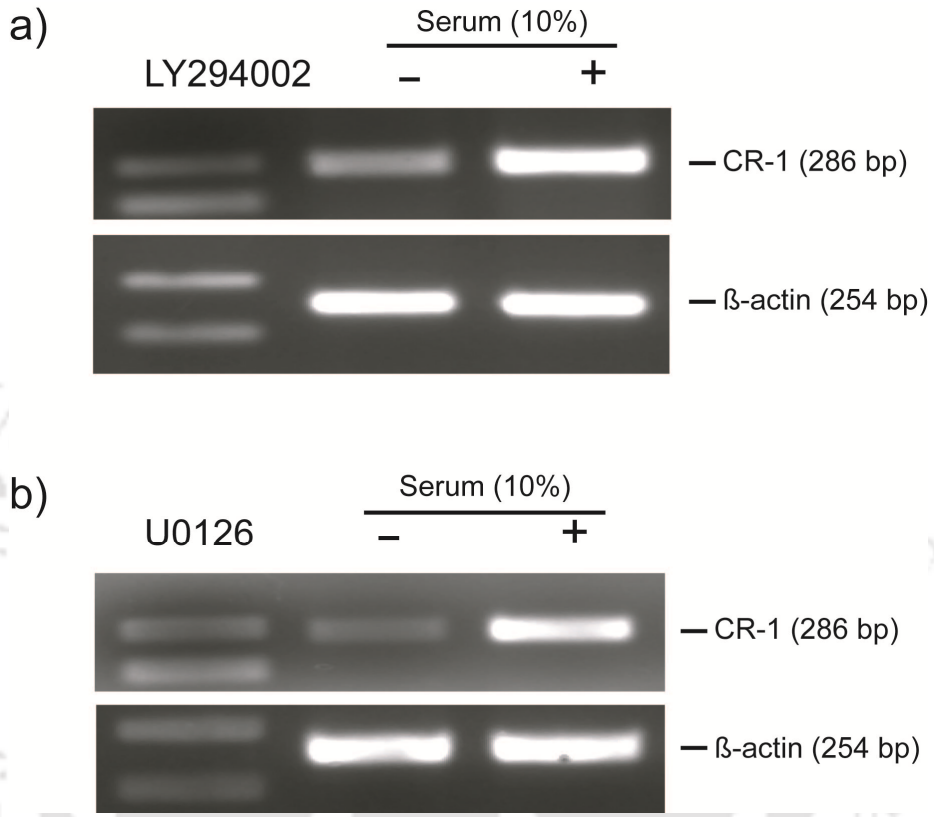

Figure 4.33: Expression of CR-1 in presence of a) PI3K inhbitor, LY294002 (1.5 μM), and b) MAPK inhibitor, U0126 (6 μM). U-87 MG cells were treated for 24 hr in presence of serum (10%). Expression of CR-1 was checked by RT-PCR.

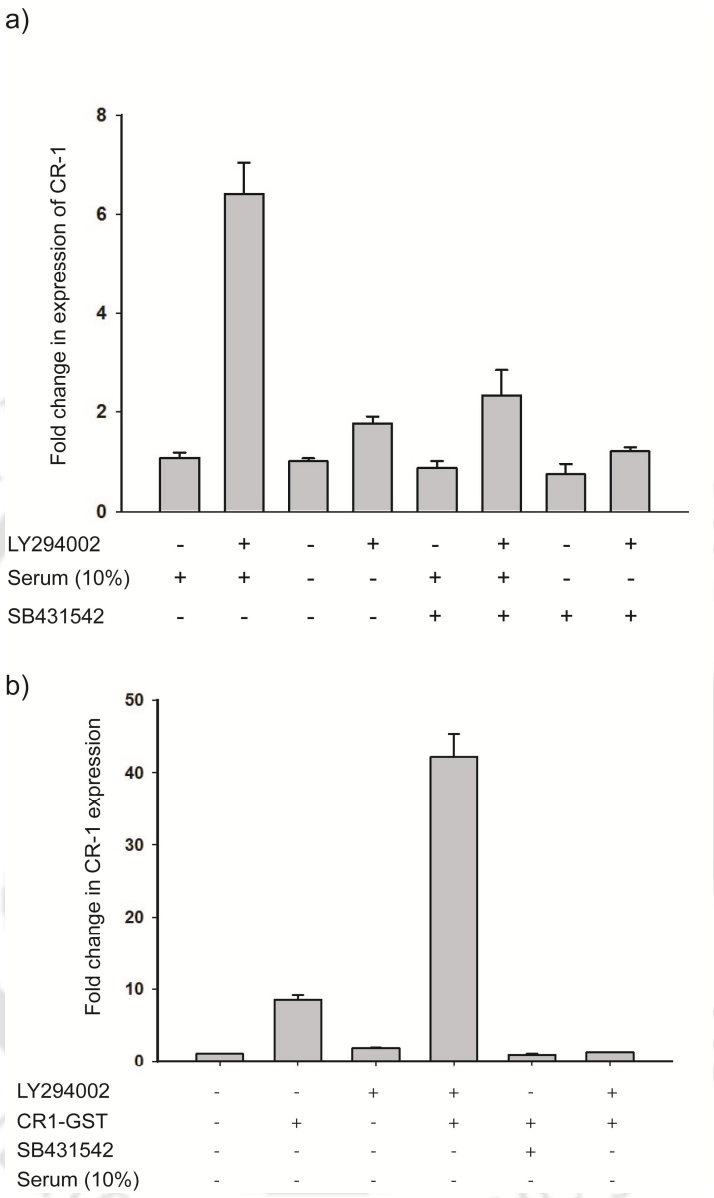

Figure 4.34: Expression of CR-1 in U-87 MG cells treated with different inhibitors and activators. a) Treated with or without LY294002, serum (10%) and CR1-GST (200 ng/ml). b) Treated with or without LY294002, SB431542, serum (10%) and CR1-GST (200 ng/ml). Expression of CR-1 was measured using real-time PCR. Each data point represents average of four independent experiments.

4.15: Combinatorial control of CR-1 expression:

In this work, we have shown that CR-1 can induce its own expression through Alk4/SMAD2/3 pathway. This creates a possible autoregulatory positive feedback. Positive feedback often enhances heterogeneity in gene expression and triggers formation of two subpopulations. Corresponding to this, we have also observed that induction of CR-1/Nodal/Alk4/SMAD2/3 pathway leads to heterogeneous expression of CR-1, with a minority subpopulation having induction in expression of CR-1.

We have also shown that induction in expression of CR-1 through Alk4/SMAD2/3 pathway is negatively regulated by two cardinal growth factor pathways, PI3K/Akt and MAPK/Erk. These two pathways are often activated during embryonic development and in cancer cells. Even CR-1 can also activate these two pathways in certain cellular systems. Taken together, one can conclude that expression of CR-1 is controlled through multiple pathways in a combinatorial fashion.

Signaling pathways are not isolated from each other but are interconnected to form a complex network. Cells receive information through multiple signaling pathways and they must then integrate this information to achieve a particular cellular function [191, 192]. Combinatorial effects of multiple pathways, often working against each other, eventually lead to regulated and balanced expression of a particular gene [193, 194]. Being a molecule involved in embryonic development, expression of CR-1 requires fine spatial and temporal control. Combinatorial control through multiple pathways, with non-linear components like feedback, can fine tune such expression. Our present work opens a window to further investigate such combinatorial control.

5 Conclusions

In this work, we have explored the transcriptional circuit of human Cripto-1. Based on the existing information in literature, we hypothesized that CR-1 can activate its own expression through Nodal/Alk4/SMAD2/3 pathway. By treating U-87 MG cells with exogenous recombinant CR-1, we have shown that, indeed CR-1 can induce its own expression through this pathway. We have confirmed that such induction involves only the transcript variant-1 of CR-1, coding for the full-length protein, and confirmed that CR-3, the Cripto pseudogene, is not expressed or induced in this system. We have shown that such induction increases both CR-1 transcript and protein. We have proved that treatment with recombinant CR-1 does not affect the stability of CR-1 mRNA. This confirmed that CR-1 mediated activation of Alk4/SMAD2/3 pathway, increases transcription of CR-1 in these cells. Interestingly, CR-1 mediated induction of CR-1 expression has sigmoidal dose-response behavior, with Hill-coeffecient greater than one, indicating that this system is ultra-sensitive and may involve cooperativity among transcription factors.

Induction of CR-1 expression, by CR-1 itself, creates an autoregulatory positive feedback. Theoretical and experimental works have shown that an ultra-sensitive transcriptional circuit with positive feedback can lead to bimodal gene expression. This led us to hypothesize that induction of CR-1 expression, by CR-1, may lead to bimodal gene expression. We investigated cell-to-cell variation in CR-1 expression using flow cytometry. Similar to our hypothesis, we observed that CR-1 mediated induction led to formation of two subpopulations, one with higher expression of CR-1 and the other having lower basal level expression. The size of the subpopulation having higher expression of CR-1 is smaller and it increases with increase in the inducing signal. However, we have not observed clear bimodality with two distinct peaks in our flow cytometry data. Bimodality gets obscured when background readings are high and the difference in two subpopulations is small. We looked into the noise in CR-1 expression and used the behavior of noise to substantiate the existence of two subpopulations having different level of CR-1 expression.

We have also observed that expression of CR-1 and MDR1, a gene related to drug resistance, are correlated. We have shown that treatment with CR-1 co-induces CR-1 and MDR1 expression in the same subpopulation of cells.

Going beyond the Alk4/SMAD2/3 pathway, we also proved the involvement of PI3K/Akt and MAPK pathways in control of CR-1 expression. We have shown that PI3K/Akt pathway negatively regulate Alk4/SMAD2/3 mediated induction of CR-1 expression.

Off late, designs in molecular circuits in biology have got much attention. Over the years, extensive theoretical development has happened to understand the design and function of such circuits. However, those theoretical/mathematical ideas are not extensively used in experimental exploration of molecular pathways. Theoretical and experimental works in model systems have shown that architecture of transcriptional circuits affects gene expression heterogeneity. In the present work, we used this idea to explore transcriptional control and expression of CR-1.

Cell-to-cell variability in gene expression is very crucial in embryonic development. We have established that two subpopulations of cells, having high and low expression of CR-1, emerge through an autoregulatory pathway. This would help further to understand the role of CR-1 in cellular pattern formation during development.

Such heterogeneity in CR-1 expression would be useful also to understand its role in cancer. Cellular heterogeneity in a tumor is a well-established phenomenon. Stochastic accumulation of mutations/genetic alternations is usually blamed for such heterogeneity. Our key observation that CR-1 mediated induction leads to heterogeneity in CR-1 expression would help to substantiate the role of non-genetic heterogeneity in development and progression of cancer. If investigated, one may find autoregulatory positive feedback in transcriptional control of many more molecules involved oncogenesis. Many of those genes may have bimodal expression emerging spontaneously due to the very nature of the transcriptional circuit. Investigating such heterogeneity in gene expression would enrich our understanding of origin and progression of cancer.

In this work we have focused on the autoregulatory mechanism of transcriptional control of CR-1 expression. Dynamics and the noise in gene expression also depend on some other factors, like state of the promoter. Epigenetic modifications, like DNA-methylation and histone acetylation,

changes the local chromatin architecture of a promoter. Such changes affect the probabilities of promoter transition between ON and OFF states. Changes in transition probabilities would affect the heterogeneity in gene expression. Genes involved in embryonic developments are often controlled through epigenetic modifications. It would be interesting to investigate the role of such epigenetic changes on the heterogeneity of CR-1 expression.

The correlated induction of CR-1 and MDR-1 expression in a subpopulation of cells is a critical observation in this work. Future investigations in this direction would help to understand spontaneous emergence of drug resistance in cancer.

Involvement of PI3K/Akt pathway in negative regulation of Alk4/SMAD2/3 mediated CR-1 expression is one of the novel observations in this work. Further study is required to identify the connections between these two pathways in regulation of CR-1. PI3k/Akt and MAPK pathways are cardinal pathways in oncogenic signaling. Several drugs have been developed to inhibit signaling through these pathways. Our observations indicate that use of those pathway blockers may eventually increase expression of CR-1. Being a mitogen, such increase in CR-1 expression would affect the efficacy of the drug itself. Chemotherapy induced activation of pro-oncogenic pathways is an active area of research. This is shifting our focus from mutations in pathway molecules, to the crosstalk of different pathways, to understand development of drug resistance in cancer. Our observations provide a new clue in that direction.

6 Bibliography

1. Ciccodicola A, Dono R, Obici S, Simeone A, Zollo M, Persico MG: **Molecular characterization of a gene of the 'EGF family' expressed in undifferentiated human NTERA2 teratocarcinoma cells**. *EMBO J* 1989, **8**(7):1987-1991.
2. Shen MM, Wang H, Leder P: **A differential display strategy identifies Cryptic, a novel EGF-related gene expressed in the axial and lateral mesoderm during mouse gastrulation**. *Development* 1997, **124**(2):429-442.
3. Kinoshita N, Minshull J, Kirschner MW: **The identification of two novel ligands of the FGF receptor by a yeast screening method and their activity in Xenopus development**. *Cell* 1995, **83**(4):621-630.
4. Zhang J, Talbot WS, Schier AF: **Positional cloning identifies zebrafish one-eyed pinhead as a permissive EGF-related ligand required during gastrulation**. *Cell* 1998, **92**(2):241-251.
5. Scognamiglio B, Baldassarre G, Cassano C, Tucci M, Montuori N, Dono R, Lembo G, Barra A, Lago CT, Viglietto G *et al*: **Assignment of human teratocarcinoma derived growth factor (TDGF) sequences to chromosomes 2q37, 3q22, 6p25 and 19q13.1**. *Cytogenet Cell Genet* 1999, **84**(3-4):220-224.
6. Saloman DS, Bianco C, Ebert AD, Khan NI, De Santis M, Normanno N, Wechselberger C, Seno M, Williams K, Sanicola M *et al*: **The EGF-CFC family: novel epidermal growth factor-related proteins in development and cancer**. *Endocr Relat Cancer* 2000, **7**(4):199-226.
7. Harari PM: **Epidermal growth factor receptor inhibition strategies in oncology**. *Endocr Relat Cancer* 2004, **11**(4):689-708.
8. Watanabe K, Bianco C, Strizzi L, Hamada S, Mancino M, Bailly V, Mo W, Wen D, Miatkowski K, Gonzales M *et al*: **Growth factor induction of Cripto-1 shedding by glycosylphosphatidylinositol-phospholipase D and enhancement of endothelial cell migration**. *The Journal of biological chemistry* 2007, **282**(43):31643-31655.
9. Bianco C, Wechselberger C, Ebert A, Khan NI, Sun Y, Salomon DS: **Identification of Cripto-1 in human milk**. *Breast Cancer Res Treat* 2001, **66**(1):1-7.

10. Bianco C, Strizzi L, Mancino M, Rehman A, Hamada S, Watanabe K, De Luca A, Jones B, Balogh G, Russo J *et al*: **Identification of cripto-1 as a novel serologic marker for breast and colon cancer**. *Clin Cancer Res* 2006, **12**(17):5158-5164.
11. Rosa FM: **Cripto, a multifunctional partner in signaling: molecular forms and activities**. *Sci STKE* 2002, **2002**(158):pe47.
12. Strizzi L, Bianco C, Normanno N, Salomon D: **Cripto-1: a multifunctional modulator during embryogenesis and oncogenesis**. *Oncogene* 2005, **24**(37):5731-5741.
13. Bianco C, Kannan S, De Santis M, Seno M, Tang CK, Martinez-Lacaci I, Kim N, Wallace-Jones B, Lippman ME, Ebert AD *et al*: **Cripto-1 indirectly stimulates the tyrosine phosphorylation of erb B-4 through a novel receptor**. *The Journal of biological chemistry* 1999, **274**(13):8624-8629.
14. Shi S, Ge C, Luo Y, Hou X, Haltiwanger RS, Stanley P: **The threonine that carries fucose, but not fucose, is required for Cripto to facilitate Nodal signaling**. *The Journal of biological chemistry* 2007, **282**(28):20133-20141.
15. Minchiotti G, Manco G, Parisi S, Lago CT, Rosa F, Persico MG: **Structure-function analysis of the EGF-CFC family member Cripto identifies residues essential for nodal signalling**. *Development* 2001, **128**(22):4501-4510.
16. Yan YT, Liu JJ, Luo Y, E C, Haltiwanger RS, Abate-Shen C, Shen MM: **Dual roles of Cripto as a ligand and coreceptor in the nodal signaling pathway**. *Mol Cell Biol* 2002, **22**(13):4439-4449.
17. Bianco C, Adkins HB, Wechselberger C, Seno M, Normanno N, De Luca A, Sun Y, Khan N, Kenney N, Ebert A *et al*: **Cripto-1 activates nodal- and ALK4-dependent and -independent signaling pathways in mammary epithelial Cells**. *Mol Cell Biol* 2002, **22**(8):2586-2597.
18. Bianco C, Strizzi L, Rehman A, Normanno N, Wechselberger C, Sun Y, Khan N, Hirota M, Adkins H, Williams K *et al*: **A Nodal- and ALK4-independent signaling pathway activated by Cripto-1 through Glypican-1 and c-Src**. *Cancer research* 2003, **63**(6):1192-1197.
19. De Luca A, Lamura L, Strizzi L, Roma C, D'Antonio A, Margaryan N, Pirozzi G, Hsu MY, Botti G, Mari E *et al*: **Expression and functional role of CRIPTO-1 in cutaneous melanoma**. *Br J Cancer* 2011, **105**(7):1030-1038.
20. Bianco C, Normanno N, De Luca A, Maiello MR, Wechselberger C, Sun Y, Khan N, Adkins H, Sanicola M, Vonderhaar B *et al*: **Detection and localization of Cripto-1**

binding in mouse mammary epithelial cells and in the mouse mammary gland using an immunoglobulin-cripto-1 fusion protein. *J Cell Physiol* 2002, **190**(1):74-82.

21. Baldassarre G, Romano A, Armenante F, Rambaldi M, Paoletti I, Sandomenico C, Pepe S, Staibano S, Salvatore G, De Rosa G *et al*: **Expression of teratocarcinoma-derived growth factor-1 (TDGF-1) in testis germ cell tumors and its effects on growth and differentiation of embryonal carcinoma cell line NTERA2/D1**. *Oncogene* 1997, **15**(8):927-936.
22. De Santis ML, Kannan S, Smith GH, Seno M, Bianco C, Kim N, Martinez-Lacaci I, Wallace-Jones B, Salomon DS: **Cripto-1 inhibits beta-casein expression in mammary epithelial cells through a p21ras-and phosphatidylinositol 3'-kinase-dependent pathway**. *Cell Growth Differ* 1997, **8**(12):1257-1266.
23. Brandt R, Normanno N, Gullick WJ, Lin JH, Harkins R, Schneider D, Jones BW, Ciardiello F, Persico MG, Armenante F *et al*: **Identification and biological characterization of an epidermal growth factor-related protein: cripto-1**. *The Journal of biological chemistry* 1994, **269**(25):17320-17328.
24. Das AB, Loying P, Bose B: **Human recombinant Cripto-1 increases doubling time and reduces proliferation of HeLa cells independent of pro-proliferation pathways**. *Cancer Lett* 2012, **318**(2):189-198.
25. Shen MM, Schier AF: **The EGF-CFC gene family in vertebrate development**. *Trends Genet* 2000, **16**(7):303-309.
26. Bhattacharya B, Miura T, Brandenberger R, Mejido J, Luo Y, Yang AX, Joshi BH, Ginis I, Thies RS, Amit M *et al*: **Gene expression in human embryonic stem cell lines: unique molecular signature**. *Blood* 2004, **103**(8):2956-2964.
27. International Stem Cell I, Adewumi O, Aflatoonian B, Ahrlund-Richter L, Amit M, Andrews PW, Beighton G, Bello PA, Benvenisty N, Berry LS *et al*: **Characterization of human embryonic stem cell lines by the International Stem Cell Initiative**. *Nat Biotechnol* 2007, **25**(7):803-816.
28. Aasen T, Raya A, Barrero MJ, Garreta E, Consiglio A, Gonzalez F, Vassena R, Bilic J, Pekarik V, Tiscornia G *et al*: **Efficient and rapid generation of induced pluripotent stem cells from human keratinocytes**. *Nat Biotechnol* 2008, **26**(11):1276-1284.
29. Bianco C, Rangel MC, Castro NP, Nagaoka T, Rollman K, Gonzales M, Salomon DS: **Role of Cripto-1 in stem cell maintenance and malignant progression**. *Am J Pathol* 2010, **177**(2):532-540.

30. Bamford RN, Roessler E, Burdine RD, Saplakoglu U, dela Cruz J, Splitt M, Goodship JA, Towbin J, Bowers P, Ferrero GB *et al*: **Loss-of-function mutations in the EGF-CFC gene CFC1 are associated with human left-right laterality defects**. *Nat Genet* 2000, **26**(3):365-369.

31. Minchiotti G, Parisi S, Liguori GL, D'Andrea D, Persico MG: **Role of the EGF-CFC gene cripto in cell differentiation and embryo development**. *Gene* 2002, **287**(1-2):33-37.

32. Xu C, Liguori G, Persico MG, Adamson ED: **Abrogation of the Cripto gene in mouse leads to failure of postgastrulation morphogenesis and lack of differentiation of cardiomyocytes**. *Development* 1999, **126**(3):483-494.

33. Ding J, Yang L, Yan YT, Chen A, Desai N, Wynshaw-Boris A, Shen MM: **Cripto is required for correct orientation of the anterior-posterior axis in the mouse embryo**. *Nature* 1998, **395**(6703):702-707.

34. Xu C, Liguori G, Adamson ED, Persico MG: **Specific arrest of cardiogenesis in cultured embryonic stem cells lacking Cripto-1**. *Dev Biol* 1998, **196**(2):237-247.

35. Sonntag KC, Simantov R, Bjorklund L, Cooper O, Pruszak J, Kowalke F, Gilmartin J, Ding J, Hu YP, Shen MM *et al*: **Context-dependent neuronal differentiation and germ layer induction of Smad4-/- and Cripto-/- embryonic stem cells**. *Mol Cell Neurosci* 2005, **28**(3):417-429.

36. Gritsman K, Zhang J, Cheng S, Heckscher E, Talbot WS, Schier AF: **The EGF-CFC protein one-eyed pinhead is essential for nodal signaling**. *Cell* 1999, **97**(1):121-132.

37. Warga RM, Kane DA: **One-eyed pinhead regulates cell motility independent of Squint/Cyclops signaling**. *Dev Biol* 2003, **261**(2):391-411.

38. Bianco C, Strizzi L, Normanno N, Khan N, Salomon DS: **Cripto-1: an oncofetal gene with many faces**. *Curr Top Dev Biol* 2005, **67**:85-133.

39. Normanno N, De Luca A, Bianco C, Maiello MR, Carriero MV, Rehman A, Wechselberger C, Arra C, Strizzi L, Sanicola M *et al*: **Cripto-1 overexpression leads to enhanced invasiveness and resistance to anoikis in human MCF-7 breast cancer cells**. *J Cell Physiol* 2004, **198**(1):31-39.

40. Shankar V, Ciardiello F, Kim N, Derynck R, Liscia DS, Merlo G, Langton BC, Sheer D, Callahan R, Bassin RH *et al*: **Transformation of an established mouse mammary epithelial cell line following transfection with a human transforming growth factor alpha cDNA**. *Mol Carcinog* 1989, **2**(1):1-11.

41. Ciardiello F, Dono R, Kim N, Persico MG, Salomon DS: **Expression of cripto, a novel gene of the epidermal growth factor gene family, leads to in vitro transformation of a normal mouse mammary epithelial cell line**. *Cancer research* 1991, **51**(3):1051-1054.
42. Wechselberger C, Strizzi L, Kenney N, Hirota M, Sun Y, Ebert A, Orozco O, Bianco C, Khan NI, Wallace-Jones B *et al*: **Human Cripto-1 overexpression in the mouse mammary gland results in the development of hyperplasia and adenocarcinoma**. *Oncogene* 2005, **24**(25):4094-4105.
43. Normanno N, De Luca A, Maiello MR, Bianco C, Mancino M, Strizzi L, Arra C, Ciardiello F, Agrawal S, Salomon DS: **CRIPTO-1: a novel target for therapeutic intervention in human carcinoma**. *Int J Oncol* 2004, **25**(4):1013-1020.
44. Bianco C, Strizzi L, Ebert A, Chang C, Rehman A, Normanno N, Guedez L, Salloum R, Ginsburg E, Sun Y *et al*: **Role of human cripto-1 in tumor angiogenesis**. *J Natl Cancer Inst* 2005, **97**(2):132-141.
45. Strizzi L, Bianco C, Normanno N, Seno M, Wechselberger C, Wallace-Jones B, Khan NI, Hirota M, Sun Y, Sanicola M *et al*: **Epithelial mesenchymal transition is a characteristic of hyperplasias and tumors in mammary gland from MMTV-Cripto-1 transgenic mice**. *J Cell Physiol* 2004, **201**(2):266-276.
46. Savagner P: **Leaving the neighborhood: molecular mechanisms involved during epithelial-mesenchymal transition**. *Bioessays* 2001, **23**(10):912-923.
47. Ebert AD, Wechselberger C, Nees M, Clair T, Schaller G, Martinez-Lacaci I, Wallace-Jones B, Bianco C, Weitzel HK, Salomon DS: **Cripto-1-induced increase in vimentin expression is associated with enhanced migration of human Caski cervical carcinoma cells**. *Exp Cell Res* 2000, **257**(1):223-229.
48. Massague J: **TGF-beta signal transduction**. *Annu Rev Biochem* 1998, **67**:753-791.
49. Schier AF: **Nodal morphogens**. *Cold Spring Harb Perspect Biol* 2009, **1**(5):a003459.
50. Wu MY, Hill CS: **Tgf-beta superfamily signaling in embryonic development and homeostasis**. *Dev Cell* 2009, **16**(3):329-343.
51. Schier AF: **Nodal signaling in vertebrate development**. *Annu Rev Cell Dev Biol* 2003, **19**:589-621.
52. Schier AF, Shen MM: **Nodal signalling in vertebrate development**. *Nature* 2000, **403**(6768):385-389.
53. Foley SF, van Vlijmen HW, Boynton RE, Adkins HB, Cheung AE, Singh J, Sanicola M, Young CN, Wen D: **The CRIPTO/FRL-1/CRYPTIC (CFC) domain of human Cripto.**

Functional and structural insights through disulfide structure analysis. *Eur J Biochem* 2003, **270**(17):3610-3618.

54. Kirkbride KC, Ray BN, Blobe GC: **Cell-surface co-receptors: emerging roles in signaling and human disease**. *Trends Biochem Sci* 2005, **30**(11):611-621.
55. Yeo C, Whitman M: **Nodal signals to Smads through Cripto-dependent and Cripto-independent mechanisms**. *Mol Cell* 2001, **7**(5):949-957.
56. Kruithof-de Julio M, Alvarez MJ, Galli A, Chu J, Price SM, Califano A, Shen MM: **Regulation of extra-embryonic endoderm stem cell differentiation by Nodal and Cripto signaling**. *Development* 2011, **138**(18):3885-3895.
57. Parisi S, D'Andrea D, Lago CT, Adamson ED, Persico MG, Minchiotti G: **Nodal-dependent Cripto signaling promotes cardiomyogenesis and redirects the neural fate of embryonic stem cells**. *J Cell Biol* 2003, **163**(2):303-314.
58. Adkins HB, Bianco C, Schiffer SG, Rayhorn P, Zafari M, Cheung AE, Orozco O, Olson D, De Luca A, Chen LL *et al*: **Antibody blockade of the Cripto CFC domain suppresses tumor cell growth in vivo**. *J Clin Invest* 2003, **112**(4):575-587.
59. Shi Y, Bao YL, Wu Y, Yu CL, Huang YX, Sun Y, Zheng LH, Li YX: **Alantolactone inhibits cell proliferation by interrupting the interaction between Cripto-1 and activin receptor type II A in activin signaling pathway**. *J Biomol Screen* 2011, **16**(5):525-535.
60. Chang F, Lee JT, Navolanic PM, Steelman LS, Shelton JG, Blalock WL, Franklin RA, McCubrey JA: **Involvement of PI3K/Akt pathway in cell cycle progression, apoptosis, and neoplastic transformation: a target for cancer chemotherapy**. *Leukemia* 2003, **17**(3):590-603.
61. Roberts PJ, Der CJ: **Targeting the Raf-MEK-ERK mitogen-activated protein kinase cascade for the treatment of cancer**. *Oncogene* 2007, **26**(22):3291-3310.
62. Bianco C, Mysliwiec M, Watanabe K, Mancino M, Nagaoka T, Gonzales M, Salomon DS: **Activation of a Nodal-independent signaling pathway by Cripto-1 mutants with impaired activation of a Nodal-dependent signaling pathway**. *FEBS Lett* 2008, **582**(29):3997-4002.
63. Ebert AD, Wechselberger C, Frank S, Wallace-Jones B, Seno M, Martinez-Lacaci I, Bianco C, De Santis M, Weitzel HK, Salomon DS: **Cripto-1 induces phosphatidylinositol 3'-kinase-dependent phosphorylation of AKT and glycogen**

synthase kinase 3beta in human cervical carcinoma cells. *Cancer research* 1999, **59**(18):4502-4505.

64. Kannan S, De Santis M, Lohmeyer M, Riese DJ, 2nd, Smith GH, Hynes N, Seno M, Brandt R, Bianco C, Persico G *et al*: **Cripto enhances the tyrosine phosphorylation of Shc and activates mitogen-activated protein kinase (MAPK) in mammary epithelial cells**. *The Journal of biological chemistry* 1997, **272**(6):3330-3335.
65. Kelber JA, Panopoulos AD, Shani G, Booker EC, Belmonte JC, Vale WW, Gray PC: **Blockade of Cripto binding to cell surface GRP78 inhibits oncogenic Cripto signaling via MAPK/PI3K and Smad2/3 pathways**. *Oncogene* 2009, **28**(24):2324-2336.
66. Shani G, Fischer WH, Justice NJ, Kelber JA, Vale W, Gray PC: **GRP78 and Cripto form a complex at the cell surface and collaborate to inhibit transforming growth factor beta signaling and enhance cell growth**. *Mol Cell Biol* 2008, **28**(2):666-677.
67. Dono R, Montuori N, Rocchi M, De Ponti-Zilli L, Ciccodicola A, Persico MG: **Isolation and characterization of the CRIPTO autosomal gene and its X-linked related sequence**. *Am J Hum Genet* 1991, **49**(3):555-565.
68. Sun C, Orozco O, Olson DL, Choi E, Garber E, Tizard R, Szak S, Sanicola M, Carulli JP: **CRIPTO3, a presumed pseudogene, is expressed in cancer**. *Biochem Biophys Res Commun* 2008, **377**(1):215-220.
69. Kenney NJ, Huang RP, Johnson GR, Wu JX, Okamura D, Matheny W, Kordon E, Gullick WJ, Plowman G, Smith GH *et al*: **Detection and location of amphiregulin and Cripto-1 expression in the developing postnatal mouse mammary gland**. *Mol Reprod Dev* 1995, **41**(3):277-286.
70. Hu XF, Xing PX: **Cripto as a target for cancer immunotherapy**. *Expert Opin Ther Targets* 2005, **9**(2):383-394.
71. Ciardiello F, Kim N, Saeki T, Dono R, Persico MG, Plowman GD, Garrigues J, Radke S, Todaro GJ, Salomon DS: **Differential expression of epidermal growth factor-related proteins in human colorectal tumors**. *Proc Natl Acad Sci U S A* 1991, **88**(17):7792-7796.
72. Qi CF, Liscia DS, Normanno N, Merlo G, Johnson GR, Gullick WJ, Ciardiello F, Saeki T, Brandt R, Kim N *et al*: **Expression of transforming growth factor alpha, amphiregulin and cripto-1 in human breast carcinomas**. *Br J Cancer* 1994, **69**(5):903-910.
73. Fontanini G, De Laurentiis M, Vignati S, Chine S, Lucchi M, Silvestri V, Mussi A, De Placido S, Tortora G, Bianco AR *et al*: **Evaluation of epidermal growth factor-related**

growth factors and receptors and of neoangiogenesis in completely resected stage I-IIIA non-small-cell lung cancer: amphiregulin and microvessel count are independent prognostic indicators of survival. *Clin Cancer Res* 1998, **4**(1):241-249.

74. D'Antonio A, Losito S, Pignata S, Grassi M, Perrone F, De Luca A, Tambaro R, Bianco C, Gullick WJ, Johnson GR *et al*: **Transforming growth factor alpha, amphiregulin and cripto-1 are frequently expressed in advanced human ovarian carcinomas**. *Int J Oncol* 2002, **21**(5):941-948.
75. Friess H, Yamanaka Y, Buchler M, Kobrin MS, Tahara E, Korc M: **Cripto, a member of the epidermal growth factor family, is over-expressed in human pancreatic cancer and chronic pancreatitis**. *Int J Cancer* 1994, **56**(5):668-674.
76. Mancino M, Strizzi L, Wechselberger C, Watanabe K, Gonzales M, Hamada S, Normanno N, Salomon DS, Bianco C: **Regulation of human Cripto-1 gene expression by TGF-beta1 and BMP-4 in embryonal and colon cancer cells**. *J Cell Physiol* 2008, **215**(1):192-203.
77. Mallikarjuna K, Vaijayanthi P, Krishnakumar S: **Cripto-1 expression in uveal melanoma: an immunohistochemical study**. *Exp Eye Res* 2007, **84**(6):1060-1066.
78. Wu Z, Li G, Wu L, Weng D, Li X, Yao K: **Cripto-1 overexpression is involved in the tumorigenesis of nasopharyngeal carcinoma**. *BMC Cancer* 2009, **9**:315.
79. Gong YP, Yarrow PM, Carmalt HL, Kwun SY, Kennedy CW, Lin BP, Xing PX, Gillett DJ: **Overexpression of Cripto and its prognostic significance in breast cancer: a study with long-term survival**. *Eur J Surg Oncol* 2007, **33**(4):438-443.
80. Zhong XY, Zhang LH, Jia SQ, Shi T, Niu ZJ, Du H, Zhang GG, Hu Y, Lu AP, Li JY *et al*: **Positive association of up-regulated Cripto-1 and down-regulated E-cadherin with tumour progression and poor prognosis in gastric cancer**. *Histopathology* 2008, **52**(5):560-568.
81. Tysnes BB, Satran HA, Mork SJ, Margaryan NV, Eide GE, Petersen K, Strizzi L, Hendrix MJ: **Age-Dependent Association between Protein Expression of the Embryonic Stem Cell Marker Cripto-1 and Survival of Glioblastoma Patients**. *Transl Oncol* 2013, **6**(6):732-741.
82. Pilgaard L, Mortensen JH, Henriksen M, Olesen P, Sorensen P, Laursen R, Vyberg M, Agger R, Zachar V, Moos T *et al*: **Cripto-1 Expression in Glioblastoma Multiforme**. *Brain Pathol* 2014.

83. Chan YS, Yang L, Ng HH: **Transcriptional regulatory networks in embryonic stem cells**. *Prog Drug Res* 2011, **67**:239-252.
84. Herreros-Villanueva M, Bujanda L, Billadeau DD, Zhang JS: **Embryonic stem cell factors and pancreatic cancer**. *World J Gastroenterol* 2014, **20**(9):2247-2254.
85. Watanabe K, Meyer MJ, Strizzi L, Lee JM, Gonzales M, Bianco C, Nagaoka T, Farid SS, Margaryan N, Hendrix MJ *et al*: **Cripto-1 is a cell surface marker for a tumorigenic, undifferentiated subpopulation in human embryonal carcinoma cells**. *Stem Cells* 2010, **28**(8):1303-1314.
86. Bianco C, Cotten C, Lonardo E, Strizzi L, Baraty C, Mancino M, Gonzales M, Watanabe K, Nagaoka T, Berry C *et al*: **Cripto-1 is required for hypoxia to induce cardiac differentiation of mouse embryonic stem cells**. *Am J Pathol* 2009, **175**(5):2146-2158.
87. Hamada S, Watanabe K, Hirota M, Bianco C, Strizzi L, Mancino M, Gonzales M, Salomon DS: **beta-Catenin/TCF/LEF regulate expression of the short form human Cripto-1**. *Biochem Biophys Res Commun* 2007, **355**(1):240-244.
88. Bianco C, Castro NP, Baraty C, Rollman K, Held N, Rangel MC, Karasawa H, Gonzales M, Strizzi L, Salomon DS: **Regulation of human Cripto-1 expression by nuclear receptors and DNA promoter methylation in human embryonal and breast cancer cells**. *J Cell Physiol* 2013, **228**(6):1174-1188.
89. Hentschke M, Kurth I, Borgmeyer U, Hubner CA: **Germ cell nuclear factor is a repressor of CRIPTO-1 and CRIPTO-3**. *The Journal of biological chemistry* 2006, **281**(44):33497-33504.
90. Shi Y, Massague J: **Mechanisms of TGF-beta signaling from cell membrane to the nucleus**. *Cell* 2003, **113**(6):685-700.
91. Elowitz MB, Levine AJ, Siggia ED, Swain PS: **Stochastic gene expression in a single cell**. *Science* 2002, **297**(5584):1183-1186.
92. Newman JR, Ghaemmaghami S, Ihmels J, Breslow DK, Noble M, DeRisi JL, Weissman JS: **Single-cell proteomic analysis of S. cerevisiae reveals the architecture of biological noise**. *Nature* 2006, **441**(7095):840-846.
93. Cohen AA, Kalisky T, Mayo A, Geva-Zatorsky N, Danon T, Issaeva I, Kopito RB, Perzov N, Milo R, Sigal A *et al*: **Protein dynamics in individual human cells: experiment and theory**. *PLoS One* 2009, **4**(4):e4901.
94. Friedman N, Cai L, Xie XS: **Linking stochastic dynamics to population distribution: an analytical framework of gene expression**. *Phys Rev Lett* 2006, **97**(16):168302.

95. Cai L, Friedman N, Xie XS: **Stochastic protein expression in individual cells at the single molecule level**. *Nature* 2006, **440**(7082):358-362.
96. Furusawa C, Suzuki T, Kashiwagi A, Yomo T, Kaneko K: **Ubiquity of Log-normal Distributions in Intra-cellular Reaction Dynamics**. *Biophysics* 2005, **1**:25-31.
97. Kaern M, Elston TC, Blake WJ, Collins JJ: **Stochasticity in gene expression: from theories to phenotypes**. *Nat Rev Genet* 2005, **6**(6):451-464.
98. Huang S: **Non-genetic heterogeneity of cells in development: more than just noise**. *Development* 2009, **136**(23):3853-3862.
99. Shahrezaei V, Swain PS: **The stochastic nature of biochemical networks**. *Curr Opin Biotechnol* 2008, **19**(4):369-374.
100. McAdams HH, Arkin A: **Stochastic mechanisms in gene expression**. *Proc Natl Acad Sci U S A* 1997, **94**(3):814-819.
101. Raj A, Peskin CS, Tranchina D, Vargas DY, Tyagi S: **Stochastic mRNA synthesis in mammalian cells**. *PLoS Biol* 2006, **4**(10):e309.
102. Golding I, Paulsson J, Zawilski SM, Cox EC: **Real-time kinetics of gene activity in individual bacteria**. *Cell* 2005, **123**(6):1025-1036.
103. Yu J, Xiao J, Ren X, Lao K, Xie XS: **Probing gene expression in live cells, one protein molecule at a time**. *Science* 2006, **311**(5767):1600-1603.
104. Bar-Even A, Paulsson J, Maheshri N, Carmi M, O'Shea E, Pilpel Y, Barkai N: **Noise in protein expression scales with natural protein abundance**. *Nat Genet* 2006, **38**(6):636-643.
105. Carey LB, van Dijk D, Sloot PM, Kaandorp JA, Segal E: **Promoter sequence determines the relationship between expression level and noise**. *PLoS Biol* 2013, **11**(4):e1001528.
106. Shahrezaei V, Swain PS: **Analytical distributions for stochastic gene expression**. *Proc Natl Acad Sci U S A* 2008, **105**(45):17256-17261.
107. Taniguchi Y, Choi PJ, Li GW, Chen H, Babu M, Hearn J, Emili A, Xie XS: **Quantifying E. coli proteome and transcriptome with single-molecule sensitivity in single cells**. *Science* 2010, **329**(5991):533-538.
108. Birtwistle MR, von Kriegsheim A, Dobrzynski M, Kholodenko BN, Kolch W: **Mammalian protein expression noise: scaling principles and the implications for knockdown experiments**. *Mol Biosyst* 2012, **8**(11):3068-3076.
109. Ozbudak EM, Thattai M, Kurtser I, Grossman AD, van Oudenaarden A: **Regulation of noise in the expression of a single gene**. *Nat Genet* 2002, **31**(1):69-73.

110. Lillacci G, Khammash M: **The signal within the noise: efficient inference of stochastic gene regulation models using fluorescence histograms and stochastic simulations**. *Bioinformatics* 2013, **29**(18):2311-2319.

111. Gupta PB, Fillmore CM, Jiang G, Shapira SD, Tao K, Kuperwasser C, Lander ES: **Stochastic state transitions give rise to phenotypic equilibrium in populations of cancer cells**. *Cell* 2011, **146**(4):633-644.

112. Mariani L, Schulz EG, Lexberg MH, Helmstetter C, Radbruch A, Lohning M, Hofer T: **Short-term memory in gene induction reveals the regulatory principle behind stochastic IL-4 expression**. *Mol Syst Biol* 2010, **6**:359.

113. Bengtsson M, Stahlberg A, Rorsman P, Kubista M: **Gene expression profiling in single cells from the pancreatic islets of Langerhans reveals lognormal distribution of mRNA levels**. *Genome Res* 2005, **15**(10):1388-1392.

114. Narsinh KH, Sun N, Sanchez-Freire V, Lee AS, Almeida P, Hu S, Jan T, Wilson KD, Leong D, Rosenberg J *et al*: **Single cell transcriptional profiling reveals heterogeneity of human induced pluripotent stem cells**. *J Clin Invest* 2011, **121**(3):1217-1221.

115. Shalek AK, Satija R, Adiconis X, Gertner RS, Gaublomme JT, Raychowdhury R, Schwartz S, Yosef N, Malboeuf C, Lu D *et al*: **Single-cell transcriptomics reveals bimodality in expression and splicing in immune cells**. *Nature* 2013, **498**(7453):236-240.

116. Larson DR, Singer RH, Zenklusen D: **A single molecule view of gene expression**. *Trends Cell Biol* 2009, **19**(11):630-637.

117. Davidson EH: **Emerging properties of animal gene regulatory networks**. *Nature* 2010, **468**(7326):911-920.

118. Garcia-Ojalvo J: **Physical approaches to the dynamics of genetic circuits: A tutorial**. *Contemporary Physics* 2011, **52**(5):439-464.

119. Chalancon G, Ravarani CN, Balaji S, Martinez-Arias A, Aravind L, Jothi R, Babu MM: **Interplay between gene expression noise and regulatory network architecture**. *Trends Genet* 2012, **28**(5):221-232.

120. Becskei A, Seraphin B, Serrano L: **Positive feedback in eukaryotic gene networks: cell differentiation by graded to binary response conversion**. *EMBO J* 2001, **20**(10):2528-2535.

121. Okano H, Kobayashi TJ, Tozaki H, Kimura H: **Estimation of the source-by-source effect of autorepression on genetic noise**. *Biophys J* 2008, **95**(3):1063-1074.

122. Dublanche Y, Michalodimitrakis K, Kummerer N, Foglierini M, Serrano L: **Noise in transcription negative feedback loops: simulation and experimental analysis**. *Mol Syst Biol* 2006, **2**:41.

123. Austin DW, Allen MS, McCollum JM, Dar RD, Wilgus JR, Sayler GS, Samatova NF, Cox CD, Simpson ML: **Gene network shaping of inherent noise spectra**. *Nature* 2006, **439**(7076):608-611.

124. Thieffry D, Huerta AM, Perez-Rueda E, Collado-Vides J: **From specific gene regulation to genomic networks: a global analysis of transcriptional regulation in Escherichia coli**. *Bioessays* 1998, **20**(5):433-440.

125. Alon U: **An Introduction to Systems Biology: Design Principles of Biological Circuits**. *Chapman & Hall* 2006.

126. Rossi FM, Kringstein AM, Spicher A, Guicherit OM, Blau HM: **Transcriptional control: rheostat converted to on/off switch**. *Mol Cell* 2000, **6**(3):723-728.

127. Shah NA, Sarkar CA: **Robust network topologies for generating switch-like cellular responses**. *PLoS Comput Biol* 2011, **7**(6):e1002085.

128. May T, Eccleston L, Herrmann S, Hauser H, Goncalves J, Wirth D: **Bimodal and hysteretic expression in mammalian cells from a synthetic gene circuit**. *PLoS One* 2008, **3**(6):e2372.

129. Kramer BP, Fussenegger M: **Hysteresis in a synthetic mammalian gene network**. *Proc Natl Acad Sci U S A* 2005, **102**(27):9517-9522.

130. Venturelli OS, El-Samad H, Murray RM: **Synergistic dual positive feedback loops established by molecular sequestration generate robust bimodal response**. *Proc Natl Acad Sci U S A* 2012, **109**(48):E3324-3333.

131. Maamar H, Dubnau D: **Bistability in the Bacillus subtilis K-state (competence) system requires a positive feedback loop**. *Mol Microbiol* 2005, **56**(3):615-624.

132. Park BO, Ahrends R, Teruel MN: **Consecutive positive feedback loops create a bistable switch that controls preadipocyte-to-adipocyte conversion**. *Cell Rep* 2012, **2**(4):976-990.

133. Yao G, Lee TJ, Mori S, Nevins JR, You L: **A bistable Rb-E2F switch underlies the restriction point**. *Nat Cell Biol* 2008, **10**(4):476-482.

134. Booth IR: **Stress and the single cell: intrapopulation diversity is a mechanism to ensure survival upon exposure to stress**. *Int J Food Microbiol* 2002, **78**(1-2):19-30.

135. Thattai M, van Oudenaarden A: **Stochastic gene expression in fluctuating environments**. *Genetics* 2004, **167**(1):523-530.

136. Acar M, Mettetal JT, van Oudenaarden A: **Stochastic switching as a survival strategy in fluctuating environments**. *Nat Genet* 2008, **40**(4):471-475.

137. Sureka K, Ghosh B, Dasgupta A, Basu J, Kundu M, Bose I: **Positive feedback and noise activate the stringent response regulator rel in mycobacteria**. *PLoS One* 2008, **3**(3):e1771.

138. Simpson P: **Notch signalling in development: on equivalence groups and asymmetric developmental potential**. *Curr Opin Genet Dev* 1997, **7**(4):537-542.

139. Chang HH, Hemberg M, Barahona M, Ingber DE, Huang S: **Transcriptome-wide noise controls lineage choice in mammalian progenitor cells**. *Nature* 2008, **453**(7194):544-547.

140. Graf T, Stadtfeld M: **Heterogeneity of embryonic and adult stem cells**. *Cell Stem Cell* 2008, **3**(5):480-483.

141. Hayashi K, Lopes SM, Tang F, Surani MA: **Dynamic equilibrium and heterogeneity of mouse pluripotent stem cells with distinct functional and epigenetic states**. *Cell Stem Cell* 2008, **3**(4):391-401.

142. Singh AM, Reynolds D, Cliff T, Ohtsuka S, Mattheyses AL, Sun Y, Menendez L, Kulik M, Dalton S: **Signaling network crosstalk in human pluripotent cells: a Smad2/3-regulated switch that controls the balance between self-renewal and differentiation**. *Cell Stem Cell* 2012, **10**(3):312-326.

143. Raj A, Rifkin SA, Andersen E, van Oudenaarden A: **Variability in gene expression underlies incomplete penetrance**. *Nature* 2010, **463**(7283):913-918.

144. Burrell RA, McGranahan N, Bartek J, Swanton C: **The causes and consequences of genetic heterogeneity in cancer evolution**. *Nature* 2013, **501**(7467):338-345.

145. Roesch A, Fukunaga-Kalabis M, Schmidt EC, Zabierowski SE, Brafford PA, Vultur A, Basu D, Gimotty P, Vogt T, Herlyn M: **A temporarily distinct subpopulation of slow-cycling melanoma cells is required for continuous tumor growth**. *Cell* 2010, **141**(4):583-594.

146. Magee JA, Piskounova E, Morrison SJ: **Cancer stem cells: impact, heterogeneity, and uncertainty**. *Cancer Cell* 2012, **21**(3):283-296.

147. Chaffer CL, Brueckmann I, Scheel C, Kaestli AJ, Wiggins PA, Rodrigues LO, Brooks M, Reinhardt F, Su Y, Polyak K *et al*: **Normal and neoplastic nonstem cells can**

spontaneously convert to a stem-like state. *Proc Natl Acad Sci U S A* 2011, **108**(19):7950-7955.

148. Pisco AO, Brock A, Zhou J, Moor A, Mojtahedi M, Jackson D, Huang S: **Non-Darwinian dynamics in therapy-induced cancer drug resistance**. *Nat Commun* 2013, **4**:2467.
149. Brock A, Chang H, Huang S: **Non-genetic heterogeneity--a mutation-independent driving force for the somatic evolution of tumours**. *Nat Rev Genet* 2009, **10**(5):336-342.
150. Pfaffl MW, Horgan GW, Dempfle L: **Relative expression software tool (REST) for group-wise comparison and statistical analysis of relative expression results in real-time PCR**. *Nucleic Acids Res* 2002, **30**(9):e36.
151. Laemmli UK: **Cleavage of structural proteins during the assembly of the head of bacteriophage T4**. *Nature* 1970, **227**(5259):680-685.
152. Sobell HM: **Actinomycin and DNA transcription**. *Proc Natl Acad Sci U S A* 1985, **82**(16):5328-5331.
153. Henness S, van Thoor E, Ge Q, Armour CL, Hughes JM, Ammit AJ: **IL-17A acts via p38 MAPK to increase stability of TNF-alpha-induced IL-8 mRNA in human ASM**. *Am J Physiol Lung Cell Mol Physiol* 2006, **290**(6):L1283-1290.
154. Overton WR: **Modified histogram subtraction technique for analysis of flow cytometry data**. *Cytometry* 1988, **9**(6):619-626.
155. Massague J, Gomis RR: **The logic of TGFbeta signaling**. *FEBS Lett* 2006, **580**(12):2811-2820.
156. Wasserman WW, Sandelin A: **Applied bioinformatics for the identification of regulatory elements**. *Nat Rev Genet* 2004, **5**(4):276-287.
157. Baldassarre G, Tucci M, Lembo G, Pacifico FM, Dono R, Lago CT, Barra A, Bianco C, Viglietto G, Salomon D *et al*: **A truncated form of teratocarcinoma-derived growth factor-1 (cripto-1) mRNA expressed in human colon carcinoma cell lines and tumors**. *Tumour Biol* 2001, **22**(5):286-293.
158. Nevozhay D, Adams RM, Murphy KF, Josic K, Balazsi G: **Negative autoregulation linearizes the dose-response and suppresses the heterogeneity of gene expression**. *Proc Natl Acad Sci U S A* 2009, **106**(13):5123-5128.
159. Derynck R, Zhang Y, Feng XH: **Smads: transcriptional activators of TGF-beta responses**. *Cell* 1998, **95**(6):737-740.

160. Stroschein SL, Wang W, Luo K: **Cooperative binding of Smad proteins to two adjacent DNA elements in the plasminogen activator inhibitor-1 promoter mediates transforming growth factor beta-induced smad-dependent transcriptional activation**. *The Journal of biological chemistry* 1999, **274**(14):9431-9441.

161. Clarke DC, Brown ML, Erickson RA, Shi Y, Liu X: **Transforming growth factor beta depletion is the primary determinant of Smad signaling kinetics**. *Mol Cell Biol* 2009, **29**(9):2443-2455.

162. Inman GJ, Nicolas FJ, Callahan JF, Harling JD, Gaster LM, Reith AD, Laping NJ, Hill CS: **SB-431542 is a potent and specific inhibitor of transforming growth factor-beta superfamily type I activin receptor-like kinase (ALK) receptors ALK4, ALK5, and ALK7**. *Mol Pharmacol* 2002, **62**(1):65-74.

163. Isaacs FJ, Hasty J, Cantor CR, Collins JJ: **Prediction and measurement of an autoregulatory genetic module**. *Proc Natl Acad Sci U S A* 2003, **100**(13):7714-7719.

164. To TL, Maheshri N: **Noise can induce bimodality in positive transcriptional feedback loops without bistability**. *Science* 2010, **327**(5969):1142-1145.

165. Martinez Arias A, Brickman JM: **Gene expression heterogeneities in embryonic stem cell populations: origin and function**. *Curr Opin Cell Biol* 2011, **23**(6):650-656.

166. Toyooka Y, Shimosato D, Murakami K, Takahashi K, Niwa H: **Identification and characterization of subpopulations in undifferentiated ES cell culture**. *Development* 2008, **135**(5):909-918.

167. Kalmar T, Lim C, Hayward P, Munoz-Descalzo S, Nichols J, Garcia-Ojalvo J, Martinez Arias A: **Regulated fluctuations in nanog expression mediate cell fate decisions in embryonic stem cells**. *PLoS Biol* 2009, **7**(7):e1000149.

168. Strizzi L, Margaryan NV, Gilgur A, Hardy KM, Normanno N, Salomon DS, Hendrix MJ: **The significance of a Cripto-1 positive subpopulation of human melanoma cells exhibiting stem cell-like characteristics**. *Cell Cycle* 2013, **12**(9):1450-1456.

169. Scheidenhelm DK, Cresswell J, Haipek CA, Fleming TP, Mercer RW, Gutmann DH: **Akt-dependent cell size regulation by the adhesion molecule on glia occurs independently of phosphatidylinositol 3-kinase and Rheb signaling**. *Mol Cell Biol* 2005, **25**(8):3151-3162.

170. Palani S, Sarkar CA: **Transient noise amplification and gene expression synchronization in a bistable mammalian cell-fate switch**. *Cell Rep* 2012, **1**(3):215-224.

171. Zechner C, Ruess J, Krenn P, Pelet S, Peter M, Lygeros J, Koeppl H: **Moment-based inference predicts bimodality in transient gene expression**. *Proc Natl Acad Sci U S A* 2012, **109**(21):8340-8345.

172. Strizzi L, Abbott DE, Salomon DS, Hendrix MJ: **Potential for cripto-1 in defining stem cell-like characteristics in human malignant melanoma**. *Cell Cycle* 2008, **7**(13):1931-1935.

173. Bianco C, Salomon DS: **Targeting the embryonic gene Cripto-1 in cancer and beyond**. *Expert Opin Ther Pat* 2010, **20**(12):1739-1749.

174. Clarke MF, Dick JE, Dirks PB, Eaves CJ, Jamieson CH, Jones DL, Visvader J, Weissman IL, Wahl GM: **Cancer stem cells--perspectives on current status and future directions: AACR Workshop on cancer stem cells**. *Cancer research* 2006, **66**(19):9339-9344.

175. Abdullah LN, Chow EK: **Mechanisms of chemoresistance in cancer stem cells**. *Clin Transl Med* 2013, **2**(1):3.

176. Hu XF, Li J, Yang E, Vandervalk S, Xing PX: **Anti-Cripto Mab inhibit tumour growth and overcome MDR in a human leukaemia MDR cell line by inhibition of Akt and activation of JNK/SAPK and bad death pathways**. *Br J Cancer* 2007, **96**(6):918-927.

177. Nakai E, Park K, Yawata T, Chihara T, Kumazawa A, Nakabayashi H, Shimizu K: **Enhanced MDR1 expression and chemoresistance of cancer stem cells derived from glioblastoma**. *Cancer Invest* 2009, **27**(9):901-908.

178. Comerford KM, Wallace TJ, Karhausen J, Louis NA, Montalto MC, Colgan SP: **Hypoxia-inducible factor-1-dependent regulation of the multidrug resistance (MDR1) gene**. *Cancer research* 2002, **62**(12):3387-3394.

179. Yamada T, Takaoka AS, Naishiro Y, Hayashi R, Maruyama K, Maesawa C, Ochiai A, Hirohashi S: **Transactivation of the multidrug resistance 1 gene by T-cell factor 4/beta-catenin complex in early colorectal carcinogenesis**. *Cancer research* 2000, **60**(17):4761-4766.

180. Utsunomiya Y, Hasegawa H, Yanagisawa K, Fujita S: **Enhancement of mdr1 gene expression by transforming growth factor-beta1 in the new adriamycin-resistant human leukemia cell line ME-F2/ADM**. *Leukemia* 1997, **11**(6):894-895.

181. Dohgu S, Yamauchi A, Takata F, Naito M, Tsuruo T, Higuchi S, Sawada Y, Kataoka Y: **Transforming growth factor-beta1 upregulates the tight junction and P-glycoprotein**

of brain microvascular endothelial cells. *Cellular and molecular neurobiology* 2004, **24**(3):491-497.

182. Zhang M, Wang M, Tan X, Li TF, Zhang YE, Chen D: **Smad3 prevents beta-catenin degradation and facilitates beta-catenin nuclear translocation in chondrocytes**. *The Journal of biological chemistry* 2010, **285**(12):8703-8710.
183. Kim Y, Kugler MC, Wei Y, Kim KK, Li X, Brumwell AN, Chapman HA: **Integrin alpha3beta1-dependent beta-catenin phosphorylation links epithelial Smad signaling to cell contacts**. *J Cell Biol* 2009, **184**(2):309-322.
184. Daschner PJ, Ciolino HP, Plouzek CA, Yeh GC: **Increased AP-1 activity in drug resistant human breast cancer MCF-7 cells**. *Breast Cancer Res Treat* 1999, **53**(3):229-240.
185. Liberati NT, Datto MB, Frederick JP, Shen X, Wong C, Rougier-Chapman EM, Wang XF: **Smads bind directly to the Jun family of AP-1 transcription factors**. *Proc Natl Acad Sci U S A* 1999, **96**(9):4844-4849.
186. Imajo M, Tsuchiya Y, Nishida E: **Regulatory mechanisms and functions of MAP kinase signaling pathways**. *IUBMB Life* 2006, **58**(5-6):312-317.
187. Courtney KD, Corcoran RB, Engelman JA: **The PI3K pathway as drug target in human cancer**. *J Clin Oncol* 2010, **28**(6):1075-1083.
188. Gharbi SI, Zvelebil MJ, Shuttleworth SJ, Hancox T, Saghir N, Timms JF, Waterfield MD: **Exploring the specificity of the PI3K family inhibitor LY294002**. *Biochem J* 2007, **404**(1):15-21.
189. Favata MF, Horiuchi KY, Manos EJ, Daulerio AJ, Stradley DA, Feeser WS, Van Dyk DE, Pitts WJ, Earl RA, Hobbs F *et al*: **Identification of a novel inhibitor of mitogen-activated protein kinase kinase**. *The Journal of biological chemistry* 1998, **273**(29):18623-18632.
190. Guo X, Wang XF: **Signaling cross-talk between TGF-beta/BMP and other pathways**. *Cell Res* 2009, **19**(1):71-88.
191. Eliceiri BP: **Integrin and growth factor receptor crosstalk**. *Circ Res* 2001, **89**(12):1104-1110.
192. Aksamitiene E, Kiyatkin A, Kholodenko BN: **Cross-talk between mitogenic Ras/MAPK and survival PI3K/Akt pathways: a fine balance**. *Biochem Soc Trans* 2012, **40**(1):139-146.

193. McKenna NJ, O'Malley BW: **Combinatorial control of gene expression by nuclear receptors and coregulators**. *Cell* 2002, **108**(4):465-474.

194. Hoffmann E, Dittrich-Breiholz O, Holtmann H, Kracht M: **Multiple control of interleukin-8 gene expression**. *J Leukoc Biol* 2002, **72**(5):847-855.

Appendix

General Reagents: Acetic acid, Chloroform, di-sodium hydrogen phosphate, Glycerol, Hydrochloric acid, Isopropyl Alcohol, Methanol, Ethanol, Potassium acetate, Sulphuric acid, Sodium chloride (all of AR grade) from SRL, India and Merck, India.

Molecular biology grade reagents/chemicals: Acrylamide, APS, Bis-acrylamide, EDTA, IPTG, Lysozyme, TEMED, G418, Phenol, Tween 20, Triton X 100, Alk4 inhibitor, Actinomycin D from Sigma-Aldrich, U.S.A. or SRL, India. PCR Master Mix, dNTPs from Bioline, UK. Cyber green Master Mix from Applied Biosystem, U.S.A. Agarose, Magnesium chloride, Disodium citrate, Boric acid, SDS, Tris base from Merck, India. Ampicillin, Chloramphenicol, Tetracycline from Himedia, India. PI3K inhibitor, MEK1/2 inhibitor from Cell Signaling Technology, U.S.A.

Components for bacterial culture medium: Bacto-agar, Tryptone, Yeast extract from Himedia, India.

Components for mammalian cell culture medium: DMEM and antibiotic from Invitrogen, Fetal Calf Serum from PAA, Sodium bicarbonate from Sigma-Aldrich, U.S.A.

Enzymes: RNase from Sigma-Aldrich, DNase from Promega, Reverse transcriptase from Thermo Scientific, U.S.A. All restriction enzymes from New England Biolabs, U.K.

Blotting membranes and Filters: PVDF membrane (0.2 µm), Syringe driven filter (0.2 µm & 0.45 µm) from Millipore and 3 mm filter paper from Whatman, USA.

DNA and protein markers: 100 bp and 1 kb DNA ladder and protein molecular weight marker (14-100 kDa) from Bangalore Genei, India.

Plastic and Glassware: PCR tubes from Axygen, U.S.A. Micro-pipette tips, Micro-centrifuge tubes, Petri-dishes, Falcon tubes and other plastic wares from Tarsons Product Pvt. Ltd., India. All glassware from Borosil International, India.

Table A1. List of Buffers and Solutions

Buffers/Solutions	Compositions
Tris-EDTA (TE) buffer	0.01 M Tris-HCl (pH 7.4), 0.001 M Na_2-EDTA (pH 8.0)
TAE – Tris Acetate EDTA buffer, 50X (100 mL)	24.2 g Tris base, 5.71 ml CH_3COOH, 10 ml of 0.5 M EDTA
Phosphate buffer saline (PBS)	0.137 M NaCl, 2.68 mM KCl, 7.98 mM Na_2HPO_4, 1.4 mM KH_2PO_4, pH 7.2
PBST	PBS containing 0.1% Tween-20
TBS	50 mM Tris base, 150 mM NaCl
TBST	TBS containing 0.1% Tween 20
Trypsin-EDTA	0.05% Trypsin, 0.53 mM EDTA in PBS
RIPA buffer	50 mM Tris-HCl, pH 7.5, 150 mM NaCl, 1% Nonidet P40, 0.5% sodium deoxycholate, 0.1% SDS

Table A2. Culture medium for Bacteria

Media	Constitutes	Concentration (%)	pH
2xTY	Bactotryptone Yeast extract NaCl	1.6 1.0 0.5	7.2

Table A3. List of Plasmid Vector

Name	Use	Promoter	Selection marker (s)	Cloning Site
pGEX-4T-2 (GE healthcare)	Bacterial Expression Vector	ptac	Amp^R	CR1ΔC cloned at BamHI/XhoI site
pCI-Neo (Promega)	Mammalian Expression Vector	pCMV	Amp^R, Neo^R	Full length CR-1 cloned at EcoRI site (gifted by Dr. D.S. Salomon , NIH, USA
pCI-Neo (Promega)	Mammalian Expression Vector	pCMV	Amp^R, Neo^R	CR1ΔC cloned at XhoI/NotI site

Table A4. List of Bacterial Strain

Strain	Selection marker (s)	Description
Escherichia coli Rosetta Gami (DE3) (Novagen)	Cam^R, Tet^R, Kan^R	F^- *ompT hsdS*$_B$ ($r_B^- m_B^-$) *gal dcm lacY1 ahpC* (DE3) *gor 522*:: Tn*10 trxB* pRARE

Table A5. Culture media for mammalian cells

Media	Constituents	pH
DMEM	DMEM powder with high glucose for 1 liter, 3.7 gm $NaHCO_3$	7.4, adjusted with 1N HCl
DMEM with serum	DMEM, 10% serum, 1x Antibiotic	7.4

Table A6. List of Primers

Target	Primers	Sequence	Tm (°C)	Final Conc. (nM)	Product Size (bp)
Nodal	Forward	CCCAAGCAGTACAACGCCTA	60	200	105
	Reverse	ACGTTTCAGCAGACTCTGGAT			
Alk4	Forward	CTCCAAAGACAAGACGCTCC	60	200	402
	Reverse	CCAGCTTAATCATCCCCTCA			
ActRIIB	Forward	CACAGCCGTGCTGGCTGACT	60	200	211
	Reverse	TGCAGCCTTGCAGCGAGACA			
SMAD2	Forward	AAGAAGTCAGCTGGTGGGT	60	200	246
	Reverse	GCCTGTTGTATCCCACTGA			
SMAD3	Forward	CAGAACGTCAACACCAAGT	60	200	308
	Reverse	ATGGAATGGCTGTAGTCGT			
SMAD4	Forward	CCAGGATCAGTAGGTGGAAT	60	200	243
	Reverse	GTCTAAAGGTTGTGGGTCTG			
CR-1	Forward	GATACAGCACAGTAAGGAGC	60	200	286
	Reverse	TAGTTCTGGAGTCCTGGAAG			
CR-1, transcript-1	Forward	AAGCTATGGACTGCAGGAAGATGG	60	200	156
	Reverse	GCTGTCATCTCTGAAGGCCAGGTA			
CR-3	Forward	GCGTGTGCTGCCCATGGGA	60	200	432
	Reverse	CGGGTCATGAAATTTGCATA			
MDR-1	Forward	GCCTGGCAGCTGGAAGACAAATAC ACAAAATT	60	200	286
	Reverse	CAGACAGCAGCTGACAGTCCAAGA ACAGGACT			
Oct4	Forward	GAGAACCGAGTGAGAGGCAACC	60	200	166
	Reverse	CATAGTCGCTGCTTGATCGCTTG			
Nanog	Forward	AATACCTCAGCCTCCAGCAGATG	60	200	148
	Reverse	TGCGTCACACCATTGCTATTCTTC			

Table A6. List of Primers

Target	Primers	Sequence	Tm (°C)	Final Conc. (nM)	Product Size (bp)
CD133	Forward	ATGACAAGCCCATCACAACA	60	200	197
	Reverse	AGCACTACCCAGAGACCAATG			
Sox2	Forward	GCTCGCAGACCTACATGAAC	60	200	144
	Reverse	GGGAGGAAGAGGTAACCACA			
Endogenous controls:					
β-actin	Forward	CTGTCTGGCGGCACCACCAT	60	200	254
	Reverse	GCAACTAAGTCATAGTCCGC			
Cyclophilin	Forward	ACACGCCATAATGGCACTGG	60	200	105
	Reverse	ATTTGCCATGGACAAGATGCC			
GAPDH	Forward	GAAGGTGAAGGTCGGAGTC	6	200	226
	Reverse	GAAGATGGTGATGGGATTTC			
Primers set for cloning:					
Cripto-1	Forward	TAGCCTCGAGATGGACTGCAGGAA GATGG ***Xho I*** (underlined) for cloning in pCI-neo vector	60	200	507
	Reverse	GGAAGCGGCCGCTCACGGTGGTAG TTCTGG ***Not I*** (underlined) for cloning in pCI-neo vector			

Table A7. Buffers and Solutions for SDS-PAGE

30% acrylamide-bisacrylamide solution (100 ml)	29.2 g Acrylamide, 0.8 g Bis-acrylamide
Tris HCl, pH 6.8, 0.5 M (100 ml)	6.06 g Tris base, pH adjusted to 6.8 with 2 N HCl
Tris HCl, pH 8.8, 1.5 M (100 ml)	18.18 g Tris base, pH adjusted to 8.8 with 2 N HCl
Gel Running Buffer	25 mM Tris base, 0.1% SDS
Sample Loading Buffer (1X)	50 mM Tris-HCl pH 6.8, 2% SDS, 10% glycerol, 1% β-mercaptoethanol, 0.02% bromophenol blue
Staining solution	50% Methanol, 10% Acetic acid, 40% water, 0.25% CBB R250
Destaining solution	30% Methanol, 10% Acetic acid, 60% Water.

Table A8. Buffers and solutions for western blot

Transfer buffer	25 mM Tris base, 39 mM Glycine, 20% Methanol
Ponceau solution (Sigma)	0.1% PonceauS in 5% acetic acid
Blocking Solution	3% BSA in TBST
Washing buffer	TBST

Table A9. List of Antibody

Name	Source/Type	Working condition	Working Dilution	Use
Anti-human Cripto-1 (R&D Systems, U.S.A, #AF145)	Goat/ monoclonal	4 ^{o}C/ ON	1:500	WB
Anti-human phospho-Smad2 (Ser465/467) (Cell Signaling, U.S.A, # 3108)	Rabbit/ Monoclonal	4 ^{o}C/ ON	1:1000	WB
Anti-human Smad2 (Cell Signaling, U.S.A, # 3102)	Rabbit/ Monoclonal	4 ^{o}C/ ON	1:3000	WB
Anti-human COXIV (Cell Signaling, U.S.A, # 4850)	Rabbit/ Monoclonal	4 ^{o}C/ ON	1:3000	WB
Anti-human β-actin (Cell Signaling, U.S.A, # 4970)	Rabbit/ Monoclonal	4 ^{o}C/ ON	1:3000	WB
Anti Rabbit-HRP (Cell Signaling, U.S.A, # 7074)	Goat	RT/2 hr	1:6000	WB
Anti Goat-HRP (Bangalore Genei, India, #105500)	Rabbit	RT/2 hr	1:3000	WB
Anti-human Cripto-1 Phycoerythrin (R&D Systems, U.S.A, #FAB2772P)	Mouse/	4 ^{o}C/45 min	As per recommendation	FACS
Anti-P Glycoprotein antibody [UIC2] (FITC) (Abcam, U.K., #ab66250)	Mouse/ Monoclonal	4 ^{o}C/45 min	As per recommendation	FACS
Mouse IgG1 κ Isotype control (BD Pharmingen, U.S.A, #554121)	Mouse/ Monoclonal	4 ^{o}C/45 min	As per recommendation	FACS
FITC-Rat Anti-mouse IgG2a, κ (BD Pharmingen, U.S.A, #553335)	Rat/ Monoclonal	4 ^{o}C/45 min	As per recommendation	FACS
PE-Goat Anti-mouse Ig (BD Pharmingen, U.S.A, #550589)	Goat/ Polyclonal	4 ^{o}C/45 min	As per recommendation	FACS

RT: Room Temperature, ON: Over Night, WB: Western Blot

Table A10. List of Inhibitors

Name	Stock Conc. (mM)	Working Conc. (μM)	Solvent
Alk4 Inhibitor (SB 431542)	10	10	DMSO
PI3K Inhibitor (LY294002)	10	1.5	DMSO
MEK1/2 Inhibitor (U0126)	10	6	DMSO

Table A11. List of Inhibitors

Name	Stock Conc. (mg/ml)	Working Conc. (μg/ml)	Solvent
Ampicillin	100	50-100	Water
Chloramphenicol	50	50	50% Ethanol
Tetracycline	25	12.5	70% Ethanol
G418	20	400-800	HEPES buffer

Figure A1. Melting curve profile of amplicon of each primer set using SYBR Green as a reporter dye

Cripto-1

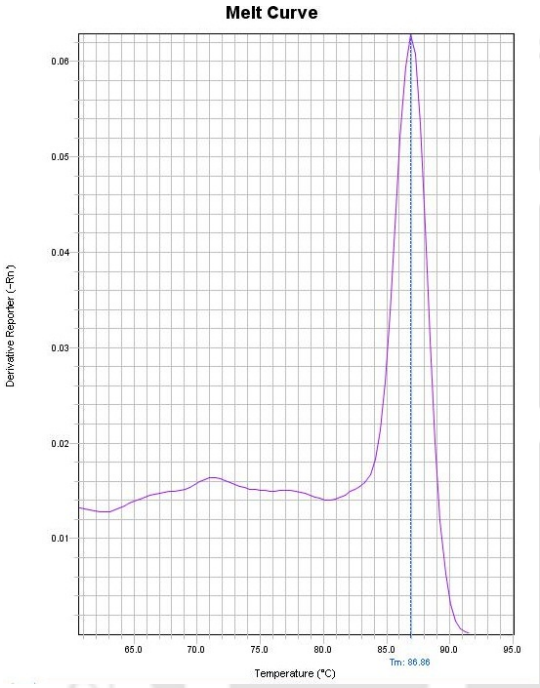

Cyclophilin

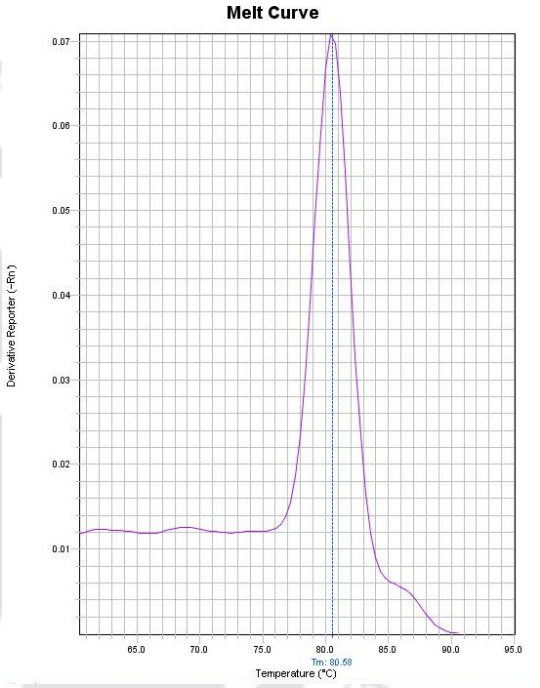

Publications

Publications in Journals:

1. Autoregulation and heterogeneity in expression of human cripto-1. (Communicated)
2. Asim Bikas Das, **Pojul Loying**, Biplab Bose. Human recombinant Cripto-1 increases doubling time and reduce proliferation of HeLa cells independent of pro-proliferation pathways. Cancer Letters 318(2012) 189-198.

Abstracts presented in Conferences:

1. Design Principle of the Transcriptional Circuit of Human Cripto-1.
   Pojul Loying, Ritika Chaturvedi and Biplab Bose
   ICSCC-2012, New Delhi, INDIA
2. Transcription circuit of human cripto-1: Exploring expression heterogeneity.
   Pojul Loying, Mahesh Agarwal and Biplab Bose
   Cell Signaling in Metabolism, Inflammation and Cancer-2013,
   Cold Spring Harbor Asia, Suzhou, CHINA
3. Involvement of Mitogenic Pathways in Expression of Human Cripto-1.
   Pojul Loying, Mahesh Agarwal and Biplab Bose
   ICSCC-2013, Mumbai, INDIA

Workshop attended:

1. **EMBO practical course** on *'Single Cell Gene Expression Analysis'* at **EMBL Heidelberg**, Germany from 19th to 23rd March 2012.